Development And Comparative Assessment Of Continuous And Semi-Continuous Processes For Upgrading Oil From Electrified E-Waste Plastic Pyrolysis

Yasaman Barati

A Thesis

in the Department

of

Chemical and Materials Engineering

Presented in Partial Fulfillment of the Requirements for the Degree of

Master of Applied Science

at

Concordia University

Montréal, Québec, Canada

December, 2025

Concordia University

School of Graduate Studies

This is to certify that the thesis prepared

By: **Yasaman Barati**

Entitled: **Development And Comparative Assessment Of Continuous And Semi-Continuous Processes For Upgrading Oil From Electrified E-Waste Plastic Pyrolysis**

and submitted in partial fulfillment of the requirements for the degree of

Master of Applied Science (Chemical Engineering)

complies with the regulations of this University and meets the accepted standards with respect to originality and quality.

Signed by the Final Examining Committee:

_____Chair
Dr. Alex De Visscher

_____Examiner
Dr. Nhat Truong Nguyen

_____Supervisor
Dr. Yaser Khojasteh-Salkuyeh

_____Co-Supervisor
Dr. Sana Jahanshahi Anbuhi

_____Industry Supervisor
Dr. Sherif Farag

Approved by _____
Dr. Sana Jahanshahi Anbuhi, Graduate Program Director

December 2025 _____
Dr. Mourad Debbabi, Dean of the Gina Cody School of Engineering and Computer Science

Abstract

Development And Comparative Assessment Of Continuous And Semi-Continuous Processes For Upgrading Oil From Electrified E-Waste Plastic Pyrolysis

Yasaman Barati

One of the main challenges for plastic waste conversion plants is low profitability due to variations in feedstock conditions and the small percentage of valuable components in the product. In this study, we designed the pyrolytic oil and gas upgrading process based on the innovative microwave-assisted pyrolysis method. The process is designed to recover energy and chemicals from 17.5 tonnes of oil feed per day, produced from the pyrolysis of 25 tonnes of pre-treated electronic waste plastic. A continuous distillation train with five columns is designed to recover toluene, ethylbenzene, and styrene at chemical grade purity with recovery rates between 70% and 90%. While considering no price for the feed oil, the configuration had a net present value of $2.24 million. When the feed oil price was increased to $262 per tonne, the net present value dropped to -5.80 million, requiring an external credit of $90.80 per tonne of waste to reach the break-even point. This highlights how the economic performance of upstream pyrolysis and metal recovery affects overall feasibility. Life cycle assessment showed that chemical recovery through pyrolysis outperformed conventional incineration when the electricity mix emitted less than 0.582 kg CO_2-eq per kWh. In Quebec, replacing incineration with pyrolysis reduced the global warming impact by 145% from 40,545 to -16,155 kg CO_2-eq per day for the treatment of 25 tonnes of e-waste. Due to uncertainties in the composition and flow rate of the waste stream, and to lower the capital cost of the plant, we designed the alternative semi-continuous upgrading process with only one column. Overall, more than 320 different scenarios were designed and analyzed. Results showed that the proposed system can achieve recoveries between 66-90% and 90% and requires the external credit as low as $18.89 per tonne of waste. Furthermore, adding a second column to the semi-continuous plant produced a profitable design with a net present value of $0.99 million, with no external financial support.

Acknowledgement

Throughout the course of this work, I was fortunate enough to be surrounded by strong support. I would like to express my sincere gratitude to my supervisor, Dr. Yaser Khojasteh-Salkuyeh, for his continuous guidance and for generously sharing his extensive engineering experience. His practical insight and approachable manner helped me learn many useful concepts that I will carry into my future career.

I am also grateful to my co-supervisor, Dr. Sana Jahanshani Anbuhi, for her steady support and encouragement throughout this project. I would like to thank Dr. Sherif Farag and Dr. Mai Attai from GreeNovel, the industry partner, for introducing me to their facilities and making this project possible.

Finally, my deepest gratitude goes to my parents for their patience and their unconditional support and confidence in me.

Table of Contents

List of Figures

List of Tables

1. Introduction

1.1. Background and motivation

Electronic waste (e-waste) is among the fastest-growing global waste streams, increasing by 3-5% each year and by 82% since 2010, reaching a record 62 million tons in 2022 [1], [2]. The e-waste generated worldwide is expected to surpass 74 Mt by 2030, while only a fraction is collected correctly or recycled [2], [3]. E-waste contains both hazardous compounds and valuable metals, making its management technically complex and environmentally critical. Conventional disposal routes, such as landfilling and incineration, release toxic emissions, including halogenated dioxins and furans from flame retardants found in many electronic plastics. Although incineration can recover some energy, it typically produces large volumes of flue gas and requires extensive gas-cleaning systems.

Pyrolysis has emerged as a lower-temperature thermal treatment option for the non-metallic fractions of e-waste. Compared to incineration, pyrolysis can cut gas emissions by 90-95%, limit the formation of toxic compounds, and produce valuable byproducts such as pyrolysis oil, char, and gas[4], [5]. Microwave-assisted pyrolysis (MAP) can further improve heating efficiency and reduce dioxin formation. However, despite these benefits, pyrolysis oil from e-waste plastics is difficult to use directly as fuel or a petrochemical feedstock due to the presence of halogens, metals, high olefin content, and unstable aromatic compounds, which can cause corrosion.

The MAP process that generates the pyrolysis oil used in this study already includes upstream dehalogenation and metal-removal steps, thereby narrowing the problem to upgrading the treated oil. Even after pretreatment, pyrolysis oil must be further refined to recover high-value monomers such as styrene, ethylbenzene, and toluene. The distillation process developed in this work is specifically designed to overcome key obstacles, such as azeotrope formation and repolymerization, while maintaining high purity and practical operation.

Considering the scale of the e-waste problem and the potential value of recovered monomers, there is a strong incentive to assess whether upgrading e-waste-derived pyrolysis oil is technically feasible, economically viable, and environmentally friendly. Therefore, this project aims to design and simulate both continuous and semi-continuous distillation processes for upgrading pyrolysis oil recovered from e-waste, and to evaluate their performance through technoeconomic and life cycle assessments.

1.2. Research objectives

This research aims to evaluate the environmental and economic performance of different valorization routes for pyrolytic oil derived from e-waste plastics, a challenging and emerging waste stream. The study focuses on the feasibility of microwave-assisted pyrolysis and the

subsequent recovery of valuable chemicals from the resulting pyrolytic oil, resulting from hazardous e-waste plastic.

The work includes four main components:

- Conceptual design and simulation of the pyrolytic oil upgrading to high-purity chemicals.
- Techno-economic analysis of the process by estimating capital costs, operating costs, annual revenues, and net present value of the continuous process while performing sensitivity analysis to find the key performance indicators.
- Life cycle assessment of the process to evaluate the environmental impacts of the pyrolysis and chemical recovery process and to compare it with conventional waste treatment and energy recovery routes. The functional unit is the treatment of 25 tonnes of e-waste plastic per day.
- Development and comparative economic analysis of a semi-continuous process for chemical recovery in Aspen Plus V14, providing greater operational flexibility.

1.3. Thesis layout

Chapter 2 presents a literature review on e-waste plastics, available treatment options, the advantages of the pyrolysis method, and the properties of the resulting pyrolytic oil. Chapter 3 describes in detail the process modeled in Aspen Plus, including the baseline incineration route and the continuous and semi-continuous distillation processes. Chapter 4 presents the results and discussion section of the thesis. The simulation results for the continuous process are reported in Chapter 4.1, while Chapters 4.2 and 4.3 assess the continuous design from economic and environmental perspectives, respectively, using techno-economic analysis (TEA) and life cycle assessment (LCA). Lastly, the performance of the semi-continuous process is outlined in Chapter 4.4, along with a brief cost analysis. Lastly, the main conclusions of this work are summarized in Chapter 5.

2. Literature review

2.1. The e-waste plastic problem

Electronic waste (e-waste) is among the fastest-growing waste streams, increasing at an annual rate of 3–5% [1]. In 2022, e-waste generation reached a record 62 million tonnes (Mt), marking an 82% increase since 2010 [2]. In 2022, each EU resident generated 11.2 kg of electronic waste. The e-waste generation worldwide is projected to surpass 74 million metric tons by 2030 [2], [3]. Uncontrolled accumulation and unsafe recycling practices pose serious risks to both human health and the environment. As a result, WEEE recycling has emerged as a major issue in recent decades because of the toxic compounds released during recycling [6].

Printed circuit boards (PCBs) also make up approximately 30% of the total E-waste generated [7]. The most common types of plastics in e-wastes are styrene-based polymers, such as acrylonitrile butadiene styrene (ABS), polystyrene (PS), high-impact polystyrene (HIPS), and epoxy resins [4], [8], [9], [10]. Additional polymers, including PVC, PE, PP, PU, PA, PC, PET, and PBT, are present in smaller quantities [4], [11]**.** An example WEEE composition as reported is: PP 3 wt%, PBT 3 wt%, PVC 4 wt%, styrene-based polymers 50 wt%, thermosetting resins 24 wt%, inorganic fraction 16 wt% [12].

E-waste plastics are frequently contaminated with heavy metals such as Pb, Hg, Cd, and brominated flame retardants (BFRs), especially tetrabromobisphenol A (TBBPA) and its derivatives [8]**.** Addressing the additives and the heterogeneous nature of e-waste poses challenges for the recycling of this waste stream.

2.1.1. E-waste recycling

Electronic waste contains both hazardous and valuable chemicals and is a challenging waste stream to manage. E-waste is primarily recycled through four main methods: incineration, mechanical treatment, hydrometallurgy, and pyrolysis. Mechanical treatment is often the first step in e-waste management. This process generally includes shredding and grinding materials into smaller fragments, and then using separation techniques like gravity, eddy current, and floatation methods to sort metals, glass, and different plastic types [10], [13]. The resulting plastics could be blended into lower-value products such as bins and garden furniture if sufficiently pure [9].

However, achieving such purity is difficult. As discussed previously, e-waste plastics contain numerous additives and heavy metals that complicate mechanical recycling [12]. Traditional techniques like grinding and melting are also ineffective for thermosetting polymers [14]. Moreover, mechanical treatment can result in a significant loss of valuable metal portions [15]. Due to these limitations, mechanical treatment is rarely used in isolation, and it is typically followed by thermal or chemical processes like pyrolysis [16].

Traditionally, the non-metallic fractions of e-waste were disposed of through incineration or landfilling. While incineration reduces waste volume and recovers some energy in the form of

electricity, it can lead to the release of toxic emissions [9], [15]. Heat treatment processes such as combustion, may cayse BFRs in e-waste plastics to generate brominated aromatic compounds that can ultimately lead to the production of polybrominated dibenzo-p-dioxins (PBDD) and polybrominated dibenzo furans (PBDF) [8], [9]. In contrast, the emissions in pyrolysis are more controlled, and the amount of toxic gas produced is significantly lower than in incineration [15]. Lee et al. estimated that opting for pyrolysis over incineration in waste-to-energy schemes could avoid about 0.26 t CO_2 per tonne of plastic waste [17]. Moreover, while incineration focuses on energy recovery, pyrolysis produces products that can be further processed. [4]

Pyrolysis is a thermochemical conversion process that decomposes long-chain polymers into smaller molecules at moderate temperatures, typically between 300 and 500 °C, in the absence of oxygen [17] Conducted at atmospheric pressure, it converts waste into gas, liquid, and solid products and does not require extensive sorting of mixed plastic streams [18], [19]. The products of pyrolysis, particularly the oil, are compositionally similar to petrochemical fuels, as they have a high calorific value and can be considered a valuable energy source. Additionally, pyrolysis oils have potential application in producing value-added products, such as phenolic resins, carbon nanotubes, porous carbon materials, and asphalt modifiers [7].

Gasification is a process that thermally treats waste in a partially oxidative environment to generate syngas. This process takes place at high temperatures, reaching up to 1600 °C under pressures of up to 150 bar. The primary valuable product from gasification is a hydrogen-rich synthesis gas [5], [10]. One of the advantages of pyrolysis over gasification is its ability to generate a higher quantity of olefins. Re-polymerizing these unsaturated hydrocarbons enables the production of new recycled plastics, contributing to a circular economy [19]. Furthermore, studies have shown that pyrolysis could have lower energy consumption compared to other methods of treating the non-metal fraction of e-waste, such as gasification. [10]

An important advantage of pyrolysis is its ability to decrease flue gas volume, thereby reducing the requirements for gas cleaning and purification, and ultimately simplifying and reducing the costs of the process. [4] Compared to incineration, pyrolysis reduces gas emissions by 90-95%, keeping contaminants in the residue rather than releasing them into the environment through gas [5]. Choosing pyrolysis instead of incineration in waste-to-energy plans could prevent approximately 0.26 tons of CO_2 per ton of plastic waste. [17]

2.1.2. Microwave-assisted pyrolysis of e-waste plastics

A microwave pyrolysis reactor uses microwave high-frequency heating. This method offers advantages over traditional pyrolysis because microwave-assisted pyrolysis enables direct and rapid heat transfer into the feedstock through convective heat transfer, ensuring quick and even internal heating of waste particles [20]. This method eliminates the need for extensive feedstock crushing and allows for better temperature control and faster processing, unlike conventional pyrolysis [4], [16], [21], [22]**.** Rapid heating can help reduce the production of toxic by-products like dioxins and furans can also be minimized [15].

Huang and Lo demonstrated that waste printed circuit boards (PCBs) can be effectively pyrolyzed at 300 W, reaching 323 °C within 10 minutes. Their study also highlighted improved metal recovery efficiency through microwave-assisted pyrolysis [23]. The scalability of MAP remains a challenge, particularly in maintaining efficient and uniform heating in large batch reactors. Continuous reactors, where the feedstock moves through a microwave-heated zone, have shown better performance and are more suitable for larger-scale applications [4]. Another limitation of this technology might be its high electricity demand, which can lead to high operating costs. Integrating pyrolysis with other processes has been suggested as a strategy to reduce the electricity costs. For example, combining biomass gasification with pyrolysis reduced recycling fuel costs by 26–29% compared to using pyrolysis alone [24].

2.2. Pyrolysis products

Pyrolysis of different waste materials produces three main products: char, oil, and gas. For instance, pyrolysis of printed circuit boards (PCBs) produced 48 wt% char, 20 wt% oil, and 32 wt% gas. [24]. In plastic pyrolysis, the liquid fraction is rich in organic compounds, while the gas contains Hydrogen, carbon monoxide, methane, and light hydrocarbons from C_2 to C_7. The solid residue mainly consists of carbon. The distribution and composition of these products are affected by factors like plastic type, reactor design, operating temperature, catalysts, and heating method [25].

Pyrolysis may be performed under different conditions, with fast pyrolysis noted for its high heating rates and short vapor residence times [20]. According to Joo et al. (2021), fast pyrolysis could operates at rapid heating rates of 300–1000 °C per minute and residence times of 0.5 to 2 seconds, which can yield up to 75% liquid product [20].

2.2.1. Pyrolysis char properties

The char generated from the pyrolysis of electronic and plastic waste contains valuable materials, particularly metals and carbonaceous compounds [11]. In the case of PCBs, the char has been shown to contain precious metals such as Au, Ag, and Cu, along with metalloids, alkali metals, and transition metals. The dominant elements identified in PCB char were Si (16 wt%), Ca (9 wt%), and Al (4.7 wt%). For waste cable (WC) char, calcium was the most abundant element at 15.5 wt**%** [24]**.** In contrast, char from polystyrene pyrolysis mainly consisted of carbon (87.6%), hydrogen (11.09%), and sulfur (0.51%) [26].

Elements such as Al, Cu, and Fe were present in relatively high concentrations in PCB-derived char [27]. While hydrometallurgical processes such as leaching or smelting are commonly used for metal recovery, the high carbon content in the char can hinder these methods by promoting coke formation. Incineration inhibits coke formation and could be a more practical approach when metal recovery is the main goal [4].

Microwave-assisted pyrolysis (MAP) offers enhanced metal recovery compared to conventional pyrolysis. MAP has been reported to achieve up to 96% copper recovery, whereas conventional

methods typically reach 75%. Thermogravimetric analysis (TGA) also showed that MAP led to 3 to 5% higher weight loss in waste PCB, suggesting more complete decomposition [23].

In addition to metal recovery, pyrolysis char has potential for use in secondary applications. It can serve as raw material for activated carbon, pigment, asphalt components, and a low-grade carbon black substitute [28]. Other possible uses include its application as an adsorbent material, solid fuel, or soil amendments [29].

2.2.2. Pyrolysis gas properties

Non-condensable gases typically make up around 15 percent of total pyrolysis products from WEEE [18]. These gases often contain methane and other light hydrocarbons (C_1 to C_5) along with carbon monoxide and carbon dioxide, making them a potential energy source for the pyrolysis plant [28]**.** For example, HIPS and ABS polymers release significant amounts of hydrogen during thermal cracking and dehydrogenation. The polycarbonate content in waste printed-circuit boards contributes oxygen to the gas phase, which reacts with carbon to form CO and CO_2 [1]. The gas stream additionally contains molecular halogens such as chlorine and bromine, and hydrogen halides like HCl and HBr. The concentrations of these compounds tend to increase with temperature [4].

The pyrolysis gas can be utilized as a fuel to supply the reactor's thermal energy requirement. For instance, in the process developed by Fivga et al., the combined energy content of the char and gas products reached 156.7 kW_{th}, which was sufficient to meet the reactor's energy demand of 41.16 kW_{th} without requiring any external heat source [30]. Jadhao et al**.** reported that in their experiment, the gas product from PCB pyrolysis had a heating value of 28 MJ/kg [1].

2.2.3. Dehalogenation of e-waste pyrolysis products

Halogenated plastics in electronic waste break down differently from conventional polyolefins during pyrolysis. Uddin et al. demonstrated that PVC, brominated ABS, and HIPS release a range of chlorinated and brominated organic compounds. As a result, the pyrolysis oil produced by these plastics is unsuitable for direct use as fuel or petrochemical feedstock unless these heteroatoms are removed. During thermal degradation, the carbon-halogen bonds break, producing hydrogen chloride and hydrogen bromide [9]. Higher reactor temperatures accelerate the breakdown of heavier brominated compounds into lighter molecules that migrate to the liquid and gas phases [21].

In most e-waste plastics, halogens originate from flame-retardant additives such as tetrabromobisphenol A (TBBA), decabromodiphenyl ether, and brominated phenyl phosphates, which are widely added to polystyrene-based resins [8], [10], [31]. Chlorine, however, is mainly associated with PVC jacketing in electrical cables [19]. TBBA begins to decompose between 200 and 500 °C, releasing HBr with brominated phenols that ultimately produce polybrominated dioxins and furans [27]. During pyrolysis of the non-metal fraction of waste PCBs, compounds such as bromoethane, methyl bromide, brominated C_3 species, brominated acetone, and

dibromophenols were detected [32]. These acids cause severe corrosion and fouling of downstream equipment, and their coexistence with low-boiling alkyl bromides and bromophenols requires effective debromination before any hydrotreating, steam cracking, or fuel blending step.

2.2.3.1. Dehalogenation strategies

Several studies have explored ways to reduce halogen content in pyrolysis products. Gao and Xu used $CaCO_3$ during pyrolysis to capture bromine as solid $CaBr_2$, which could later be recovered by water leaching [33]. A similar approach was used by López et al. for chlorine removal. They also demonstrated that a stepwise pyrolysis method could achieve comparable halogen removal efficiency [34]. In another study, under microwave-induced rapid heating, more than 50 wt% of the brominated flame retardants in WPCBs were converted into HBr, which was captured by an overhead layer of $CaCO_3$. This resulted in pyrolysis oils with bromine levels below 5 wt% [35].

Alkali-based additives can also be used to remove halogens from gas and liquid products [4]. Shen et al. pre-treated non-metallic PCB waste with alkali before pyrolysis and successfully fixed 54% of HBr as solid NaBr in the char [36]. Zhang et al. expanded on this method by adding K_2CO_3, Na_2CO_3, or NaOH directly to the reactor. These additives reached bromine fixation efficiencies of up to 99.80%, 96.39%, and 86.69%, respectively [21]. NaOH solution has also been employed in different studies to scrub HBr from pyrolytic gas [15]**.** In addition, certain metal oxides display strong scavenging behaviour. Al_2O_3, ZnO, Fe_2O_3, La_2O_3, CaO, and CuO all suppress HBr formation and other brominated volatiles when co-fed with WPCBs [37].

Catalytic cracking also aids debromination. Zeolite-based catalysts such as ZSM-5 and YZ efficiently cleave organobromine species during pyrolysis [10], [38]. Chinnathan Areeprasert and Chanoknunt Khaobang reported that using ZSM-5, YZ, biochar, or Fe-rich electronic-waste char reduced the bromine content of ABS/PC pyrolysis oil from approximately 2 wt% to 0.39–0.85 wt% [27].

Complementary pre-treatment steps have also been explored to enhance dehalogenation. Evangelopoulos et al. investigated solvent leaching of e-waste plastics with toluene, derived from pyrolysis oil, and isopropanol.[6] However, bromine removal remained limited under the tested conditions, suggesting that a combination of pre-treatment and in-situ capture may be required. Pre-treatment methods typically include solvent extraction methods such as Soxhlet extraction, and more rapid methods such as supercritical fluid extraction, pressurized liquid extraction, ultrasonic-assisted extraction, and microwave-assisted extraction, which may use less solvent [9], [39], [40].

The current study is based on the process developed by GreeNovel, which conducts dehalogenation in two stages of the process to ensure thorough treatment. The process begins with the pretreatment of washed and shredded waste materials, followed by gas purification using a patented dehalogenation agent. This method effectively reduces the levels of HF, HCl, and HBr in the gas to below 0.74 ppm, 0.36 ppm, and 0.15 ppm, respectively [41].

2.2.4. Pyrolytic oil properties: Influence of operating conditions

The yield and quality of pyrolysis products are influenced by the feedstock and process parameters, including temperature, pressure, reactor type, residence time, and catalyst use. When optimized, these parameters can increase the yield of valuable light oil fractions and promote the formation of monoaromatics, enhancing the fuel and feedstock value of the liquid product [12], [18], [42].

The type of plastic feedstock determines the composition of the oil. Styrene-based plastics, such as polystyrene (PS), produce oils rich in valuable monoaromatic compounds like styrene, ethylbenzene, toluene, and α-methylstyrene [9]. Microwave-assisted pyrolysis of PS has been shown to produce up to 92.7% single-ring aromatics with boiling points below 200 °C [22]. In contrast, pyrolysis of e-waste, particularly waste circuit boards (WCBs) and printed circuit boards (PCBs), tends to result in oils with a lower content of light fractions. WCB pyrolysis oil has been reported to contain 9.66% non-ring compounds, 38.97% single-ring aromatics, and 6.07% chlorinated species [24]. When oxygenated polymers such as PET, PC, PLA, or PMMA are present, phenols and other oxygen-containing compounds appear in the oil [9], [10], [28], [38].

Temperature governs the extent of polymer chain degradation during pyrolysis [43]. Many researchers have attempted to optimize temperature and reactor design for specific qualities in oil. Park et al. targeted higher BTEX yields and lower styrene formation by coupling an auger reactor with a fluidized-bed reactor in a continuous two-stage setup. At 780 °C, using recycled pyrolysis gas as the fluidizing medium, they achieved a maximum BTEX yield of 26.3%. The resulting oil exceeded 40 MJ kg^{-1} in calorific value and met diesel and gasoline standards for density, viscosity, and flash point, although its aromatic-hydrocarbon content remained above regulatory limits [42].

Some studies aimed to maximise styrene recovery. Artexte et al. improved styrene monomer recovery by modifying the temperature and nitrogen flow rate during flash pyrolysis in a conical spouted bed reactor [44]. Hassibi et al. increased the styrene content from 59.3% to 81.2% by integrating a reflux reactor operating at 200 °C. Notably, this adjustment lowered the pyrolysis temperature to 480°C, compared to the conventional 600°C [26]. Zayoud et al. lowered the optimum temperature for maximum styrene yield (55.9%) from 600 to 550 °C by operating at a vacuum pressure of 0.02 bar, thereby reducing pyrolysis energy consumption [45].

Catalytic pyrolysis can promote desired reactions while reducing the required temperature and reaction time. Muhammad et al. demonstrated that ZSM-5 and Y zeolites increased concentrations of aromatic compounds such as benzene, toluene, and ethylbenzene. However, this also resulted in a decrease in styrene content and overall liquid yield [46]. Terapalli et al. reported that a plastic-to-KOH ratio of 27.5 g to 7.5 g in microwave-assisted pyrolysis of polystyrene produced a 95 wt per cent oil yield. The presence of KOH favoured saturated hydrocarbons, which improved heating value and lowered viscosity and flash point [47]. Despite these improvements, catalysts introduce challenges that include toxicity, high costs, coke deposition, and the need for regeneration.

Removing catalysts from char is difficult, and carbon deposition on active sites progressively reduces catalytic performance [9], [29], [48].

2.3. Upgrading oil quality

When targeting oil quality improvement, most studies have focused on reducing halogenated compounds due to their environmental and processing concerns. Besides heteroatoms, another challenge for fuel use is the high olefin content and unsaturated compounds in the oil. These molecules promote corrosion and thermal-oxidative instability, leading to gum and coke formation from secondary reactions during storage and processing [19], [42], [49]. For instance, auto-polymerization of polystyrene oil can occur and form unwanted styrene dimers, trimers, or high molecular components even at moderate storage temperatures near 50 °C [42]. To mitigate these effects, a hydrotreatment process that requires substantial energy is often required to transform olefins into more stable paraffins and align the product composition with conventional diesel and naphtha products [49].

Kusenberg et al. assessed the suitability of pyrolysis oil as a feedstock for steam cracking and to achieve closed-loop plastic recycling. They reported that after hydrocracking, these oils could achieve ethylene yields exceeding those of fossil naphtha. However, its heteroatom and metal content, such as nitrogen, chlorine, and iron, contribute to fouling, catalyst deactivation, and equipment corrosion, particularly in steam crackers and separation units. Even after hydrocracking, the oils remain outside the specification limit for olefin, oxygenate, and aromatic content. Substantial upgrading is needed, such as hydrotreatment, fractionation, and desulfurization, before sending the feedstock to the steam cracker [50].

A range of upgrading processes needs to be adopted to address the disparity in quality between pyrolysis oil and traditional fossil feedstocks. These include hydrotreatment, fractionation, filtration, desulfurization, distillation, and dewatering [18], [50] These post-treatment strategies are crucial for stabilizing the oil, removing impurities, and tailoring its composition for downstream applications such as steam cracking in fuel or petrochemical production.

2.3.1. Fractionation

Fractional distillation is widely used to upgrade pyrolysis oil by separating it into narrower hydrocarbon cuts while also removing undesirable contaminants from the desired fractions. The upgraded product aligns more closely with specific applications or conventional refinery streams. Pyrolytic oil can be separated into gasoline, diesel, and heavy oil fractions for fuel recovery through distillaton, allowing for fuel recovery [51]. Gurram et al. simulated a distillation process that separates pyrolysis oil into commercially viable fractions, such as gasoline (C6–C10), naphtha (C7–C12), kerosene (C9–C14), and diesel (C12–C21) [52].

In practice, Zeb et al. reported that light and middle fractions obtained from polypropylene (PP) and mixed plastic oil (MPO) pyrolysis have densities and viscosities close to fossil naphtha and

diesel, yet their total acid numbers remain noticeably higher, above 0.5 mg KOH g^{-1}. The light PP and MPO cuts are rich in olefins (> 48 %). Fractional distillation eliminated more than 97.5% of metal contaminants, confirming its value for downstream processing [53].

Jahirul et al. applied vacuum distillation to pyrolysis oil obtained from a mixture of HDPE, PP, and PS. They collected gasoline below 170 °C, diesel between 170 and 380 °C, and a residue above 380 °C. Notably, distillation improved the calorific value, kinematic viscosity, and density of the diesel cut compared to the pyrolysis oil for engine fuel applications. The study also showed that increasing the proportion of HDPE in the feedstock resulted in increased both the cetane index and polyaromatic content in the diesel fraction, highlighting the influence of feedstock composition on product quality [54]. In the study by Lee 2021, about 70–80 wt% of the feed was collected in a diesel-like fraction with a heating value of 43–45 MJ kg^{1} and a viscosity of 1–6 cSt. This stream still exhibited a high total acid number lower than 42 mg KOH g^{-1}, likely from chlorinates and oxygenates, so hydrotreating and de-chlorination were deemed essential follow-up steps [17].

Column design and operating variables were also explored. Krywzyda and Wrzesińska distilled pyrolysis oil derived from PET and PVC into four fractions, targeting the removal of waxes and light hydrocarbons so that the heavy cut that had a flash point lower than 56 °C was required for heating oil. They showed that increasing the reflux ratio increased the yield of the heavy fraction, and adding trays enhanced the separation between components with close boiling points, until about ten theoretical stages, while column costs continued to rise [18]. Gurram et al. also investigated the effects of distillation parameters, including feed temperature and tray geometry and efficiency, on product yield and composition [52].

Zeb et al. modeled the atmospheric distillation of pyrolysis oils from polypropylene (PP) and high-density polyethylene (HDPE) in a 25-stage tower. The goal was to run a batch distillation to isolate narrow, high-purity hydrocarbon cuts. They measured bulk properties and boiling point distribution using ASTM D86 and D2887 boiling curves, verified a batch-distillation model in Aspen Plus based on these curves, and finally, scaled up the validated model to a continuous refinery tower [49].

The validated model produced typical refinery streams, including off-gas, light and heavy naphtha, kerosene, and gasoil, as well as two valuable fractions. For PP oil, a 121-151 °C cut rich in C9 iso-olefins used as a precursor of plasticizers reached 66 wt% purity (other PP cuts held 46–64 wt% of C12, C15, and C18 iso-olefins). For HDPE oil, a 230-290 °C cut contained C13–C16 α-olefins used in detergents. Continuous simulations demonstrated that drawing the C9 iso-olefin through a side stream outperformed a separate column with the same tray count, resulting in a higher yield. Thus, a side draw is advised when maximizing yield is the priority, while a dedicated column is suited for operations that value higher purity and process flexibility [49].

Distillation upgrades plastic pyrolysis oils by narrowing their boiling ranges and reducing metal content, producing gasoline, kerosene, and diesel cuts with properties closer to refinery standards. However, the resulting fractions still contain excessive olefins, aromatics, acids, and halogens. As

a result, these streams cannot yet be fed directly into refinery units or used as fuel and chemical feedstocks.

2.3.2. Monomer recovery

Early research on the chemical recycling of waste electrical and electronic equipment focused on fuel production. More recent work shows that higher economic and environmental value can be obtained by recovering monocyclic aromatics and monomers. Converting the plastic fraction of WEEE into chemicals such as styrene increases product value, lowers climate impact, and reduces the demand for fossil resources. Downstream processes like distillation can be used to recover these valuable compounds, supporting a circular economy by reducing waste disposal and decreasing reliance on virgin plastic and materials [19], [55], [56].

Techno-economic analysis proves the feasibility of the chemical route. Garcida-Alvarez et al. modeled a multiproduct refinery that upgrades HDPE pyrolysis oil into chemical-grade ethylene at 97.2% purity, propylene at 97.8% purity, and two hydrotreated streams, suitable for diesel and gasoline blending based on their molecular weight. For a plant treating 500 tonnes of plastic waste daily, the net present value reached 383 million USD, indicating economic viability. Heat integration lowered overall energy demand by 60% through the use of a methane purge stream and low-pressure steam recovery from the exothermic hydrotreatment section. Sensitivity analysis indicated that feedstock prices above 460 USD per tonne could threaten viability, but the facility remained profitable even under the highest projected increase in U.S. electricity costs [57].

Experimental work confirms the potential and challenges of monomer recovery. Rieger et al. studied the batch distillation of oil generated by the patented pyrolysis process, which focuses on metal recovery and is profitable at feed rates above 250 kg h^{-1}. Distillation produced seven fractions. The first was enriched with 88% benzene, a toluene cut at 96%, a mixed BTEX/styrene fraction, a styrene-rich fraction at 80%, and a cut dominated by phenol 35% along with naphthalene and other compounds. The operation eliminated 99 % of the halogens, however, none of the fractions reached chemical purity [55].

Extracting pure monomer streams remains difficult because many target compounds have similar boiling points and can form azeotropes, such as styrene, ethylbenzene, and alpha-methylstyrene. Obtaining high-purity styrene would require a substantial amount of energy and a large number of theoretical plates. Operating under vacuum shifts the azeotropic composition in favor of styrene, and at approximately 0.41 bar, the azeotrope disappears [58].

Another challenge is that at high operating temperatures, there is also a risk of styrene repolymerisation. Vacuum operation and polymerisation inhibitors such as dinitro-sec-butyl-phenol and p-tert-butylcatechol are often required to avoid secondary reactions [58], [59]. Liu et al. ran a continuous rectification column with 60 plates at 80 mmHg (≈0.11 bar) and dosed the distillate with the inhibitor 2,4-dinitrophenol (NSI). They obtained styrene at 99.6% purity [59].

Holtkamp et al. achieved comparable results under vacuum by adding p-tert-butylcatechol [60]. However, in this study, repolymerization of styrene has been ignored.

Many studies ran the experimental operation and built a simulation accordingly. Dahal et al. ran a 24-stage batch column at 99 mbar, keeping the bottoms between 100°C and 120°C to avoid polymerization. The bottoms were further distilled in a short-path distillation unit without reflux to isolate styrene. Data from the batch runs were used to simulate a batch model that was later scaled to a 50-stage continuous column at 50 mbar. In this configuration, styrene was withdrawn as a side stream at stage 10 with 99.6% purity, while leaving a small styrene fraction in the bottoms, which helped maintain a low temperature and prevent polymerization [61].

Recent studies have focused on more efficient distillation schemes for isolating styrene and related aromatics from plastic pyrolysis oils. Kim et al. compared several separation sequences for a feed that contained 7.0% toluene, 17.2% EB, 59.8% SM, and 12.5% AMS. The direct-indirect sequence, which first separated the light and heavy ends, and then split EB from SM, had the lowest overall column duty. Converting this train into a four-section dividing-wall column (DWC) cut utility demand by about 40%. They showed that for higher capacities, the dividing-wall design offers the best cost savings on energy. Although it might not be economical for smaller capacities because of higher initial costs related to the column's large height and diameter, its benefits become evident as capacity grows [58].

Merkel et al. designed a styrene recycling plant producing 2452 kg of styrene hourly at 99.6% purity, which could be integrated into the polystyrene production industry. They compared several separation sequences, including a three-column sloppy distillation in which styrene is drawn from the second column bottom and the third column top. Their evaluation showed that merging the second and third columns into a single unit and withdrawing styrene as a side stream lowered the overall energy use more than any other option [62].

Holtkamp et al. complemented the work of Merkel et al and proposed a robust downstream process that produces styrene at 99.6% purity from PS pyrolysis oil. They demonstrated that high levels of o-xylene, which has a boiling point similar to styrene, hinder the straightforward purification of styrene, so the authors recommended an extractive step with dialkylformamide as an option when dealing with high concentrations of o-xylene. Since real waste streams vary in composition and often contain limited polystyrene, the authors recommended identifying critical by-products in the feed and implementing alternative steps when needed. As styrene content decreases, the process requires either additional distillation columns or higher reflux ratios [60].

They also carried out a sensitivity analysis on feed composition, distillate-to-feed ratio, reflux ratio, and side-stream mass flow rate. Although the study focused on recovering and recycling styrene, the authors also considered purifying toluene and ethylbenzene. Since this purification would require installing additional distillation columns, they suggested combusting the combined toluene and ethylbenzene stream to produce energy instead [60].

Purifying styrene and related monomers from plastic pyrolysis oils is challenging due to overlapping boiling points, azeotrope formation, and high-temperature polymerization. Research indicates that carefully choosing distillation sequences combined with advanced column designs, such as side draws and dividing-wall shells, can lower energy consumption while producing styrene. Decisions regarding the further separation of by-products, such as toluene and ethylbenzene, should be based on economic benefits and environmental impact.

Most distillation studies remain at the laboratory scale, and only a few address detailed modeling or process scale-up. Continuous column models offer valuable insights, but they assume consistent feed quality and flow, conditions that are rarely met with waste streams. In practice, the composition and amount of waste plastic oils vary widely, making the flexibility of downstream processes essential. Batch columns allow for pressure and temperature adjustments for each charge and simplify the removal of tars and resins after each run [63], [64]. As a result, further exploration of batch distillation modelling could be valuable for e-waste pyrolysis oil treatment.

2.4. Environmental impacts of e-waste plastic recycling processes

Life cycle assessment of e-waste recycling processes has largely focused on metal recovery, due to its higher economic value, often neglecting the treatment of non-metallic components [13]. For instance, Ismail and Hanafiah reported that direct incineration of e-waste for energy produced lower environmental impacts than scenarios centered on metal recovery in which the plastic fraction was landfilled. However, their result may be sensitive to assumptions because the incineration case excluded the treatment of residue, and the energy recovery was calculated using an assumed average heating value of 9.97 MJ/kg for printed wire boards [65]. These assumptions may have given an advantage to the incineration route in the environmental analysis.

A few research works have begun to include the valorisation of the plastic fraction. Holtkamp et al. showed through a prospective LCA that the environmental impact of recycling PS waste depends strongly on feed composition [60]. However, regardless of its composition or by-product valorization routes, its global warming impact remains lower than that of incineration with energy recovery [60]. In contrast, Dong et al. found that incineration has a lower Global warming potential (GWP), while pyrolysis exhibited smaller impacts in terrestrial eutrophication, photochemical ozone formation, human health, and airborne human toxicity. They attributed pyrolysis's higher GWP to the emissions from the combustion of char and tar for electricity production, as well as to the process's endothermicity and the need for external energy for waste pretreatment [5]. Alston and Arnold also associated incineration with a higher climate change impact. However, the results shifted with the carbon intensity of the displaced electricity. They observed that incineration reduces the solid volume by 90 to 99%, reducing the carbon deposit impact to 14% compared to pyrolysis [9], [66].

Recovering valuable products from pyrolysis oil can improve the environmental performance of the process. Gracida et al. performed a life cycle carbon footprint analysis of a refinery upgrading HDPE pyrolysis oil, reporting emissions of 1.08, 1.10, and 1.16 kg CO_2-eq per kg of ethylene,

propylene, and aromatics, respectively, using average U.S. grid electricity. In some states, emissions could be comparable to or even lower than those from fossil-based routes, with potential reductions exceeding 25%. The monomer separation unit dominated emissions due to high electricity use [56].

Schulte et al. evaluated the climate-change impacts of several e-waste-plastic recycling pathways in Germany, using an economic-based functional unit of 1€ of marketable output. Conventional waste-to-energy incineration served as the reference system, at 7.8 kg CO_2-eq €$^{-1}$. The patented process under study pyrolyzes mixed wire and PCB residues in an auger reactor, yielding metal-rich char, oil, and gas. When the reactor is heated with electricity from the German grid, the global-warming potential is 4.5 kg CO_2-eq €$^{-1}$, and combusting the process gas to provide for the process heating demand lowers this to 3.6 kg CO_2-eq €$^{-1}$. The study also modelled four downstream distillation configurations that recover benzene, toluene, ethylbenzene, and styrene from the oil. The arrangement that isolates styrene alongside a benzene–toluene–ethylbenzene (BTE-S) blend achieved the best result at 2.0 kg CO_2-eq €$^{-1}$. This represents a 74% reduction relative to the incineration route, suggesting pyrolysis offers a clear climate advantage over incineration for treating e-waste plastics, particularly when aromatic recovery is included [67].

The inconsistent results of the LCA indicate that it is crucial to evaluate all aspects when interpreting LCA studies, as each one varies in process-related parameters such as feedstock compositions, energy sources, or LCA study elements such as impact assessment or allocation methods, and chosen system boundaries. Therefore, consistent and transparent assumptions are essential when evaluating recycling options for e-waste plastics.

2.5. Conclusion

Current research confirms that pyrolysis, supported by thorough dehalogenation, is a viable route for treating the plastic fraction of e-waste and recovering chemicals beyond the metal content. Removing halogens is important through pretreatment, during pyrolysis, or post-treatment to ensure that toxic emissions are eliminated and that the products meet fuel and chemical standards. Upgrading methods such as hydrotreatment and fractionation might improve the product; however, the high olefin content of pyrolysis oil from plastics hinders its direct use in refineries and steam crackers.

The literature generally favors targeting monomers and aromatics rather than producing fuels, since chemical recovery offers higher economic returns, reduces environmental impacts, and supports a circular economy compared to waste-to-energy incineration routes. Although existing LCA assessments are limited and often inconsistent, they suggest that combining pyrolysis with chemical separation can outperform conventional treatment options. Very few works, however, have examined the design, simulation and scaling-up of the pyrolytic oil separation, particularly with batch distillation. Batch distillation provides the flexibility needed to handle variations in feed quality and availability, and simulations can assist with scale-up and energy integration, facilitating the commercial adoption of pyrolysis and downstream processes. As a result, this study focuses on

the design and analysis of the distillation of pyrolysis oil from e-waste plastics and on the recovery of chemicals through continuous and semi-continuous routes via batch distillation. Additionally, the LCA and TEA are included to evaluate the proposed treatment route.

3. Process description

This work focuses on the distillation of pyrolysis oil derived from microwave-assisted pyrolysis of plastic waste. The process is simulated to assess the feasibility of chemical recovery and upgrading. The proposed route is evaluated against incineration, the conventional treatment method for such waste. Continuous distillation is introduced as an alternative approach that enables the recovery of value-added chemicals. This section presents a description of the process and outlines the main assumptions. In all scenarios, the facility is assumed to process 25 tonnes of e-waste plastic daily.

3.1. Incineration

Incineration is a common treatment technique for e-waste and is used as the baseline scenario for comparison in this study. The simulated incineration process is shown in Figure 1. The plastic fraction is introduced into the simulation based on ultimate and proximate analysis data available in the literature [68], which are reported in Table 1.

The ash content of the e-waste is assumed to be zero. Ash represents the non-organic, non-combustible fraction, which primarily includes metals. Since the metal fraction is already separated, the solid is assumed to be free of ash.

Table 1. Feedstock composition from Krishna et al.[68]

Ultimate Analysis %				
C	**H**	**N**	**S**	**O**
37.8	4.2	1.8	0	32
49.9	5.5	2.4	0	42.2
Proximate Analysis %				
		Volatile matter	**Fixed Carbon**	**Ash**
From the reference		61.8	14	24.2
Used in this work		81.5	18.5	0

In this scenario, it is assumed that the metal content of the waste has already been recovered, and the remaining plastic residue is combusted for energy recovery. The resulting flue gas is used to generate low-pressure steam and is then released into the atmosphere. The composition of the flue gas is reported in Table 3.

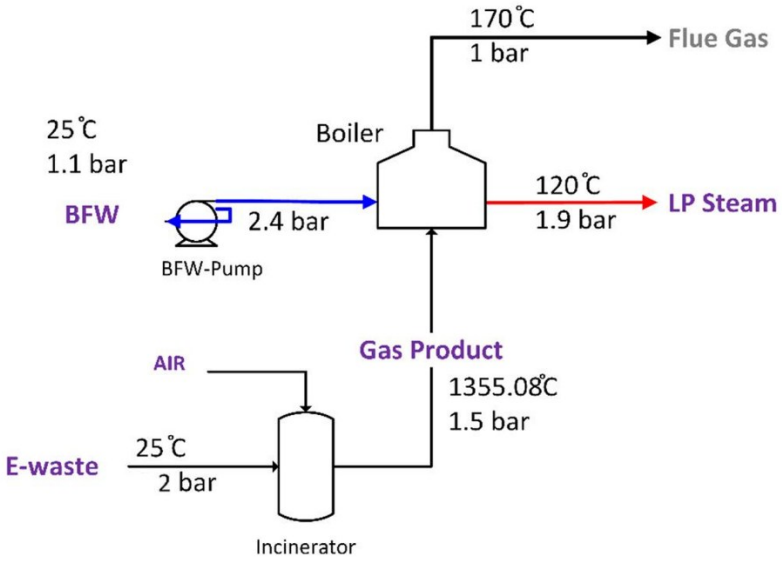

Figure 1. Process flow diagram of the incineration process

Table 2. LP steam properties from the incineration process

Property	Value
LP steam flow rate, tonne/day	90.37
Temperature, C	120
Pressure, bar	1.9

Table 3. Flue gas composition from the incineration processing route, referring to treating 25 tonnes of e-waste plastic

Compound	Quantity (tonne)
H_2O	11.23
N_2	104.89
O_2	1.14
NO_2	7.41×10^{-5}
NO	6.29×10^{-2}
CO	7.54×10^{-3}
CO_2	41.43
HBr	9.96×10^{-3}
Br_2	3.50×10^{-3}
HCl	2.86×10^{-3}
Cl_2	1.04×10^{-6}
Total	**158.69**

3.2. MW-assisted pyrolysis and oil upgrading

This section describes the alternative treatment route involving microwave-assisted pyrolysis followed by oil upgrading. The focus of the current study is on the downstream processing of the oil produced at the GreeNovel facility. A brief overview of the pyrolysis process is provided for context below.

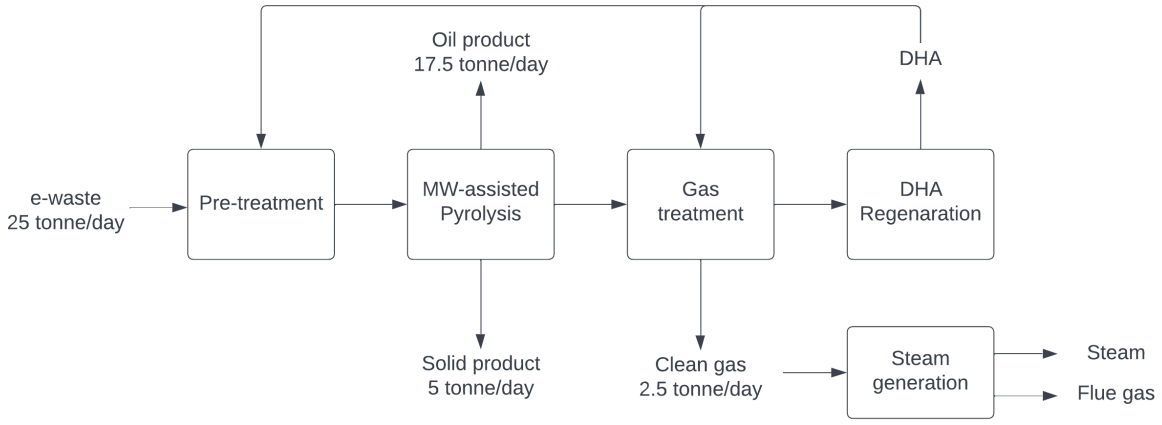

Figure 2. Block flow diagram of the base pyrolysis scenario with gas recovery

The plastic fraction of e-waste is initially washed, shredded, and treated with a dehalogenation agent (DHA) during the pretreatment stage to reduce the halogen content. The pre-treated feed is then introduced into a continuous pyrolysis reactor, heated by microwave energy. The pyrolysis process yields three product streams: a non-condensable gas (10%), solid char (20%), and liquid oil (70%).

The gas product undergoes an additional dehalogenation step with DHA to ensure the removal of residual halogen content. The cleaned gas composition is presented in Table 4. In the patented process, the DHA is regenerated and recycled for reuse in the pretreatment and gas cleaning stage [41].

Due to the presence of hydrocarbons such as methane, the pyrolytic gas has a heating value of 4.06 MJ per kilogram. This gas is combusted to recover energy and produce steam. The composition of the flue gas resulting from the combustion is provided in Table 5, after which it is released into the atmosphere.

Table 4. Cleaned gas used in the gas recovery unit in the MW-assisted pyrolysis route

Compound	Mass flow, kg/hr
CH_4	5
CO_2	76.67
CO	17.08
O_2	5.42
Total	**104.17**

Table 5. Flue gas composition from the gas recovery unit in the MW-assisted pyrolysis processing route, referring to treating 25 tonnes of e-waste plastic

Compound	Quantity (tonne)
H_2O	2.69×10^{-1}
N_2	4.03
O_2	0.64
NO_2	2.48×10^{-5}
NO	3.55×10^{-3}
N_2O	2.78×10^{-7}
CO_2	2.81
Total	**7.76**

The char stream represents 20% of the total pyrolysis output. Since the feedstock is pretreated to recover the metal fraction, and halogen content is largely reduced during pretreatment and gas cleaning, the char is predominantly carbonaceous in nature.

The oil stream accounts for the majority of the process's total output. Its composition was analyzed using GC/MS, which identified more than 100 compounds. The principal compounds, with mass fractions above 1%, are listed in Table 6. The remaining components are listed in Table A1 in the appendix.

Table 6. Pyrolytic oil composition, including components with a mass fraction above 1%

Component	Mass fraction
Styrene	21.9%
Ethylbenzene	14.0%
Bezenebutanenitrile	11.9%
Toluene	7.0%
Phenol	6.7%
1,1'-(1,3-Propanediyl)bisbenzene	6.6%
p-Cumenol	5.8%
Benzene, (1-methylethyl)-	3.2%
alpha-Methylstyrene	1.6%
2,4-Diphenyl-4-methyl-1-pentene	1.5%
Phenol, 4,4'-(1-methylethylidene)bis-	1.0%

3.3. Continuous distillation process

The continuous distillation simulations were performed using Aspen Plus V14.0. Several thermodynamic models have been applied in previous studies for pyrolytic oil, including UNIFAC [18], Peng–Robinson [30], [49], [52], [67], NRTL [69], and NRTL-RK [61]. In this work, the

UNIQUAC-RK method was selected because it combines an activity-coefficient model with an equation of state, giving more reliable VLE predictions for complex pyrolysis oils.

The oil composition was entered into the simulation platform as described in Table A1 in the appendix. For compounds not available in the Aspen database, their molecular structures were specified and parameters estimated. The pyrolytic oil was assumed to leave the upstream pyrolysis reactor at 500 °C. Before distillation, the stream was cooled, and the released heat was recovered for steam generation to partially supply process heating requirements.

REDFRAC column models were used to simulate the distillation sequence. For each column, boil-up and reflux ratios were defined through design specifications targeting specific purity or recovery levels. The lighter fraction was withdrawn from the column tops, while waxes and heavy compounds were collected from the bottom of the first column (T-100) as a by-product. This heavy fraction can be further processed or used as furnace fuel, although such applications are outside the scope of this study.

Columns T-101, T-102, T-103, and T-104 were dedicated to the recovery of the desired products. Pure toluene was recovered from the top of T-103, while ethylbenzene was withdrawn from its bottom. Column T-104 was designed for the binary separation of styrene and the remaining ethylbenzene. Due to the close boiling points of these compounds, this column required more equilibrium stages to achieve the desired purity. To improve separation and minimize styrene repolymerization, vacuum operation at 100 mbar was employed. Operating under vacuum reduced the required stage count from 70 at atmospheric pressure to 60, while keeping column temperatures below 110 °C, thereby preventing repolymerization.

The continuous simulation represents an idealized design, in which all major products are recovered at chemical-grade purity and recovery levels. In addition to the target products, toluene, ethylbenzene, and styrene, a small amount of phenol was also recovered. The system produced two additional streams: (i) a heavy oil and wax fraction, and (ii) a residual light oil stream with considerable heating value, which may be utilized as heating oil. The design specifications for each column are represented in Table 7, which allowed the recovery of each product with over 99% purity.

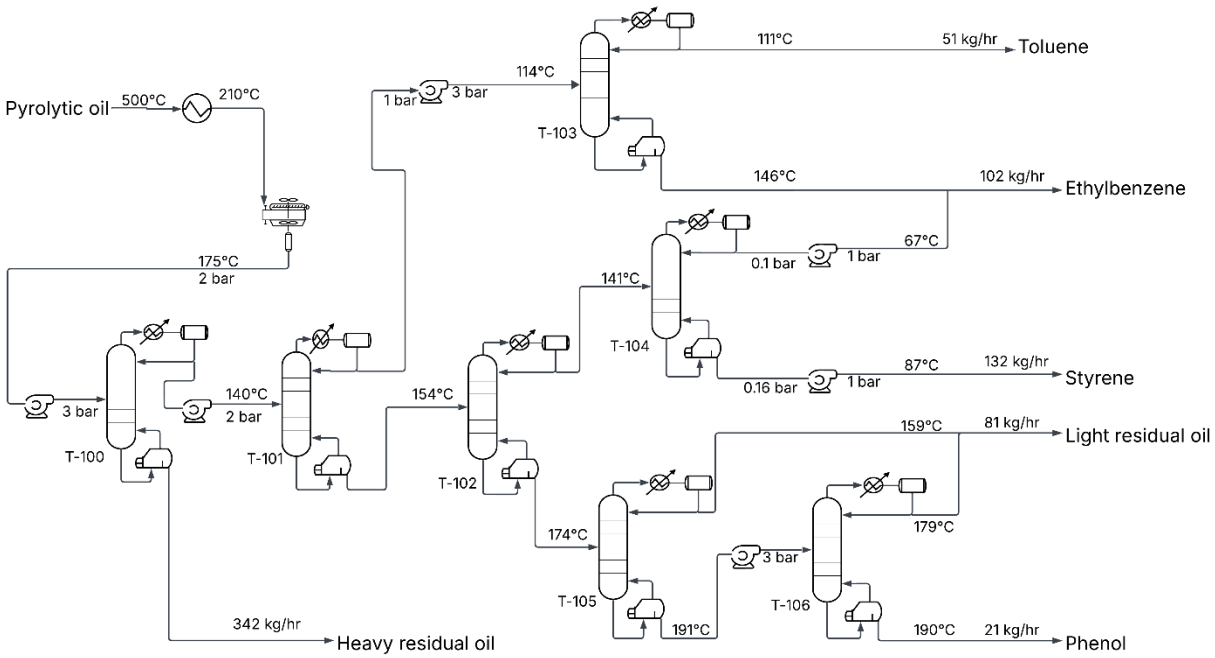

Figure 3. Process flow diagram of the continuous process

Table 7. Unit description in the continuous distillation process

Column ID	Column internal	Design spec Objective	Variable
T-100	Number of stages: 18 Type: Trayed / Sieve Total condenser Condenser pressure: 1.013 bar Feed stage: 8	Recovery of phenol from the top: 0.7 Recovery of heavier phenol (p-cresol) from the bottom: 0.997	Reflux ratio: 1.99 Boilup ratio: 2.94
T-101	Number of stages: 28 Type: Trayed / Sieve Total condenser Condenser pressure: 1.013 bar Feed stage: 15	Recovery of toluene from the top: 0.999 Recovery of styrene from the bottom: 0.999	Reflux ratio: 11.79 Boilup ratio: 2.63
T-102	Number of stages: 28 Type: Trayed / Sieve Total condenser Condenser pressure: 1.013 bar Feed stage: 15	Recovery of styrene from the top: 0.825 Recovery of isopropylbenzene and phenol from the bottom:0.999	Reflux ratio: 4.08 Boilup ratio: 11.02
T-103	Number of stages: 28 Type: Trayed / Sieve Total condenser Condenser pressure: 1.013 bar Feed stage: 15	Recovery of Toluene from the top: 0.9999 Purity of Toluene in the top: 0.998	Reflux ratio: 1.95 Boilup ratio: 14.52
T-104	Number of stages: 58 Type: Trayed / Sieve Total condenser Condenser pressure: 0.1 bar Feed stage: 30	Recovery of ethylbenzene from the top: 0.998 Recovery of Styrene from the bottom: 0.999	Reflux ratio: 21.06 Boilup ratio: 14.15
T-105	Number of stages: 28 Type: Trayed / Sieve Total condenser Condenser pressure: 1.013 bar Feed stage: 15	Recovery of alpha methyl styrene from the top: 0.99 Recovery of phenol from the bottom: 0.8	Reflux ratio: 2.74 Boilup ratio: 6.38
T-106	Number of stages: 24 Type: Trayed / Sieve Total condenser Condenser pressure: 1.013 bar Feed stage: 12	Purity of phenol in the bottom: 0.993 Recovery of phenol from the bottom: 0.75	Reflux ratio: 34.57 Boilup ratio: 14.00

3.4. Semi-continuous upgrading process

The composition and quantity of pyrolysis oil can vary significantly, making continuous distillation unsuitable for upgrading. In contrast, batch operation offers the flexibility needed for such systems. Each batch recipe can be tailored to the specific characteristics of the feed, ensuring control over the quality and purity of the final product.

The batch process was simulated in Aspen Plus V14 using the PR/BM property method and the BATCHSEP model for the column. The modeled batch distillation system consisted of a heated pot containing the oil, a rectifying column with 28 theoretical stages, a partial condenser, and multiple receivers to collect the separated products. Both atmospheric and vacuum operations are included to minimize repolymerization risk. The vacuum pressure is achieved by condensing the top-stage vapor product at a low temperature. Batch operation requires defining a sequence of operating steps in which process conditions are adjusted over time. Each step is stopped by a specified stop criterion or time limit.

3.4.1. Adjusting the reflux ratio

Unlike continuous distillation at steady state, where temperature and composition remain essentially constant, batch distillation is inherently dynamic. Under a constant reflux ratio, the removal of light compounds in the distillate causes the tray temperature to rise, and the compositions in the column and pot evolve over time. To maintain product purity, the reflux ratio must be adjusted. In this work, a controller manipulated the reflux ratio to maintain the top stage dew point setpoint on stage 2. The setpoint equals the saturation temperature of the light compound at the measured column top pressure. The partial condenser is defined as stage 1. The controller was a PI controller with a gain of 5 (would be adjusted later) and an integral time of 0.05 hr.

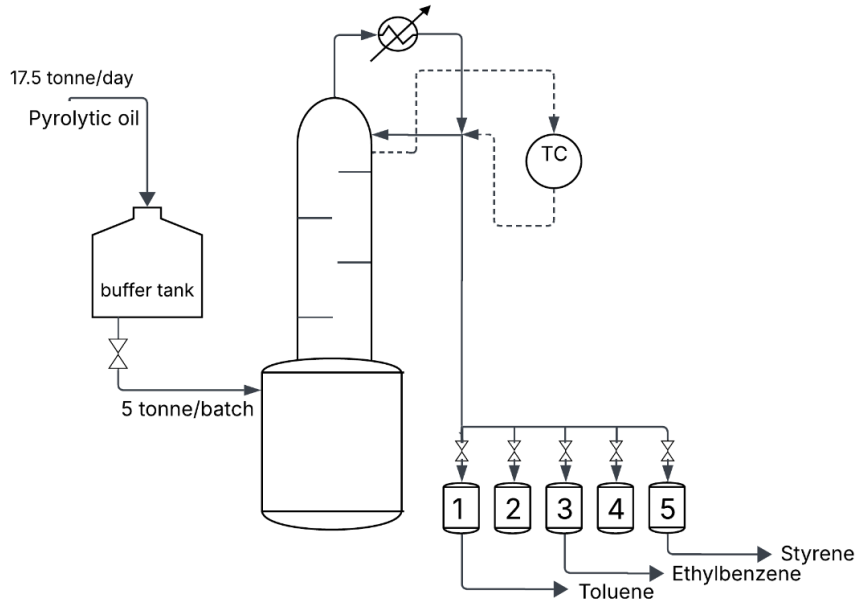

Figure 4. Diagram of the semi-continuous upgrading process with a controller adjusting the reflux ratio

3.4.2. Start-up step

The process began with a start-up step [63]. Initially, the column was assumed to be empty and filled only with nitrogen as pad gas. In the first operating step, the pot was charged with 5000 kg of oil over 15 minutes, with the feedstock composition reported in Table 8. Heating was then applied to bring the pot content to its bubble point. During this stage, the vent remained open to allow nitrogen to exit while vapor from the pot filled the column. Then, the column was operated at total reflux until a steady state was reached. This meant that no distillate was withdrawn, and all condensed overhead was returned as reflux. Operation under total reflux continued until the top vapor mass fraction of toluene reached 0.9995-0.9999. The time and energy requirements for this start-up step were recorded for both atmospheric and vacuum operations. The results are reported in Table 9.

To address convergence difficulties in the initialization step, this stage was simulated in a separate file from the main batch operation. In the main simulation, which included the subsequent steps, the initial condition was specified as total reflux. That means that the column was assumed to have already reached steady-state, and the batch operation was initiated directly from that point. The time and heating requirement of the start-up phase were then added to the results from the subsequent steps.

Table 8. Feed composition in the semi-continuous process simulation

Compound	**Mass fraction %**
Styrene	24.65%
Etylbenzene	15.77%
Toluene	7.86%
Phenol	7.54%
Phenol,-P-Isopropyl-	6.58%
1,3-Diphenylpropane	7.39%
Isopropylbenzene	3.66%
Alpha-Methyl-Styrene	1.84%
1,1-Diphenylethanol	1.72%
Bisphenol-A	1.14%
2,4-Diphenyl-4-Methylpentene-1	1.74%
P-Cumylphenol	0.95%
N-Ethylaniline	0.77%
Butane,-1,3-Diphenyl-	0.73%
1-Naphthalenecarbonitrile	0.65%
Benzenebutanenitrile	13.35%
3-Phenyl-2-pentenenitrile	1.05%
5H-Indeno[1,2-b]pyridine	0.74%
Benzene, (1,3-dimethyl-3-butenyl)-	0.99%
Benzene, 1,1'-(3-methyl-1-propene-1,3-diyl)bis-	0.88%

Table 9. The time and energy requirements of the start-up step of cases with different operating pressures

Batch process	Condenser pressure (bar)	Condenser temperature (°C)	Time (hr)	Duty (cal)
Atmospheric	1.01325	50	4.9	1.23×10^{9}
Vacuum	0.1	30	4.7	4.81×10^{8}

3.4.3. Product recovery

The next operating step was focused on recovering toluene, the lightest target product. A distillate receiver was connected, the reflux controller set point was chosen as the saturation temperature of toluene at column pressure, and the reflux ratio was adjusted automatically to maintain this overhead temperature. This step was stopped once toluene purity in the distillate receiver dropped below 99.9 percent or when the concentration of the subsequent compound exceeded 0.1 percent. A new receiver was then connected, and the controller set point was adjusted to the saturation temperature of ethylbenzene. The same procedure was repeated in the following step for styrene recovery. After styrene was collected, the batch operation was terminated, as only these three main compounds were targeted in this work.

3.4.4. Adjusting the heating rate (BATCH-A and BATCH-B)

The pot heating rate also needed to be specified. Using a constant heating for the entire batch would either be too low, leading to excessively long batch times, or too high, which would reduce separation efficiency and product recovery. Therefore, two heating policies were specified.

In the first case, “BATCH-A”, the pot heating rate was specified manually for each operating step, but kept constant within that step (x_i). The heating rates for each step were treated as decision variables and varied across different scenarios to identify more optimal operating conditions. The operating steps of this design are described in

Table 10. r_i was the pot heating rate in each step, which was adjusted in each scenario.

In the second case, “BATCH-B”, the pot heating rate was adjusted dynamically by a temperature controller. The controlled variable (set point) was the liquid temperature at the bottom of the column (stage 29), and the manipulated variable was the pot heating rate. The controller was a PI controller with a gain of 5 (would be adjusted later) and an integral time of 0.05 hr. At the beginning of each operating step, the set point was updated according to the target conditions for that step and

Table 11.

Table 10. Batch operating steps in the case of BATCH-A and vacuum operation with a constant duty rate at each step

Operating Step (i)	Setpoint of the reflux controller (°C)	Heating duty (r_i) (GJ/hr)	Receiver	Stop criterion
1	45	r_1	1	Ethylbenzene in receiver ≤ 0.01
2	45	r_2	2	Toluene in pot ≤ 0.0001
3	67	r_3	3	Styrene in receiver ≤ 0.01
4	67	r_4	4	Ethylbenzene in pot ≤ 0.001
5	75	r_5	5	Isopropylbenzene in receiver ≤ 0.01 or pot temperature ≤ 110 °C

Table 11. Batch operating steps in case BATCH-B and vacuum operation with two controllers

Operating step	Setpoint of the reflux controller (°C)	Setpoint of heating controller (°C)	Receiver	Stop criterion
1	45	82	1	Ethylbenzene in receiver ≤ 0.01
2	45	82	2	Toluene in pot ≤ 0.0001
3	67	87	3	Styrene in receiver ≤ 0.01
4	67	87	4	Ethylbenzene in pot ≤ 0.001
5	75	92	5	Isopropylbenzene in receiver ≤ 0.01 or pot temperature ≤ 110 °C

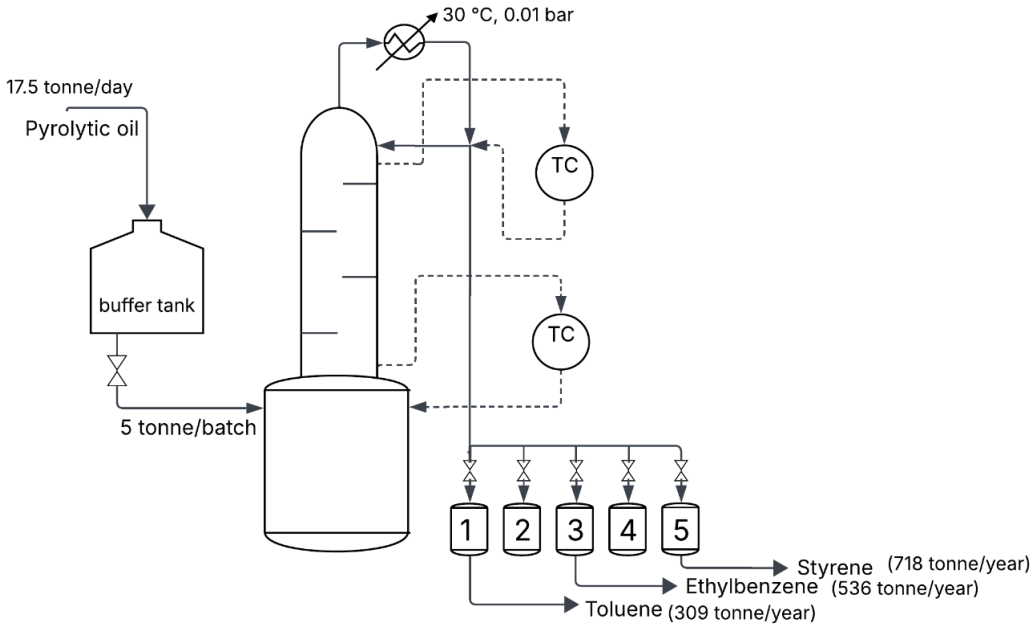

Figure 5. Diagram of the case with two controllers (BATCH-B), output data refers to one example scenario

3.4.5. Range of the manipulated variables

The upper limit for the heating rate (manipulated variable of the Pot controller) was set to 5 GJ/hr or approximately 1389 kW. This value was to be of the same order of magnitude as the highest reboiler duty in the continuous process, corresponding to the reboiler of column T-104. The reflux ratio was limited to 100, as excessively high ratios would prolong batch duration, slow distillate recovery, and increase computational time per simulation.

For each case, several scenarios were simulated, as described in Table 12 and Table 13. The recovered products and the accumulated pot duty were recorded for each batch scenario. Revenue and electricity costs were then calculated, and the scenarios were evaluated based on annual profit, defined as yearly revenue minus electricity cost. Regression analysis was applied to fit the parameters to a model equation, thereby allowing the identification of optimal scenarios for each case. The detailed results of the optimal scenarios are presented in the Results and Discussion section of this work.

Table 12. Table of adjusted process variables and their ranges in the BATCH-A scenarios with a specified constant heating rate for each operating step

Type	**Variable**	
Reflux controller	Maximum controller output (reflux ratio)	$50 \leq opmax_1 \leq 100$
	Controller gain	$1 \leq k_1 \leq 5$
Heating rate (GJ/hr)	Step 1	$1 \leq r_1 \leq 5$
	Step 2	$1 \leq r_2 \leq 5$
	Step 3	$1 \leq r_3 \leq 5$
	Step 4	$1 \leq r_4 \leq 5$
	Step 5	$1 \leq r_5 \leq 5$

Table 13. Table of adjusted process variables and their ranges in the BATCH-B scenarios with heating rate and reflux controllers

Type	**Variable**	
Reflux controller	Maximum controller output (reflux ratio)	$50 \leq opmax_1 \leq 100$
	Controller gain	$1 \leq k_1 \leq 5$
Heating rate controller	Maximum controller output (heating rate) in GJ/hr	$1 \leq opmax_2 \leq 5$
	Controller gain	$1 \leq k_2 \leq 5$

4. Results and Discussion

This section presents the results of the study in detail, beginning with the continuous chemical extraction process. The simulation products are described, and the feasibility of the process is evaluated through a technoeconomic analysis. Subsequently, the environmental performance is examined using life cycle analysis, with detailed assumptions provided. Finally, the results of the semi-continuous pyrolysis treatment are reported, and its cost is evaluated.

4.1. Continuous Process: Simulation Results

The recovered products of the continuous process are shown in Table 14. As indicated, using seven distillation columns (see Figure 3), more than 80% of toluene, ethylbenzene, and styrene were recovered with purities above 99%. Phenol had the lowest recovery rate, which raised questions about the feasibility of adding additional columns for its recovery. The extraction process is energy-intensive because of the significant reboiler duties of multiple distillation columns, listed in Table 15. Column T-104, which performs the vacuum separation of ethylbenzene and styrene, had the highest reboiler duty.

Table 14. Recovered products of the continuous chemical extraction process (see Figure 3)

Product	**Mass flow, tonne/day**	**Purity**	**Recovery rate**
Toluene	1.223	0.998	0.999
Ethylbenzene	2.452	0.997	0.996
Styrene	3.161	0.998	0.823
Phenol	0.496	0.993	0.423
Residual oil streams	**Mass flow, tonne/day**		**LHV, MJ/kg**
Light residual oil	1.954		38.263
Heavy residual oil	8.213		7.323

Table 15. Reboiler duty of distillation columns

Column	**Reboiler duty (cal/s)**
T-100	3.09×10^{4}
T-101	1.98×10^{4}
T-102	2.59×10^{4}
T-103	3.65×10^{3}
T-104	4.81×10^{4}
T-105	5.79×10^{3}
T-106	9.21×10^{3}
Total	1.44×10^{5}

Steam was generated by recovering heat from the hot streams. The recovered heat, approximately 3.95×10^4 cal/sec, could then be used to heat the reboilers in the distillation process. The properties of the generated steam are listed in Table 16.

Table 16. Properties of steam generated in the continuous process

Source	**Mass flow, kg/hr**	**Temperature, °C**	**Pressure, bar**
Hot pyrolytic oil	302.79	200	15.55
Pyrolytic gas combustion	176.12	180	9.97

4.2. Continuous Process: Techno-Economic Assessment

4.2.1. Economic assumptions

This section evaluates the economic feasibility of extracting pyrolysis oil, a key product of the E-waste Microwave-Assisted Pyrolysis process. It includes all assumptions and parameters used in the calculation. Additionally, a sensitivity analysis is conducted to consider price fluctuations. The assessment is based on 2024 data, reported in US dollars. The main profitability indicator is the net present value (NPV), with the relevant parameters listed in Table 17.

Table 17. Economic assumptions for NPV estimation

Parameters name	Value
Operation time, hr/yr	8760
Capacity factor, %	90
Operation factor, %	90
Plant lifetime, yr	30
Loan lifetime, yr	15
Construction time, yr	3
Loan interest rate, %	5
Federal and provincial tax, %	26
Debt percentage, %	40
Internal return rate, %	10
Inflation rate, %	3
Interest rate, %	7

4.2.1.1. CAPEX and OPEX estimation parameters

Capital expenditures refer to the initial investment required to start a project, including land, equipment, buildings, and installation costs. Specifically, CAPEX covers fixed capital investment, working capital, and startup expenses. In this study, equipment capital costs are calculated using the Aspen Capital Cost Estimator. Table 18 presents the parameters used in these capital cost calculations.

Operating costs (OPEX) cover the ongoing expenses for daily system operations, such as raw materials, labor, utilities, overhead, maintenance, property insurance, taxes, and general expenses. For this project, we assume one operator per shift across five shifts, following the Seider method. Each operator works 2,080 hours annually and earns $26.26 per hour [70]. Other OPEX assumptions are detailed in Table 19.

Table 18. Capital investment cost estimation parameters [64], [71]

CAPEX component	Description
Delivery costs	8% of the equipment purchased cost
Equipment erection	40% of the equipment delivered cost
Piping	70% of the equipment delivered cost
Instrumentation and Control	20% of the equipment delivered cost
Electrical	10% of the equipment delivered cost
Utility cost	10% of the equipment delivered cost
Off-sites	20% of the equipment delivered cost
Buildings	20% of the equipment delivered cost
Site preparation	10% of the equipment delivered cost
Land	6% of the equipment delivered cost
Engineering and supervision	15% of the purchased equipment
Construction overhead	18% of the purchased equipment
Project contingency	10% of the fixed capital investment
Working Capital	15% of the total capital investment
Start-up costs	9% of the fixed capital investments
Start-up costs	9% of the fixed capital investments
Site preparation	10% of the equipment delivered cost

Table 19. OPEX estimation parameters

OPEX component	Description
Labor costs	
Supervision and engineering	15% of the labour wage
Operating supplies and services	5% of the labour wages
Laboratory expenses	10% of the labour wages
Payroll charges	30% of the total labour wages and supervision & engineering costs
Maintenance costs	
Maintenance wages	3.5% of the fixed capital investment (excluding land)
Maintenance supervision and engineering	25% of the maintenance wages
Material supplies	100% of the maintenance wages
Maintenance overhead	5% of the maintenance wages
Overhead costs	
Plant overhead	7.1% of the total operating and maintenance wages, supervision and engineering expenses (TWSE)
Mechanical department services	2.4% of TWSE
Employee relations department	5.9% of TWSE
Business services	7.4% of TWSE
Property insurance and taxes	2% of the fixed capital investments (FCI)
General expenses	
Sale expenses	3% of sales
Research and development	5% of sales
Administrative expenses	3% of sales
Sale expenses	3% of sales

4.2.1.2. Prices of input and products in the market

The input and output prices are presented in Table 20. Electricity represents the main utility consumed, and its cost is determined based on the monthly large-power rate in Quebec, set at 14.234 per kW of billing demand and 3.619 cents/kWh. The rate is then converted from CAD to USD for inclusion in the study.

The pyrolysis and extraction processes are treated as independent units, with the economic assessment in this study focused primarily on the extraction stage. The pyrolytic oil obtained from the pyrolysis stage is then considered as a feedstock in the analysis. The cost of this feedstock is assumed to vary depending on the production scale and the economic gains from metal recovery. In small-scale operations and without metal recovery and sale, the cost reaches approximately $262 per tonne of oil. However, when metals are recovered from the solid stream, the oil cost can decrease significantly, reaching as low as zero, according to data provided by GreeNovel.

Table 20. Price of process input and outputs

Input/output	Market Price	Description
Electricity charge, ¢/kWh	2.678	3.619 ¢/kWh in Canadian dollars, referring to the rate for large power [72]
Electricity demand charge, $/kW	10.533	14.234 $/kW in Canadian dollars, referring to the rate for large power [72]
Pyrolytic oil, $/tonne	0 to 262	The cost of the pyrolytic oil changes depending on the scale of the pyrolysis reactor, as well as considering metals as the byproducts of the process.
Toluene, $/tonne	848	[73]
Styrene, $/tonne	1000	[74]
Ethylbenzene, $/tonne	860	[75]
Phenol, $/tonne	1422	[76]
Residue oil, $/MJ	0.029	Referring to the price data for furnace oil in Quebec [77]

4.2.2. Economic analysis results

4.2.2.1. Results summary

The following section presents the evaluation results for the base case, which assumes that the feedstock has no cost and the plant processes 25 tonnes of e-waste daily. Table 21 summarizes the economic evaluation findings. Under these assumptions, the plant has an NPV of -2.45 million dollars, requiring approximately 29 USD per tonne of e-waste in external financial support.

Table 21. Summary of economic evaluation

Economic evaluation summary	
Total operating costs, $/yr	2,236,401
Total Capital Investment, $	14,745,753
Annualized capital cost $/yr	1,309,827
Total revenue, $/yr	3,289,085
Minimum credit for e-waste, $/tonne	**29.34**
NPV, million$	**-1.81**

4.2.2.2. Equipment costs

The equipment costs were calculated using Aspen Plus Cost Estimator and are shown in Table 22. As indicated, the distillation columns are the most costly units in the system process.

Table 22. Equipment cost for the continuous process

Unit	Description	Equipment Cost
Chemical Extraction		
T-100	Removal of the heavies	$165,300
T-101	Toluene recovery	$315,300
T-102	Styrene recovery	$320,700
T-103	Toluene purification	$329,100
T-104	Separation of styrene and ethylbenzene	$1,221,400
T-105	Phenol recovery	$317,300
T-106	Phenol purification	$251,000
E-100	Cooling pyrolytic oil with heat recovery	$15,400
AC-100	Aircooler for further cooling of pyrolytic oil	$10,500
Process pump (P-100 to P-106)	Increasing fluid pressure	$5,300
Gas recovery		
P-107	Increasing pressure of feedwater	$6,000
B-100	Combustion of pyrolytic gas and heat recovery	$7,853
Total		**$2,996,953**

4.2.2.3. Feedstock and utility costs, product revenue

Table 23 and Table 24 refer to the feedstock and utility costs and the product sales and revenue, respectively.

Table 23. Feedstock and utility costs

Input	Quantity	Cost, $/yr
Electricity, MWh/yr	2,438	100,959
Pyrolysis oil, tonne/yr	3,194	-
Total Feed and Utility Costs		**100,959**

Table 24. Product sales and revenue

Products	Quantity	Revenue, $/yr
Toluene, tonne/yr	362	306,661
Ethylbenzene, tonne/yr	725	623,700
Styrene, tonne/yr	935	934,753
Phenol, tonne/yr	147	260,726
Oil (38.26 MJ/kg), MJ/yr	22100751	644,605
Oil (7.32 MJ/kg), MJ/yr	17781906	518,639
Total Revenue		**3,289,085**

4.2.2.4. CAPEX and OPEX costs

The following tables, Table 25 and Table 26, illustrate the capital and operating costs, as well as their constituent blocks.

Table 25. Capital expenditures

CAPEX component	$
Direct costs	
Total equipment cost	7,144,741
Utility cost	323,671
Off-sites	647,342
Buildings	647,342
Site preparation	323,671
Land	194,203
Total direct costs	9,280,969
Indirect costs	
Engineering and supervision	485,506
Construction overhead	582,608
Project contingency	1,149,898
Total indirect cost	2,218,012
Fixed Capital Investment (FCI)	11,498,982
Working Capital	2,211,863
Start-up costs	1,034,908
Total Capital Investment (TCI)	14,745,753
Annualized capital cost, $/yr	**1,309,827**

Table 26. Operating expenditures

OPEX component	$/yr
Utilities, $/yr	100,958.5
Raw Material, $/yr	-
Operating labour costs, $/yr	449,256
Labour wages, $/yr	273,104
Supervision and engineering, $/yr	40,966
Operating supplies and services, $/yr	13,655
Laboratory expenses, $/yr	27,310
Payroll charges, $/yr	94,221
Maintenance costs, $/yr	910,035
Maintenance wages, $/yr	395,667
Maintenance supervision and engineering, $/yr	98,917
Material supplies, $/yr	395,667
Maintenance overhead, $/yr	19,783
Overhead costs, $/yr	184,373
Plant overhead, $/yr	57,414
Mechanical department services, $/yr	19,408
Employee relations department, $/yr	47,711
Business services, $/yr	59,840
Property insurance and taxes, $/yr	229,980
General expenses, $/yr	361,799
Sale expenses, $/yr	98,672.54
Research and development, $/yr	164,454.23
Administrative expenses, $/yr	98,672.54
Operating costs, $/yr	**2,236,401**
$Million/yr	**2.2**

4.2.2.5. NPV estimation

Table 27 presents the estimation of net present value (NPV), calculated to be -1.81 million USD. This result suggests that at the current scale and under the existing process assumptions, the plant requires approximately 29.34 USD of financial credit per tonne of e-waste plastic to achieve profitability.

Table 27. NPV calculation

NPV calculation	
Total revenue, $/yr	3,289,085
Total annual costs, $/yr	2,236,401
Total Capital Investment, $	14,745,753
Gross Earning, $/yr	1,052,683
Debt needed, $	5,898,301
Equity Expended, $	8,847,452
Debt Taken, (End of 1st yr), $	495,457
Debt Taken, (End of 2nd yr), $	4,236,160
Debt Taken, (End of 3rd yr), $	6,429,797
Annual loan payment, $	619,461
Return on Investment (ROI)	5.3%
Venture Profit, $	-400,675
Land Value, $Million	0.2
NPV, $Million	**-$1.81**

4.2.3. Sensitivity Analysis

In this section, the assumptions and some parameters of the economic analysis are modified to examine the impact of different factors, such as feedstock price, plant capacity, and alternative plant designs.

4.2.3.1. Simplified design, withdrawing from phenol recovery

In the original design, phenol recovery was achieved through two additional distillation columns (T-105 and T-106, Figure 3). While the additional columns were energy and cost-intensive, only 40% of phenol was recovered from the initial pyrolytic oil. This section examines a modified scenario in which the columns T-105 and T-106 are removed, and the bottom stream from T-102 is not further distilled. Table 28 shows the changes to the product streams in the current scenario.

In this scenario, bypassing further distillation of the T-102 bottom stream resulted in a light residual oil stream with a slightly lower LHV of 36.768 MJ/kg compared to the original residual oil, which had an LHV of 38.263 MJ/kg. This change and withdrawal from selling phenol resulted in a minimal decrease of only 4% in process revenue. However, removing two distillation columns substantially reduced both energy demand and capital costs, and as shown in Figure 6. Under this configuration, the process becomes profitable, yielding an NPV of $2.24 million compared to $-1.81 million of the base case. The results are presented in Table 29.

Table 28. Describing the differences between the base and the simplified design

Case	Product	Mass flow, tonne/day	LHV, MJ/kg
Base design	Phenol	0.496	-
	Light residual oil	1.954	38.263
Simplified design	Phenol	-	-
	Light residual oil	2.45	36.768

Table 29. Results of the base and simplified design

Economic evaluation summary	Base case	Simplified case
Total input costs, $/yr	$100,959	$81,804
Operating costs, $/yr	2,236,401	$1,947,744
Total Capital Investment (TCI), $	14,745,753	$11,634,934
Annualized capital cost, $/yr	1,309,827	$1,033,501
Total revenue, $/yr	3,289,085	$3,160,518
NPV, $Million	**-1.81**	**$2.24**
Minimum credit for e-waste, $/tonne	**29.34**	**-**

Figure 6. Cost comparison of the base and simplified case

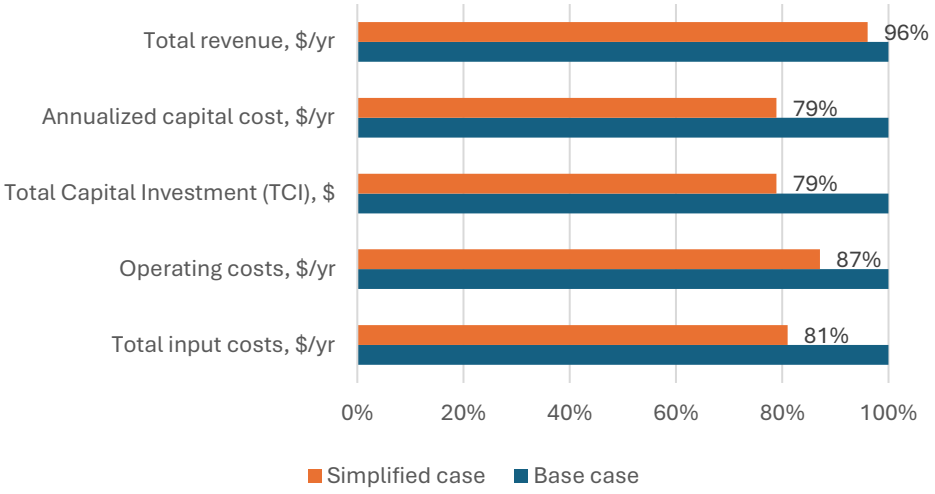

4.2.3.2. Feedstock cost

In the previous analysis, the cost of feedstock was assumed to be zero, based on the GreeNovel estimations. In this section, a fixed price of 262$/tonne of oil is considered to account for a less favorable and more costly scenario. This adjustment enables us to assess a less optimal situation and observe its impact on the results, as reported in Table 30. Considering the cost of raw material led to a larger negative NPV, and the required credit was estimated to be around $156.57 per tonne of e-waste for the base process to reach profitability at the current scale. The cost of feed oil also affected the feasibility of the simplified process, rendering it no longer self-sufficient. Even in the simplified case, an external credit of $90.80 was needed to reach profitability.

Table 30. Summary of results for the case considering the oil price of $262/tonne of oil

Economic evaluation summary	**Base case**	**Simplified case**
Raw material cost, $/yr	$836,762	$836,762
Operating costs, $/yr	$3,073,164	$2,775,233
Total Capital Investment (TCI), $	$14,745,753	$11,634,934
Annualized capital cost, $/yr	$1,309,827	$1,033,501
Total revenue, $/yr	$3,289,085	$3,160,518
NPV, $Million	-$10.06	-$5.80
Minimum credit for e-waste, $/tonne	156.57	90.80

4.2.3.3. Changing plant scale with variable oil pricing

In this analysis, the plant capacity was adjusted to assess the impact of scale on profitability. The selected scales were based on oil cost data provided by prior GreeNovel assessments, which evaluated only the upstream pyrolysis unit. The data are presented in Table 31. In the upstream study, the sale of recovered metals from e-waste was identified as the main driver of profitability. The metal recovery generates substantial revenue, which was included in the oil price calculations. he oil can be sold at a lower price as the unit's capacity increases, resulting in an oil price of zero at capacities above 13 tonnes per year.

Table 31. Pyrolytic oil price based on the scale of the pyrolysis unit, data from GreeNovel

Capacity, tonne/day	**Oil price, $/tonne**
9	398.5
10	262.3
11	148.8
12	52.7
13 and above	-30 (0)

The equipment costs were scaled up using the following equation. The capacity factor, n, is assumed to be 0.7. [64]

$$C_2 = C_1 \left(\frac{S_2}{S_1}\right)^n$$

Where $C_2 =$ cost of equipment of capacity S_2

$C_1 =$ cost of equipment of capacity S_1

At a smaller scale of 10 tonnes of e-waste per day, the process requires the highest level of government credit to maintain profitability. However, the upgrading plant with the base design reaches profitability without the need for external support for scales exceeding 29 tonnes per day. The simplified design reaches profitability at scales above 21 tonnes per day.

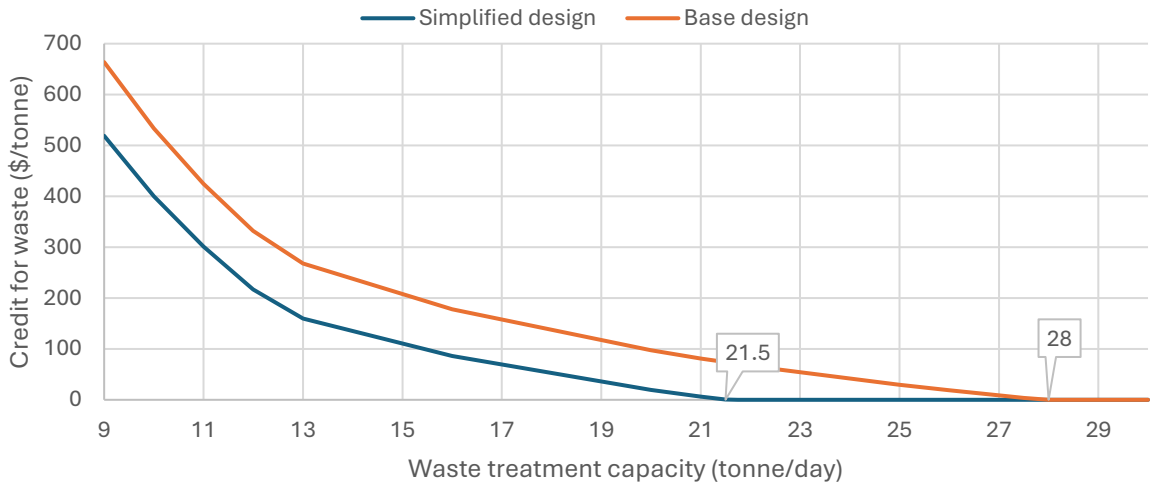

Figure 7. Minimum credit per tonne of waste required to reach profitability for different scales, accounting for changing oil prices

4.2.3.4. Changing plant scale with constant oil pricing

The results indicate that the plant is profitable when the simpler design is selected in the reference scenario of this study, when the feedstock expenses are eliminated.

This analysis takes into account the alternative scenario in which the plant's profitability is decreased due to the raw material's $262/tonne cost. Since the credit needed for the e-waste feedstock lowers with growing scale, expanding the plant's capacity increases profitability. Figure 8 provides an illustration of this impact. About 52 tonnes of e-waste per day for the base design and 40 tonnes per day for the simplified version were the minimum scales at which the facility demonstrated profitability without the requirement for outside government credit.

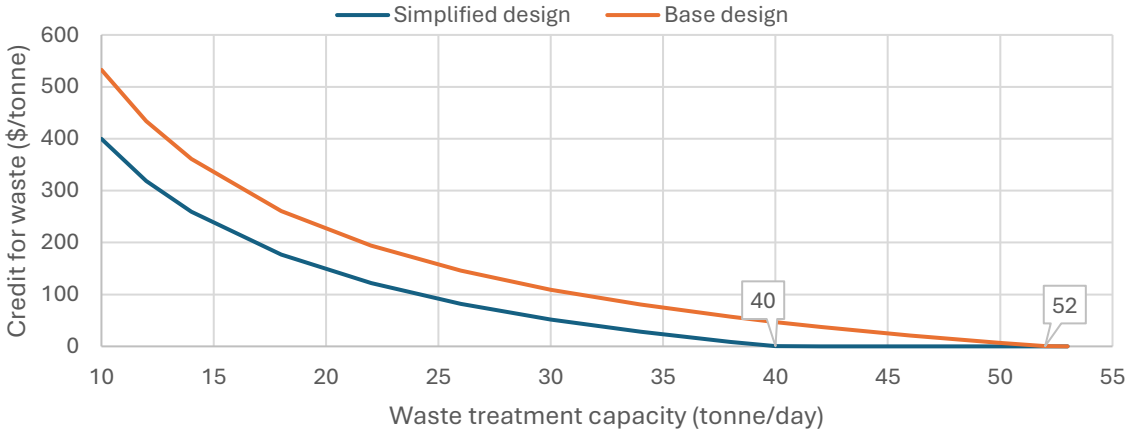

Figure 8. Minimum credit per tonne of waste required for changing plant scale, considering a constant cost for feedstock ($262/tonne oil)

4.2.3.5. Tornado plot

A sensitivity analysis was performed to identify the key variables influencing process profitability. The parameters considered were the market price of styrene, equipment cost, plant lifetime, and electricity price. These variables were selected to represent realistic fluctuations in market conditions and operating expenses. The analysis revealed that equipment cost had the greatest influence on net present value, with a 20 percent change in this parameter resulting in the largest change in profitability. On the other hand, variations in electricity price showed a relatively minor effect on the overall economic performance of the process. Figure 9 shows the results of the sensitivity analysis and the influence of each variable on the net present value using a tornado plot.

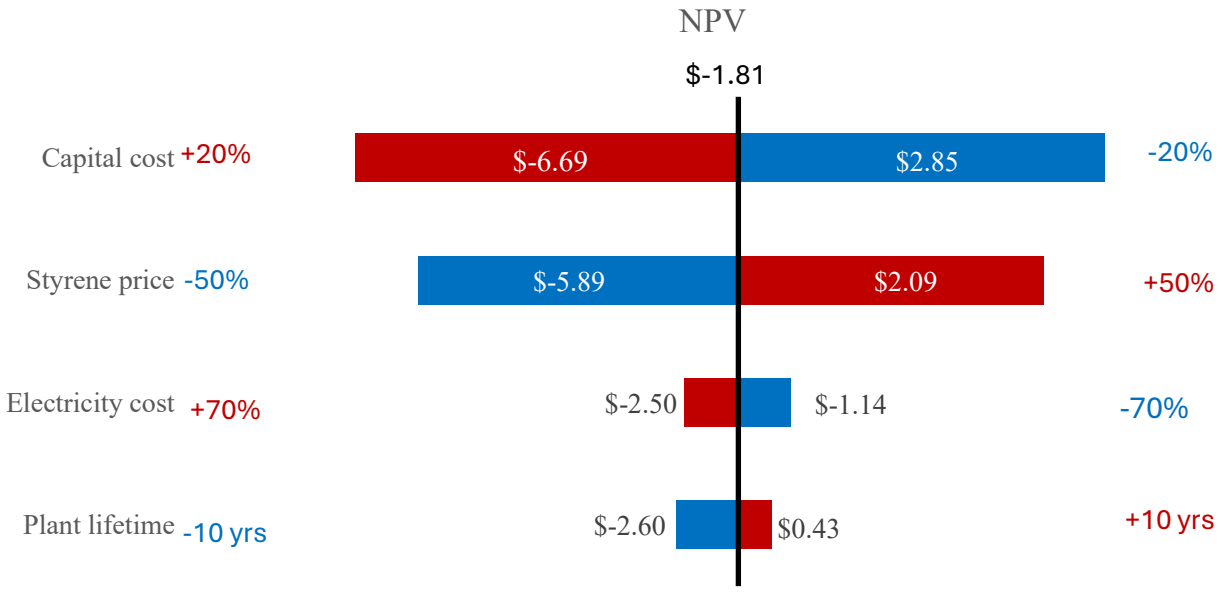

Figure 9.Tornado plot showing the impact of different factors on the NPV

4.3. Continuous Process: Life Cycle Assessment

4.3.1. Goal and scope definition

The primary aim of this study is to quantify the environmental impacts of a specific waste treatment process and compare them with incineration, the conventional treatment route. The study was based on a facility located in Quebec, Canada, invented by GreeNovel Inc. However, it also included other Canadian provinces, namely, Ontario, British Columbia, and Alberta, as well as other countries such as Brazil and China.

The established method for selecting a functional unit for waste treatment processes is to base it on the mass of waste being treated. The full-scale facility under study is expected to be able to treat 25 tonnes of E-waste daily. Therefore, to represent the process in full scale, the functional unit is chosen to be the treatment of 25 tonnes of E-waste, or in other words, **treating 25 tonnes of E-waste plastic per day**, and all the inputs and outputs of the process will be scaled accordingly.

The system boundary for this study was confined to the operations of the treatment facility, which means the environmental burden of the waste generation, collection, and its transportation to the facility was excluded. Meanwhile, the steam generation units were included to utilize the flue gas from both treatment processes. While the analysis starts from receiving the dismantled waste in the facility, the environmental impacts of the upstream electricity generation were also included. The final gate ends where the products or energy are obtained and ready to use, excluding the use and end-of-life phase of the products. This is a common approach in the LCA studies for waste treatment processes [13].

The waste treatment process, besides mitigating landfill accumulation, enables the production of valuable by-products. Specifically, the pyrolysis process generates steam and an oil product with a significant heating value, making them a promising fuel alternative. Additionally, extracting marketable products from this oil is also feasible. To avoid the allocation problem and in adherence to ISO 14044 standards, the study adopts the **system expansion** method to account for the environmental credits attributed to the production of these by-products. In other words, the emissions from the conventional process used to produce these products are subtracted from the emissions of the process under study.

The impact of the process was calculated using the OpenLCA Software. The process-specific data were collected from the GreeNovel facility, and the Ecoinvent v.3.8 database provided the background data. Data regarding the output of the processes were derived from the simulation carried out on ASPEN Plus V14.

4.3.2. Comparison Studies

4.3.2.1. Baseline Scenario – Incineration

Incineration of waste was assumed to be the baseline scenario, allowing for the comparison of the impacts of electrified pyrolysis with other treatment routes.

4.3.2.2. Geographical Location of The MW Pyrolysis

The scope of the analysis is extended to other provinces to observe the effect of the source of electricity on the life cycle impacts. The Canadian provinces under study were Quebec, Ontario, Alberta, and British Columbia. Other countries, such as Brazil and China, were also included. The Chinese province, Guangdong, was specifically selected since it has been known as the world's largest E-waste dump, importing E-waste from around the world [78].

4.3.2.3. Scenarios Including Various Oil Utilization Pathways

In this study, we consider different oil valorization scenarios. This will enable a fairer comparison with the baseline and the more established waste treatment techniques.

4.3.3. Life Cycle Inventory

4.3.3.1. The baseline: Incineration process

The incineration process outputs were identified as the process gas emissions (flue gas) and solid residues. Notably, the produced flue gas stream was used to generate low-pressure steam, with potential for heating applications. As with pyrolysis, the functional unit of the baseline scenario is also the treatment of 25 tonnes of E-waste per day. The ash content of the E-waste was assumed to be zero, and as a result, there was no solid residue in the products in the simulation.

The primary input and output of the process are documented in the Table 32.

Table 32. Life cycle inventory of the incineration route

Input	**Unit**	**Quantity**	**Output**	**Unit**	**Quantity**
E-waste	tonne	25	Heat (from steam)	kWh	5.56×10^{4}
			Flue gas	tonne	153.27

The flue gas produced by incineration contains harmful halogen compounds, originating from the additives that give E-waste its specific properties. This is not the case in the pyrolysis process at the GreeNovel facility, where the gas is treated with DHA agents to remove these corrosive compounds. Table 33 shows the composition of the flue gas emitted from the incineration process.

The LP steam is assumed to substitute for steam generation in an electric boiler. In other words, the steam produced by the waste treatment facility replaces the need to generate the same amount of steam using electricity. For this process, we assumed an efficiency of 95% for the electric boiler.

Table 33. Flue gas composition emitted from the incineration route. Data refers to the functional unit.

Compound Name	Quantity (tonne)
H_2O	11.23
N_2	104.89
O_2	1.14
NO_2	7.41×10^{-5}
NO	6.29×10^{-2}
CO	7.54×10^{-3}
CO_2	41.43
HBr	9.96×10^{-3}
Br_2	3.50×10^{-3}
HCl	2.86×10^{-3}
Cl_2	1.04×10^{-6}
Total	**158.27**

4.3.3.2. The MW-assisted pyrolysis route

4.3.3.2.1. Pyrolytic gas

The non-condensable gas product makes up 10% of the pyrolysis products. The gas is treated by the DHA agent, and then combusted to produce steam as explained in the previous sections. The composition of the released flue gas can be found in Table 34.

Table 34. Flue gas composition from the gas recovery unit in the MW-assisted pyrolysis route. Data refers to the functional unit.

Compound	Quantity (tonne)
H_2O	2.69×10^{-1}
N_2	4.03
O_2	0.64
NO_2	2.48×10^{-5}
NO	3.55×10^{-3}
N_2O	2.78×10^{-7}
CO_2	2.81
Total	**7.76**

4.3.3.2.2. Pyrolytic char

The solid product accounts for 20% of the total output from the pyrolysis process. In this study, it is assumed that the solid product is pure carbon, which is left on site as waste. This assumption is since the waste feedstock is priorly treated with a dehalogenation agent, removing its impurities. Meanwhile, the metal content of the waste is removed before it reaches the treatment facility. This approach is consistent with several waste treatment processes in the Ecoinvent database that involve incinerating plastic. However, the solid by-product, composed of carbon, can also be used for energy recovery through combustion or other applications. Nevertheless, this potential application was not included within the system boundary of this study.

4.3.3.2.3. Pyrolytic oil

Pyrolysis of plastic waste usually produces low-value hydrocarbon mixtures with a broad compositional range, extending from light alkane gases to coke, typically spanning from C5 to C28 or beyond [79]. Using different approaches, we could either recover energy or chemicals from pyrolytic oil. For the chemical recovery scenario, the energy demand (reboiler duty) and output (product mass flows and purity) were calculated from the simulation results.

Pyrolytic oils can be refined and utilized as an alternative to fossil fuels. Another case was included that prioritized fuel recycling by using oil as a fuel alternative. The impacts were assessed by considering the heating value of oil products compared to the standard value for fuel that is regarded as an avoided product. A similar approach was adopted in the literature [66]. The oil from pyrolysis can be classified as light oil, and therefore, the avoided product is chosen accordingly [80]. Additionally, it is assumed that the residue oil is transported to a nearby treatment facility or refineries in proximity to the GreeNovel facility in Granby, QC.

Table 35. Heating values of oil streams as fuel products. Data refers to the functional unit

Case	Product	Mass flow, tonne/day	LHV, MJ/kg
Scenario A	Light residual oil	1.954	38.263
	Heavy residual oil	8.213	7.323
Scenario B	Light residual oil	2.45	36.768
	Heavy residual oil	8.213	7.323
Scenario D	Pyrolytic oil	17.5	24.46

4.3.3.3. LCA scenarios: Overall summary

This LCA study investigated several scenarios that explore alternative strategies for oil valorization, either through its direct use as a fuel or through the recovery of valuable chemical components. The gas recovery unit remained the same across all scenarios.

4.3.3.3.1. Scenario A and B, credit for all products

In these scenarios, styrene, ethylbenzene, toluene, and phenol were recovered from the pyrolysis oil through a distillation process. Scenario A corresponds to the base design, which includes the recovery of all four products, whereas Scenario B represents a simplified design that excludes phenol recovery. The residual oil streams were also treated as fuel products, and their heating values were incorporated into the analysis to calculate credit gained from avoided production.

4.3.3.3.2. Scenario C, no credit for the residue oil

The input and outputs of this scenario were similar to those of scenario A, meaning that the energy demand and the recovered products remained the same. However, in this scenario, no credit is assigned for the avoided production associated with using the residual oil as a fuel, and no transportation requirements were included for sending this product to an external facility. This assumption reflects the fact that the residual oil may require additional upgrading through the addition of additives or further processing before it becomes an appropriate fuel alternative. As a result, considering fuel oil sourced from petroleum as the avoided product could introduce an unjust advantage in favour of the pyrolysis process.

4.3.3.3.3. Scenario D, oil as fuel

In this case, the pyrolysis oil was proposed as a substitute for fossil-based light fuel oils, based on its heating value of 24.47 MJ per kg. The distillation process was removed. The oil is presumed to be transported to a nearby refinery located 80 kilometers from the pyrolysis facility. The results of all scenarios are also listed in Table 36, Table 38, Table 37, and Table 39.

Table 36. Inputs and outputs of scenario A

Input	Unit	Quantity	Output	Unit	Quantity
E-waste	tonne	25	Heat (from steam)	kWh	3.96×10^3
Electricity (pyrolysis)	kWh	3.75×10^4	Styrene	tonne	3.16
Electricity (extraction)	kWh	1.60×10^4	Toluene	tonne	1.22
Transportation of residual oil	t.km	813.04	Ethylbenzene	tonne	2.45
			Phenol	tonne	0.5
			Residue oil (38.26 MJ/kg)	tonne	1.95
			Residue oil (7.32 MJ/kg)	tonne	7.94
			Flue gas	tonne	7.76
			Solid product	tonne	5

Table 37. Inputs and outputs of scenario B

Input	Unit	Quantity	Output	Unit	Quantity
E-waste	tonne	25	Heat (from steam)	kWh	3.96×10^3
Electricity (pyrolysis)	kWh	3.75×10^4	Styrene	tonne	3.16
Electricity (extraction)	kWh	1.43×10^4	Toluene	tonne	1.22
Transportation of residue oil	t.km	852.80	Ethylbenzene	tonne	2.45
			Residue oil (36.77 MJ/kg)	tonne	2.45
			Residue oil (7.32 MJ/kg)	tonne	7.94
			Flue gas	tonne	7.76
			Solid product	tonne	5

Table 38. Inputs and outputs of Scenario C

Input	Unit	Quantity	Output	Unit	Quantity
E-waste	tonne	25	Heat (from steam)	kWh	3.96×10^{3}
Electricity (pyrolysis)	kWh	3.75×10^{4}	Styrene	tonne	3.16
Electricity (extraction)	kWh	1.60×10^{4}	Toluene	tonne	1.22
			Ethylbenzene	tonne	2.45
			Phenol	tonne	0.5
			Flue gas	tonne	7.76
			Solid product	tonne	5

Table 39. Inputs and outputs of scenario D

Input	Unit	Quantity	Output	Unit	Quantity
E-waste	tonne	25	Heat (from steam)	kWh	3.96×10^{3}
Electricity (pyrolysis)	kWh	3.75×10^{4}	Pyrolytic oil (24.35 MJ/kg)	tonne	17.5
Transportation of pyrolytic oil	t.km	1400	Flue gas	tonne	7.76
			Solid product	tonne	5

4.3.4. Life cycle Impact Assessment

This study employed the ReCiPe 2016 Hierarchist method to calculate the life cycle impact assessment in both midpoint and endpoint categories, using the corresponding characterization factors. The midpoint analysis quantifies impacts across various categories, including global warming, fossil resource depletion, freshwater ecotoxicity, human toxicity, and acidification. These indicators represent intermediate effects that focus on specific environmental problems. The Hierarchist perspective of ReCiPe is the default consensus model and is widely used in scientific studies [81].

Meanwhile, the endpoint analysis focuses on three major areas of protection: ecosystem quality, human health, and resource depletion. The endpoint analysis facilitates decision-making and interpretation of the LCIA results by aggregating the results into three main areas. Figure 10 shows the relationship between LCI parameters, midpoint, and endpoint indicators in ReCiPe 2016. The tables of LCIA midpoint and endpoint results are provided in the appendix.

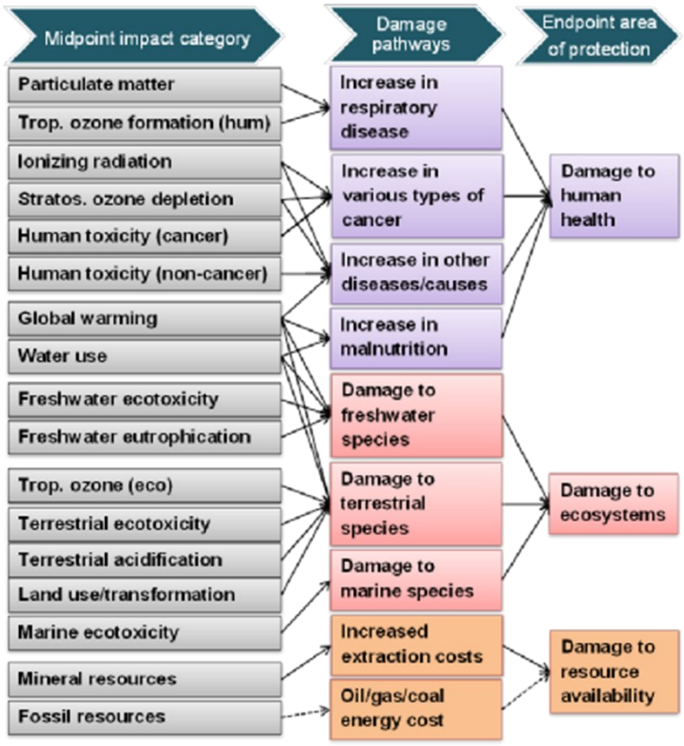

Figure 10. Overview of the structure of ReCiPe [81]

4.3.4.1. Electricity production

Given the high electricity demand of the process, it is important to compare the electricity mixes of the regions included in this study. Table A 2 in the appendix presents the midpoint impact assessment results associated with producing 1 kWh of electricity in each region. The Ecoinvent datasets used for Canadian provinces were valid for the year 2018 production mixes, while the datasets for China and Brazil reflect conditions in 2021 [80-83]. Table 40 provides an approximate breakdown of the three largest energy resources contributing to electricity generation in each region, based on the Ecoinvent 3.8 database.

Table 40. The primary sources in the electricity production mix by region, as described in ecoinvent 3.8.

Region	**Source**	**Share %**
Quebec, Canada (QC)	Hydro, reservoir	59%
	Hydro, run-of-river	35%
	Wind	4%
Alberta, Canada (AB)	Lignite	48%
	Natural gas	32%
	Heat and power co-generation, Natural gas	9%
British Columbia, Canada (BC)	Hydro, reservoir	84%
	Natural gas	7%
	Hydro, run-of-river	4%
Ontario, Canada (ON)	Nuclear, pressure water reactor	61%
	Hydro, reservoir	21%
	Wind	7%
Brazil (BR)	Hydro, reservoir	63%
	Natural gas	5%
	Biomass	3%
Guangdong, China (CN)	Hard coal	76%
	Nuclear, pressure water reactor	13%
	Hydro, run-of-river	8%

Electricity production was compared across different midpoint categories in Figure 11. Electricity production in Alberta has the highest impact in several categories, primarily due to the province's predominant use of fossil resources in its energy mix. A similar pattern is observed in China, where coal constitutes 76% of power generation. In contrast, regions with a higher share of renewable electricity demonstrate lower impacts in categories such as global warming, fossil resource scarcity, and ecotoxicity. The results highlight the energy mix's role in environmental assessments, showing regions relying on fossil fuels have higher emissions than renewable-based areas.

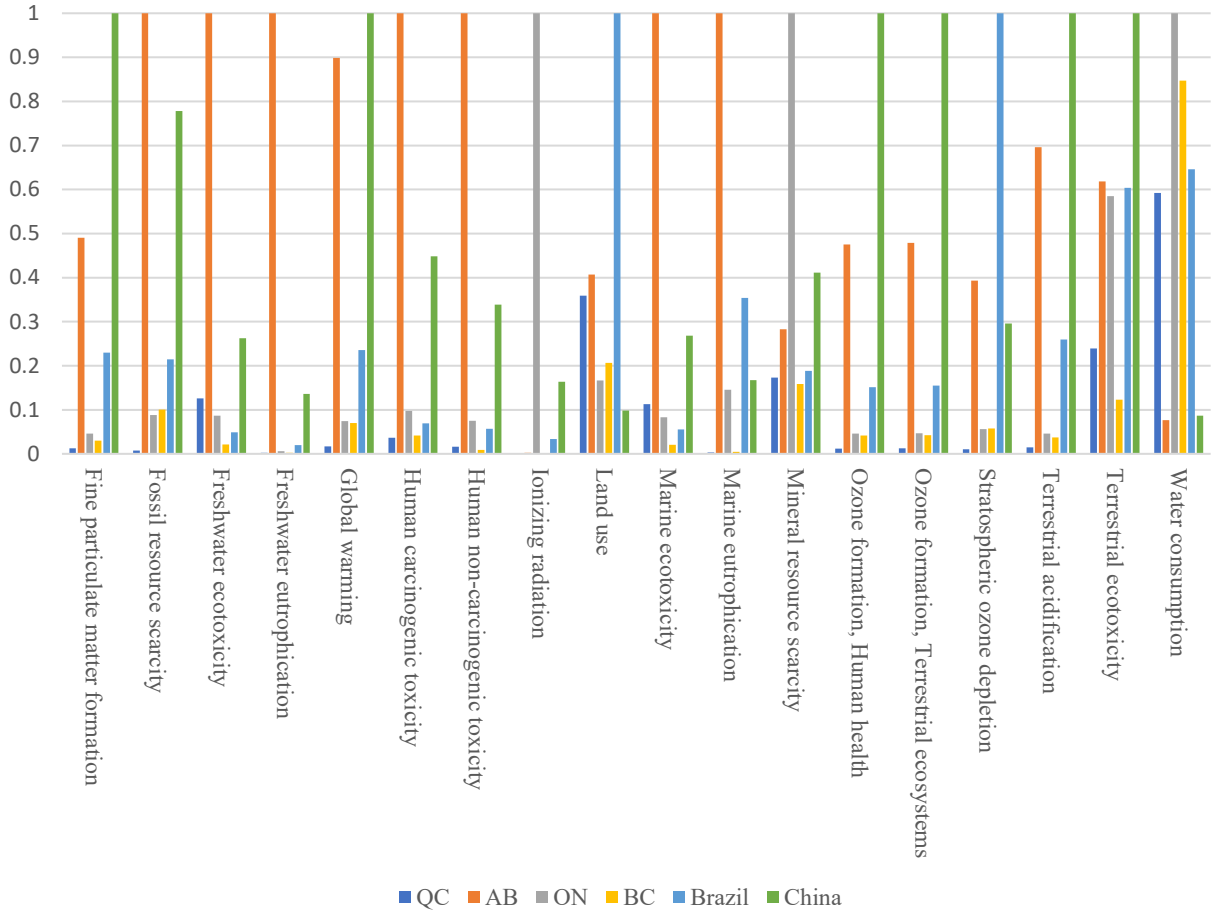

Figure 11. Normalized LCIA midpoint impact assessment for electricity production of each region, data refers to the production of 1 kwh of electricity.

4.3.4.2. Interpretation of LCIA results

This section presents an interpretation of the LCIA results. In the appendix, the midpoint results of the six regions across all scenarios are presented in detail in Table A 3 to Table A 7 in the appendix. Finally, the contribution analysis in the following section provides a more in-depth examination of the environmental impacts of the process.

4.3.4.2.1. Midpoint results

Negative values frequently appeared in the LCIA results for microwave-assisted pyrolysis, indicating a net environmental benefit. These values showed that, while the process itself had a relatively low direct impact, it avoided emissions that would have otherwise occurred in the conventional life cycle stages of the products being avoided. In the impact categories of fossil resource scarcity and global warming, the results consistently favoured pyrolysis over incineration

in Quebec, British Columbia, Ontario, and Brazil, regardless of the oil utilization scenario. These regions shared a low-emission electricity mix, enabling pyrolysis to outperform incineration despite its substantial electricity demand.

Although pyrolysis performed better than incineration in most regions, the results for Alberta and China were different. In several midpoint categories, including human carcinogenic toxicity, human non-carcinogenic toxicity, and freshwater and marine ecotoxicity, pyrolysis in Alberta showed the highest impacts, followed by China. As a result, in regions with emission-intensive electricity mixes, incineration resulted in lower overall impacts. This occurred because incineration generated a comparatively low-emission power source through steam production, which displaces the region's high-emission power supply.

In the context of global warming, and as shown in Figure 12, microwave-assisted pyrolysis produced smaller impacts than incineration in Quebec, British Columbia, Ontario, and Brazil. This pattern indicated that regions with low-emission electricity tended to favour pyrolysis over incineration. In contrast, in Alberta and China, incineration performed considerably better. For example, in Quebec, replacing incineration with pyrolysis resulted in a 145% reduction in global warming impacts, decreasing from 40,545 kg CO_2-eq to -18,155 kg CO_2-eq for the daily treatment of 25 tonnes of e-waste.

Across other impact categories, incineration was generally more water-efficient, particularly in regions with low-emission electricity. However, in the same areas, pyrolysis achieved greater reductions in global warming, fossil resource scarcity, and ozone formation impacts. This indicated a trade-off in which improved performance in mitigating global warming and other categories came at the cost of higher water consumption, particularly in areas that relied on hydroelectric power. For impacts on marine and freshwater systems, such as ecotoxicity, the results varied among low-emission regions, while Alberta and China showed a consistent preference for incineration.

The results showed only minor differences between Scenarios A, B, and C. This indicates that the credits associated with phenol and the use of residual oil as a fuel substitute contributed little to the overall environmental performance. The significant improvements were instead driven by the credits from the recovered chemical products, such as styrene and ethylbenzene, which were common to all scenarios that included chemical extraction. This interpretation is supported by the larger impacts observed in Scenario D, where the pyrolysis oil was primarily used as a fuel rather than as a chemical source.

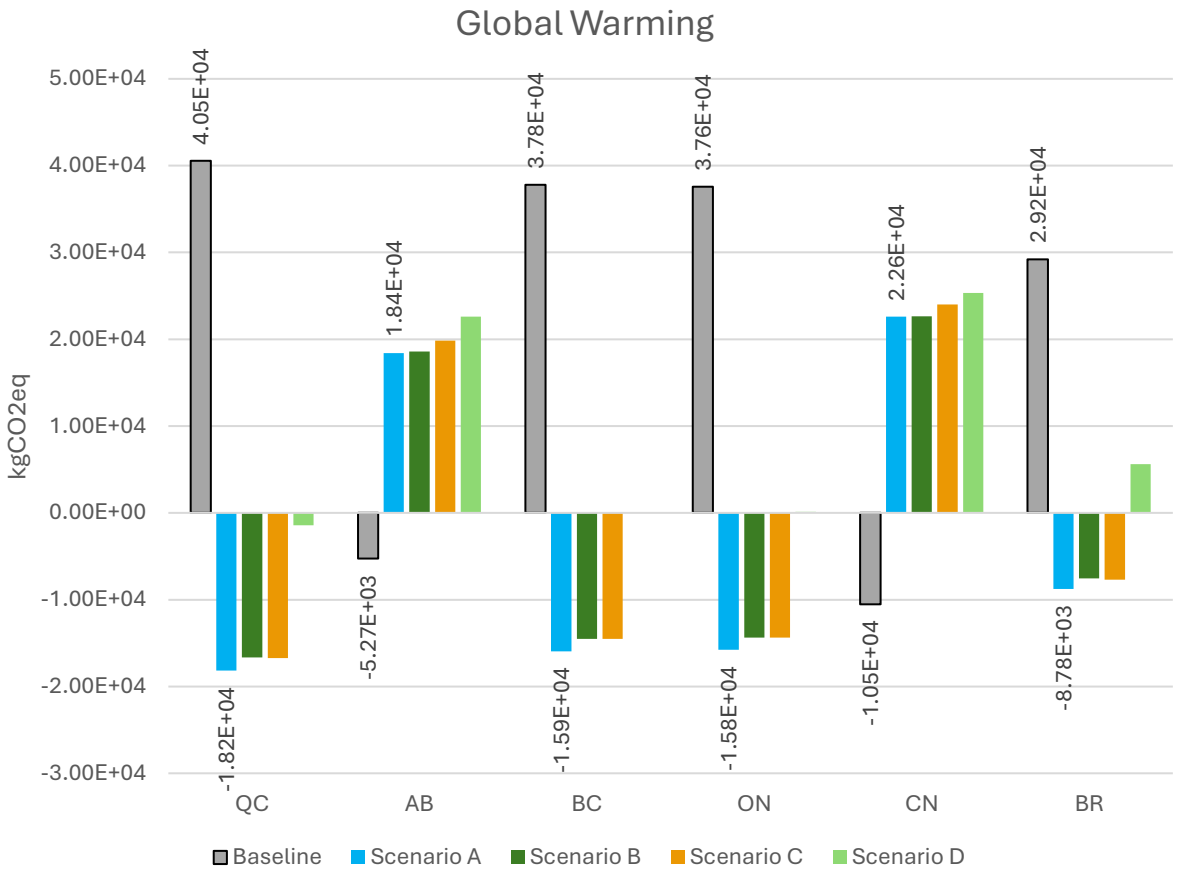

Figure 12. LCIA results in the global warming category for different scenarios

4.3.4.2.2. Endpoints results

The endpoint impact assessment results are presented in Figure 13, Figure 14, Figure 15, and also reported in Table A 8 in the appendix. These results also showed that pyrolysis produced lower environmental impacts in the areas of human health and ecosystem quality in regions with low-emission electricity. In regions like Quebec and British Columbia, these benefits were most pronounced in Scenarios A and B. Even without the chemical extraction unit, opting for pyrolysis instead of incineration reduced average damage to human health by 118%, as seen by comparing the baseline scenario with Scenario D in QC, BC, and ON. Adding the upgrading unit would improve the average reduction to 184%. In contrast, incineration was preferred in regions such as Alberta and China, where electricity generation relied heavily on fossil resources. In terms of resource availability, pyrolysis demonstrated notably better performance across all regions, regardless of the electricity mix, due to its ability to recover fuels or chemicals that would otherwise be produced from fossil resources.

When comparing different oil utilization pathways in low-emission regions, chemical recovery in Scenarios A and B resulted in lower damage than the production of fuel alternatives in Scenario D. By removing the upgrading step and switching from Scenario A to D would increase the damage to human health by 79% on average in QC, BC and ON with a more pronounced increase of 171% in Brazil. A similar trend is observed in ecosystem damage, with damage doubling on average when upgrading is removed. In regions with emission-intensive electricity, Scenario D showed a comparable performance to scenarios A, B and C with chemical extraction. In the resource availability area, Scenario D even performed slightly better than the upgrading scenarios. This difference may be due to the energy-intensive nature of the extraction process, making it more environmentally safe to avoid extraction and use the oil as a fuel alternative.

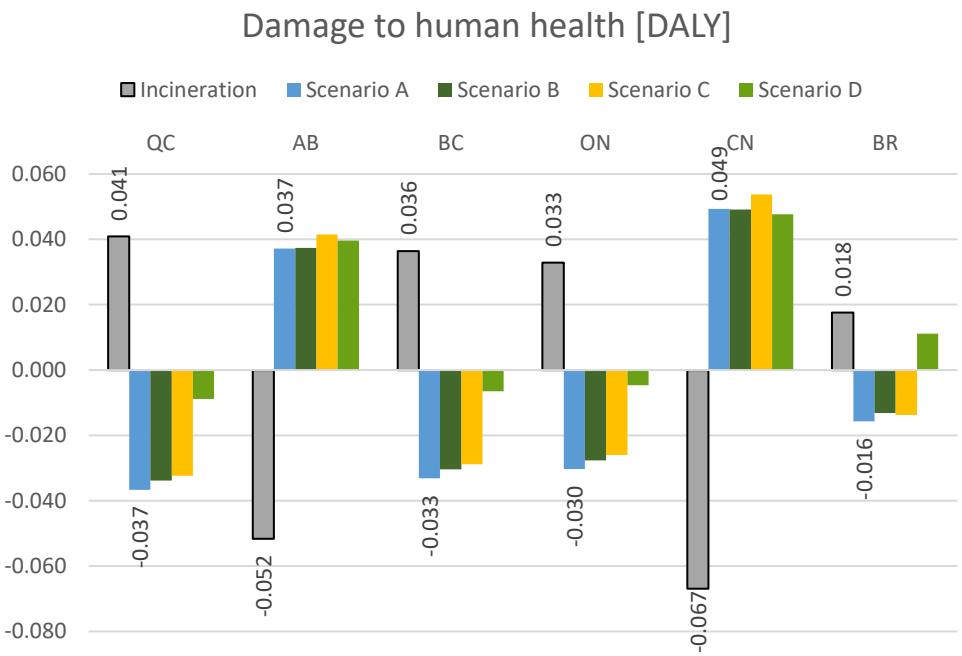

Figure 13. LCIA endpoint results of treating 25 tonne/day of e-waste through various scenarios, Damage to human health category

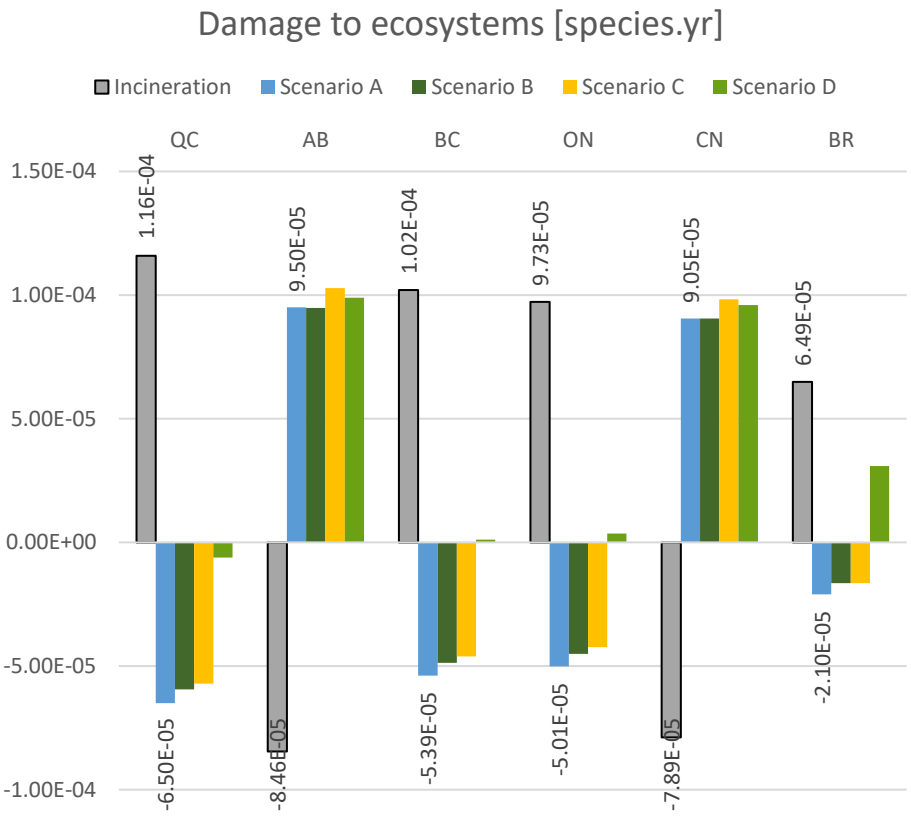

Figure 14. LCIA endpoint results of treating 25 tonne/day of e-waste through various scenarios, Damage to ecosystems category

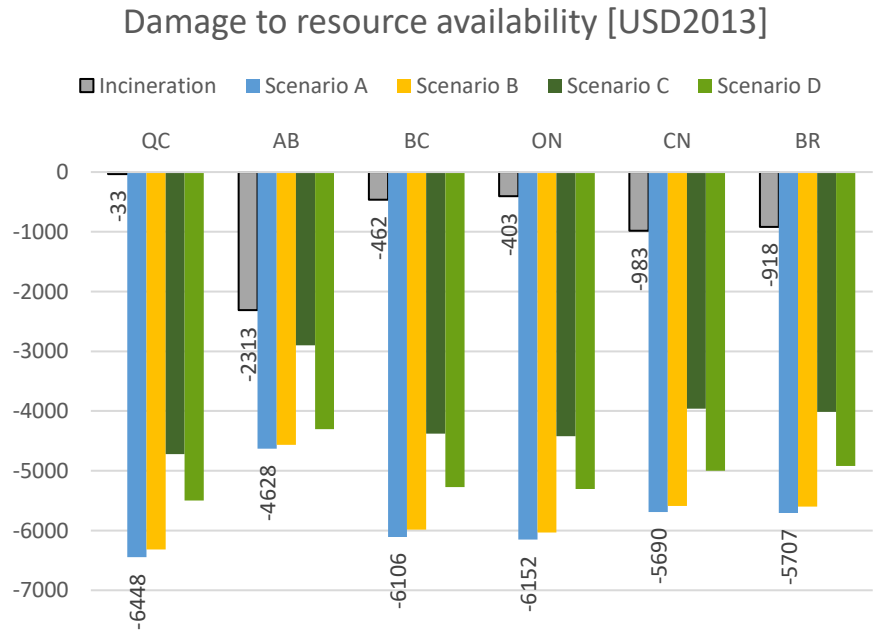

Figure 15. LCIA endpoint results of treating 25 tonne/day of e-waste through various scenarios, Damage to resource availability category

.

4.3.4.2.3. Contribution Analysis

The contribution analysis illustrates how individual processes contribute to the total impact in each category, including both direct and indirect emissions from all involved processes. The purpose of this analysis is to identify the processes with the largest impact (hotspots) across selected categories, which are global warming, fossil fuel scarcity, and water consumption. The results are based on Scenario A in Quebec, CA.

Figure 16 contributed the most to global warming, followed by indirect emissions associated with the electricity used in the pyrolysis and extraction stages. However, recycling chemicals such as styrene and ethylbenzene provides substantial environmental credits because their conventional production routes are highly emission-intensive. These credits offset the direct and indirect emissions of the system. Since the environmental burden of the pyrolysis process is smaller than the environmental credit gained from the recovered products, the overall result is a net reduction in global warming impacts.

A similar trend is observed for fossil resource scarcity, as shown in Figure 17. In this category, the direct and indirect emissions from the pyrolysis system are minor compared to the large credit associated with producing alternative fuels and recovered chemicals such as styrene and ethylbenzene. This outcome demonstrates that the avoided products are the dominant contributors to the overall benefits of the pyrolysis pathway.

For the baseline scenario, as illustrated in **Error! Reference source not found.**, direct emissions from the incineration process were the dominant contributor to the global warming impact in QC. The environmental credit was negligible since avoided emissions resulted from the steam generation, which replaced a low-emission power source in Quebec's power mix. This outcome indicates that, although incineration has relatively low electricity consumption, it provides little opportunity to recover products and generate environmental credits. As a result, incineration lacks the additional benefits that enhance the environmental performance of pyrolysis, where environmental credits are gained through chemical recovery and avoided production. In Alberta, the overall emissions from incineration are negative because of credits earned from steam production, which substitutes for Alberta's energy-intensive power mix.

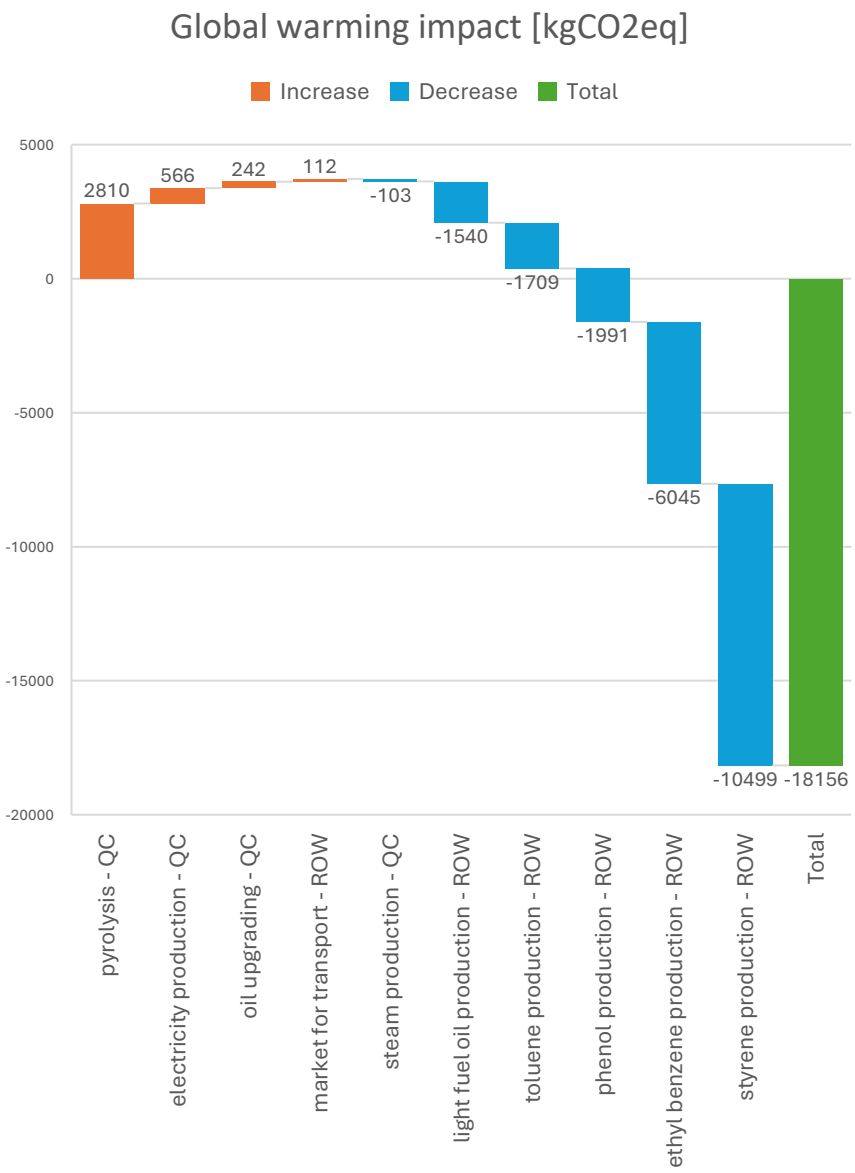

Figure 16. Contribution analysis on global warming impact, referring to QC and scenario A

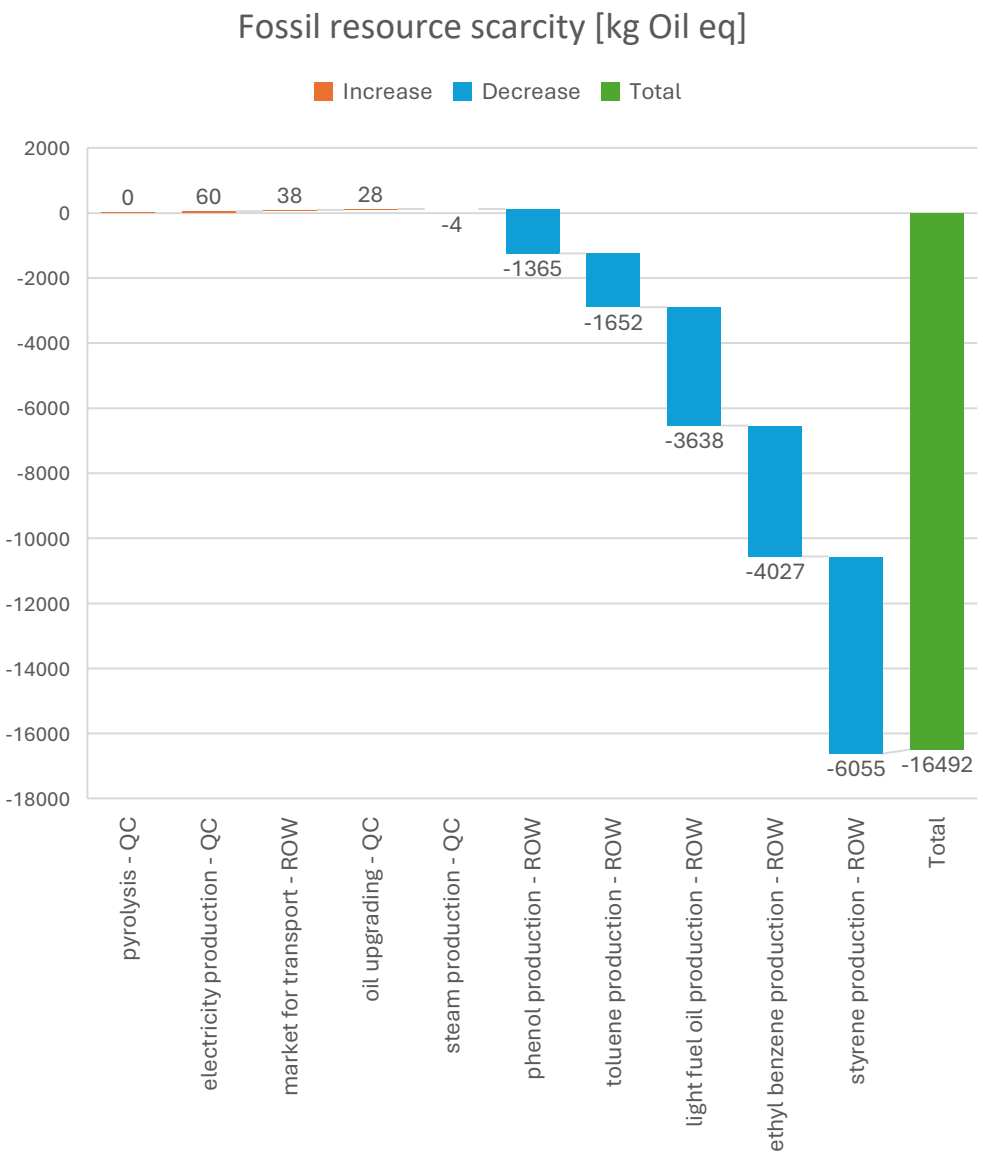

Figure 17. Contribution analysis on fossil resource scarcity, referring to QC and scenario A

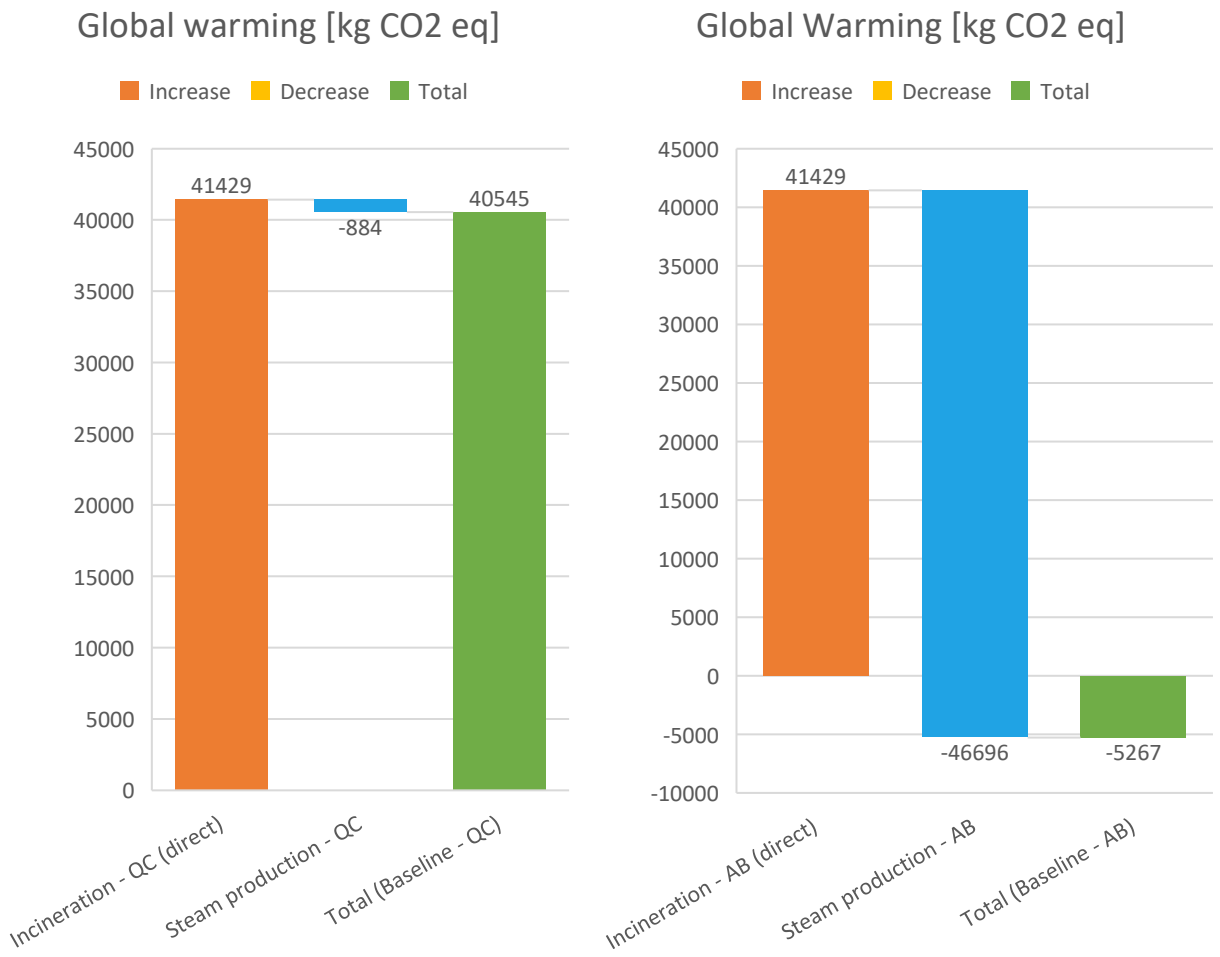

Figure 18. Contribution analysis on global warming, for the baseline scenario in QC (left) and AB (right)

4.3.4.3. Sensitivity analysis

A sensitivity analysis examined how changes in electricity-source emissions affected the performance of the two processing routes, namely the pyrolysis route with oil upgrading (Scenario A) and the baseline incineration route. The emission factor of the electricity mix was varied by adjusting the share of hard coal and run-of-river hydroelectricity. In this analysis, the electricity mix ranged from 100 percent hard coal at the high-emission end to 100 percent run-of-river hydroelectricity at the low-emission end.

The results indicated that pyrolysis's impact on global warming rises as the emissions from electricity sources increase, due to its substantial energy requirements. In contrast, the impact of incineration on global warming diminishes as electricity source emissions increase. This decline is attributed to the avoided burdens from steam generation, a co-product of incineration. When the

electricity mix has higher emissions, the environmental benefit from avoiding steam production is larger, improving the overall performance of incineration.

The findings also indicated that when the electricity mix had low emissions, such as in the case of hydroelectricity from run-of-river, pyrolysis had substantially lower global warming impacts compared to incineration. Pyrolysis remained the environmentally preferable option until the emission factor of the electricity source reached 0.582 and 0.486 kg CO_2-eq per 1 kWh for Scenario A and Scenario D, respectively. Beyond these thresholds, incineration became the more favourable option due to its lower global warming impact.

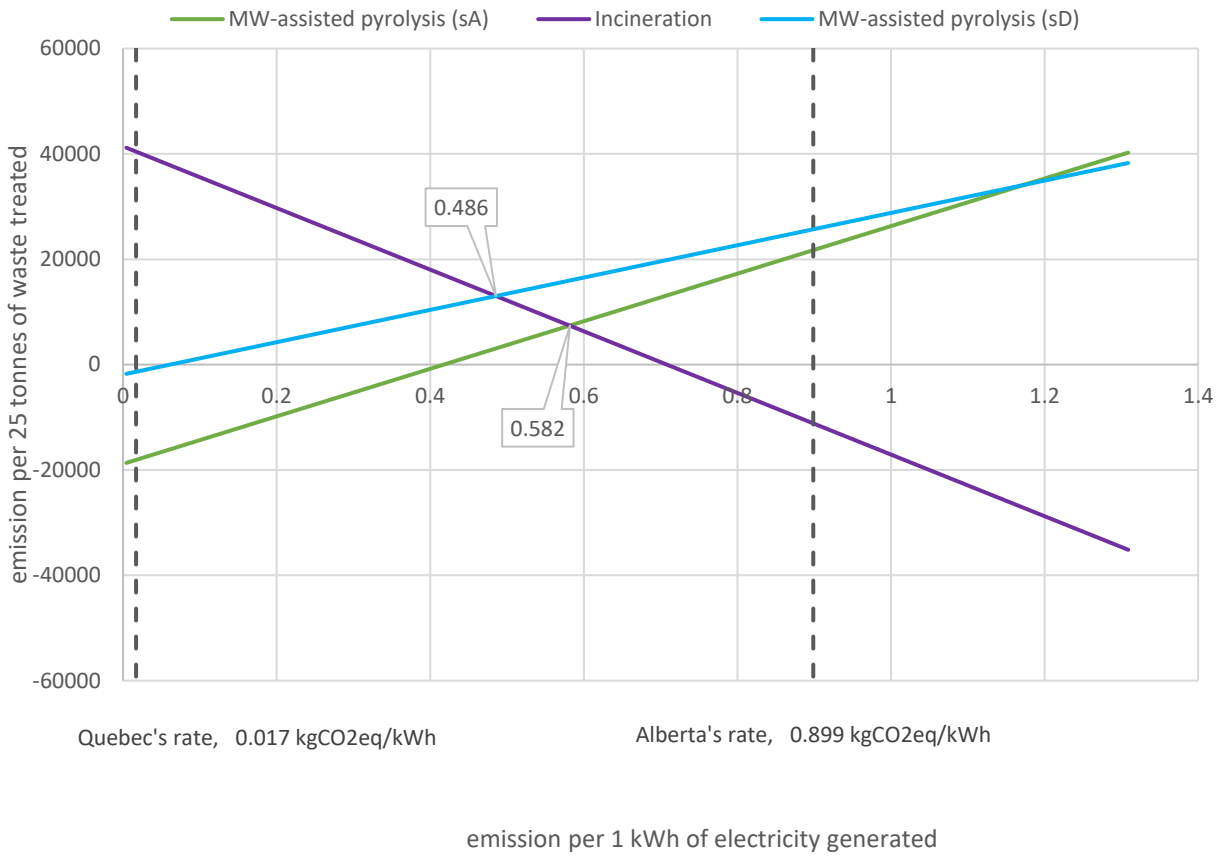

Figure 19. Sensitivity analysis of electricity source emissions on the global warming impact factor for scenarios A and D

4.4. Semi-Continuous Pyrolysis Process

4.4.1. Simulation and regression results

The results of the cases described in Section 3.4 are reported in this section. The BATCH-A configuration is discussed first. In this case, a constant heating rate was applied within each operating step under both atmospheric and vacuum conditions. Several scenarios were simulated by varying the reflux controller parameters, including the maximum controller output and controller gain, as well as the heating rate assigned to each operating step. The scenario that achieved the highest revenue is described in Table 42 and the results are reported in Table 43.

The results for BATCH-B configuration are presented next. For this case, multiple scenarios were evaluated by varying the parameters for both the reflux controller and the heating-rate controller. The scenario that led to the highest revenue, along with its associated operating conditions and outputs, is presented in Table 44 and Table 45. Figure 20 illustrates the changes in reflux ratio and stage 2 temperature over the batch cycle. During the collection of the target products in the first, third, and fifth operating steps, the stage 2 temperature remained constant at the dew point. In this case, the column operated under vacuum conditions, and the maximum reflux ratio was constrained to 65. A sharp decrease in the reflux ratio is observed when the set point is adjusted to collect the next target product.

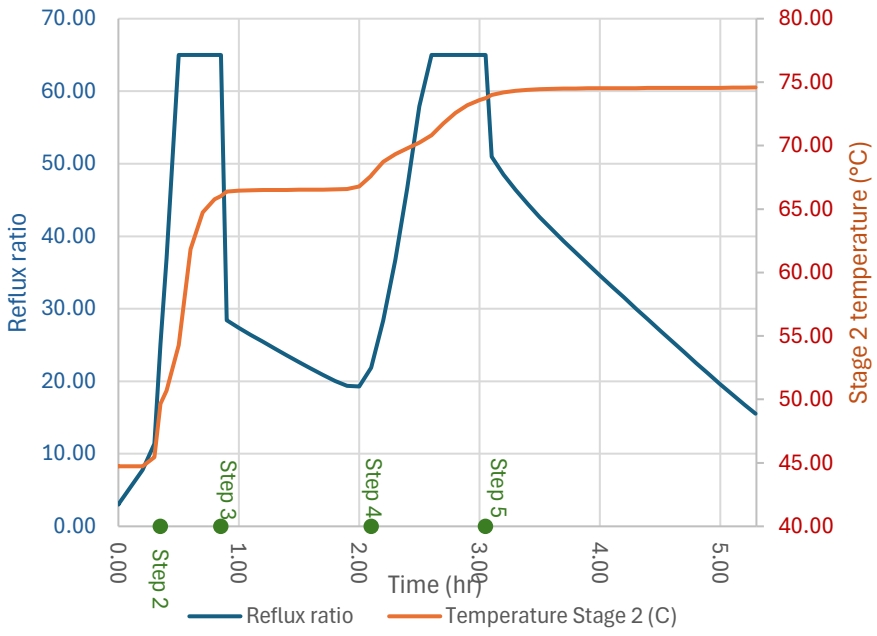

Figure 20. Reflux ratio and stage 2 temperature vs time

The dataset comprised 320 batch runs and was used to develop regression models for predicting annual revenue. Separate regression equations were derived for the BATCH-A and BATCH-B configurations under both atmospheric and vacuum operation. The R^2, reported in Table 41, varied from 0.89 to 0.99, indicating that model accuracy varied across cases.

In several cases, the optimum predicted by the regression model did not coincide with the best-performing scenario in the dataset. The predicted optimal point was therefore verified by running the simulation with the corresponding decision variables. When the simulation results did not reproduce the predicted improved revenue, the discrepancy was attributed to the limitations of the regression model rather than the Excel solver optimizer settings. The default population size was 100, and increasing it did not change the predicted optimum. In these cases, the dataset scenario producing the maximum revenue was selected for subsequent evaluation of the batch process.

Table 41. Regression models (See section 7.1.)

	Atmospheric operation	**Vacuum operation**
BATCH-A	Y_1 (R^2=0.99)	Y_2 (R^2=0.99)
BATCH-B	Y_3 (R^2=0.97)	Y_4 (R^2=0.89)

The regression models can be found in the appendix in the section 7.1. The first two equations, Y_1 and Y_2, belong to BATCH-A cases in atmospheric and vacuum conditions, respectively. In these models, X_1 represents the reflux controller maximum output, X_2 the reflux controller gain, and X_3 to X_7 the specified pot heating rate for each operating step. The following equations, Y_3 and Y_4, belong to BATCH-B cases in atmospheric and vacuum conditions, respectively. For these cases, X_1 denotes the heating rate controller output maximum, X_2 the reflux controller maximum output, X_3 the heating rate controller gain, and X_4 the reflux controller gain.

Results show that choosing vacuum pressure resulted in shorter batch times, increasing the number of batches per year and, consequently, boosting overall revenue. Meanwhile, the vacuum operation was designed to maintain a low column temperature to prevent repolymerization. The entire column temperature remained lower than in atmospheric operation.

Additionally, implementing BATCH-B instead of BATCH-A resulted in more efficient operation. The recovery rates of all products were higher, leading to increased revenue per batch when a heating rate controller was used instead of manual setting. The recovery rate of toluene increased the most compared to the others.

Table 42. Preferred scenario of case BATCH-A with a constant heating rate for each operating step

Type	Variable	Atmospheric operation	Vacuum operation
Reflux controller	Maximum controller output (reflux ratio)	55	*55*
	Controller gain	4	*5*
Heating rate (GJ/hr)	Step 1	1.5	*5*
	Step 2	5	*5*
	Step 3	5	*5*
	Step 4	5	*5*
	Step 5	5	*5*

Table 43. Simulation results of the preferred scenarios of the BATCH-A configuration

Property	Atmospheric operation		Vacuum operation	
Accumulated duty (cal)		1.32×10^{10}		6.57×10^{9}
Batch time (hr)		15.76		9.80
Product quantity (kg) and recovery rate (%)				
Toluene	339.44	85.53%	186.70	47.52%
Ethylbenzene	418.10	52.43%	549.72	69.71%
Styrene	956.10	76.46%	761.16	61.77%
Number of batches per year		555		893
Annual revenue ($)		$890,011		$1,243,410
Annual electricity cost ($)		$250,424		$200,504
Net revenue($)		$639,587		$1,042,905

Table 44. Preferred scenario of the BATCH-B configuration with two controllers

Type	Variable	Atmospheric operation	Vacuum operation
Reflux controller	Maximum controller output (reflux ratio)	60	65
	Controller gain	5	5
Heating duty controller	Maximum controller output (Heating rate)	5	5
	Controller gain	5	5

Table 45. Simulation results of the preferred scenario of the BATCH-B configuration

Property	Atmospheric operation		Vacuum operation	
Accumulated duty (cal)		1.35×10^{10}		6.71×10^{9}
Batch time (hr)		15.84		9.99
Product quantity (kg) and recovery rate (%)				
Toluene	338.02	86.03%	353.17	89.89%
Ethylbenzene	370.65	47.00%	612.16	77.63%
Styrene	980.35	79.55%	819.23	66.48%
Number of batches per year		553		876
Annual revenue ($)		$876,971		$1,441,325
Annual electricity cost ($)		$254,977		$200,805
Net revenue ($)		$621,994		$1,240,520

4.4.2. Cost analysis

The equipment cost of the batch distillation system was estimated using Capital Cost Estimator V14, based on geometry and hydraulic information from Aspen Plus V14. The distillate receivers, R-100 to R-105, were modelled as storage vessels with a height of 2 meters. The pot was represented as a jacketed process vessel with a diameter of 2.5 meters and a tangent-to-tangent height of 2 meters. The condenser was considered a heat exchanger operating at 0.1 bar, condensing the overhead vapour to 30 °C. To obtain realistic column hydraulics, a continuous RedFrac model was built in Aspen Plus V14 using a snapshot of the column profile from the batch simulation at the highest reflux ratio. The cost of the condenser was calculated using a similar method. The equipment costs are listed in Table 46.

A brief cost analysis was performed to assess the batch upgrading process. The cost analysis assumptions were similar to those of the continuous plant, which were described in Table 18, Table 19, and Table 20. Figure 21 shows that operating costs accounted for the majority of the plant's annual expenses, while annualized capital costs accounted for 22%. Table 47 summarizes the economic evaluations of BATCH-A and BATCH-B operated under vacuum pressure. Both showed slightly negative NPVs and required external credit to break even at this scale, given other current assumptions. Results showed that BATCH-B was more profitable than BATCH-A. This suggests that implementing controllers for both the reflux ratio and the pot heating rate provided a more efficient operating strategy than maintaining fixed operating conditions.

Table 46. Estimated equipment costs for the batch distillation and gas recovery unit

Unit	Description	Equipment Cost
Batch distillation unit		
D-100	Rectifying column	$510,000
R-100 to R-105	Five distillate receivers	$113,500
V-100	Jacketed process vessel as the pot	$98,800
C-100	Condenser	$22,700
Gas recovery		
P-107	Increasing pressure of feedwater	$6,000
B-100	Combustion of pyrolytic gas and heat recovery	$7,853
Total		$758,853

.

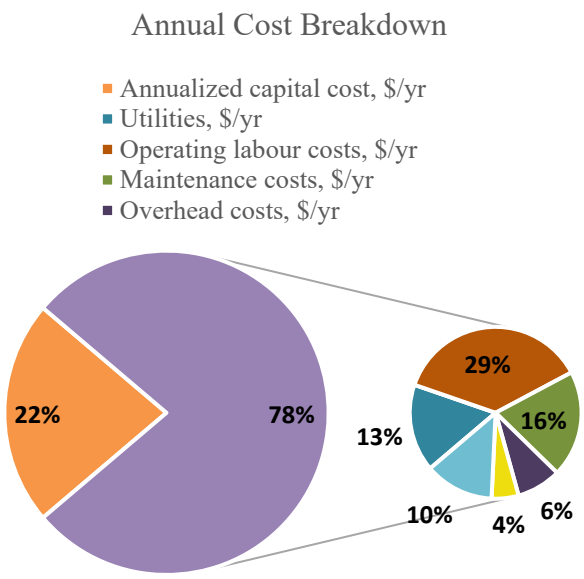

Figure 21. Annual cost breakdown for BATCH-B. Operating costs are expanded in the smaller pie

Table 47. Summary of cost analysis results for both cases operated under vacuum pressure

Economic evaluation summary	BATCH-A	BATCH-B
Raw material cost, $/yr	-	-
Utilities, $/yr	$200,504	$200,805
Operating costs, $/yr	$1,194,732	$1,216,803
Total Capital Investment (TCI), $	$3,958,641	$3,958,641
Annualized capital cost, $/yr	$351,636	$351,636
Total revenue, $/yr	$1,243,410	$1,441,325
NPV, $Million	-$2.80	-$1.06
Minimum credit for e-waste, $/tonne	**50.40**	**19.84**

4.4.3. Sensitivity analysis

4.4.3.1. Increasing the maximum heating output

During the simulation of different operating scenarios, the maximum heating capacity was identified as a key variable that could influence the economic performance of the process. To assess this effect, a sensitivity analysis was carried out by increasing the upper limit of the heating rate and evaluating the process outputs.

For consistency, this modification was applied only to the optimal scenario using the BATCH-B configuration with two controllers. The other variables, namely the reflux controller parameters and the heating rate controller's gain, were kept identical to those in the reference case, described in the previous section. The maximum heating output was previously limited to 5 GJ/hr or 1389 kW. In this section, this limit was raised to 10 GJ/hr (2778 kW) to assess the effect of a higher heating capacity.

The equipment cost was recalculated based on the updated column profile. The higher liquid and vapour flow rates increased the required column size and thus the column cost, which rose by 52% to $775,800. The condenser cost also increased by 22% to $27,800. However, the changes to the cost of the pot and the heating system were not included.

The simulation results and cost analysis are reported in Table 48 and Table 49, while the changes are plotted in Figure 22 and Figure 23. Both the total capital cost and yearly revenue increased by 36% and 26%, respectively. The higher heating rate reduced the duration of each batch by approximately 2 hours and increased the total number of batches per year by 28% or an additional 247 batches. However, the resulting increase in NPV was only around $0.01M, indicating that the higher capital and operating costs offset the increase in revenue.

Table 48. Simulation results of the sensitivity case

Property	Sensitivity scenario
Accumulated duty (cal)	7.65×10^{9}
Batch time (hr)	7.8
Product quantity (kg)	
Toluene	322.77
Ethylbenzene	631.07
Styrene	799.46
Number of batches per year	1123

Table 49. Updated economic evaluation summary for the sensitivity case

Economic evaluation summary	Sensitivity scenario
Utilities, $/yr	$293,733
Operating costs, $/yr	$1,470,988
Total Capital Investment (TCI), $	$4,189,035
Equipment Cost, $	
Column	$775,800
Condenser	$113,500
Annualized capital cost, $/yr	$477,165
Total revenue, $/yr	$1,814,952
NPV, $Million	-$1.05
Minimum credit for e-waste, $/tonne	15.45

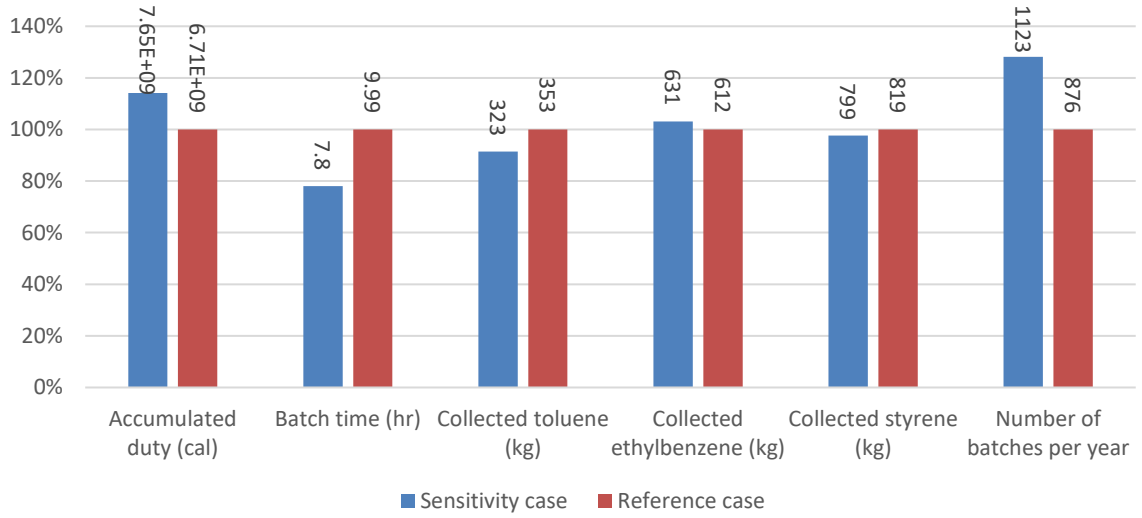

Figure 22. Comparing the batch results for the sensitivity and the reference case

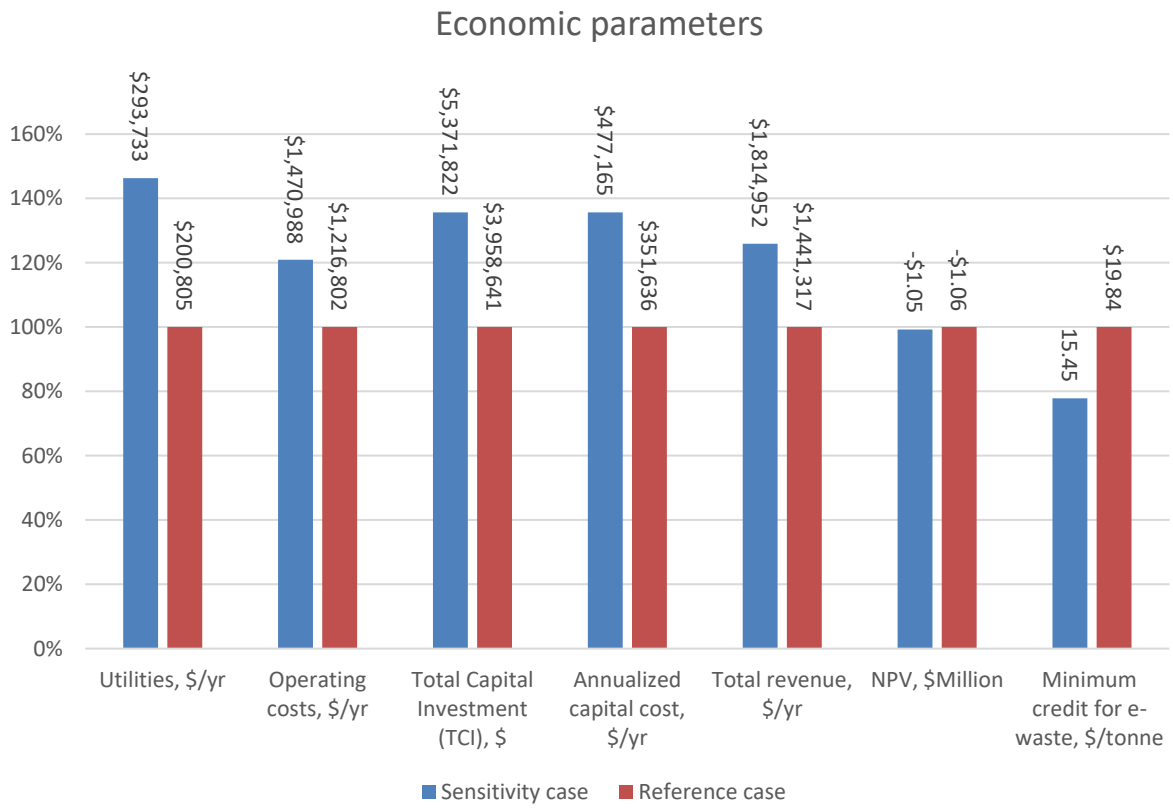

Figure 23. Comparing the economic performance of the sensitivity and the reference case

4.4.3.2. Increasing the number of columns

In the base design, the plant contained one column and one pot, which was charged with 5 tonnes of oil per batch. At this scale and in the scenarios described in Table 42 and Table 44, the plant could treat approximately 3800 to 4500 tonnes of feedstock per year, which was lower than the 6387 tonnes of feedstock available annually. To process all available feedstock, it was necessary to either increase the batch size or install additional columns. In this section, the effect of increasing the number of columns was examined, as this change did not affect the batch time, unlike increasing the batch size.

The analysis considered two identical columns operating in parallel and in a vacuum, with operating steps similar to the optimal scenarios described in Table 42 and Table 44. The total number of required yearly batches and the number of batches per column were obtained by using eq.1 and eq.2. The utilization rate was obtained from eq.3 and used to estimate the annual operating costs, since the increased capacity meant the plant did not need to operate all year.

Results are reported in Table 50, while also illustrated in Figure 24 and Figure 25. Adding a second column increased the process output and revenue. Although the capital cost was doubled, as shown in Figure 24, the net present value for BATCH-A increased by 43% and the required credit reduced by 21%. In BATCH-B, on the other hand, after adding another column, the NPV was no longer negative, indicating that the process was economically viable. Adding another column did not double the utilities and operating costs because feedstock availability limited the maximum total number of batches to 1277. As a result, the plant's utilization rate was approximately 71-73%, and this percentage was used to estimate the operating costs and account for shutdown periods.

eq.1. $$N_{batches,total} = \frac{yearly\ feed}{batch\ size} = \frac{365 \times 17.5}{5} \approx 1278\ batches\ per\ year$$

eq.2. $$N_{batches\ per\ column} = \frac{1278}{2} = 639\ batches\ per\ column\ per\ year$$

eq.3. $$\frac{639\ batches \times batch\ time}{total\ hours\ in\ a\ year} = \%utilization$$

Table 50. Summary of cost analysis results for a plant with two columns

Economic evaluation summary	**BATCH-A**	**BATCH-B**
Utilities, $/yr	$291,434	$297,196
Operating costs, $/yr	$1,278,876	$1,329,902
Total Capital Investment (TCI), $	$7,845,017	$7,845,017
Annualized capital cost, $/yr	$696,853	$696,853

Total revenue, $/yr	$1,776,697	$2,099,453
NPV, $Million	-$1.58	$0.99
Minimum credit for e-waste, $/tonne	**39.43**	-

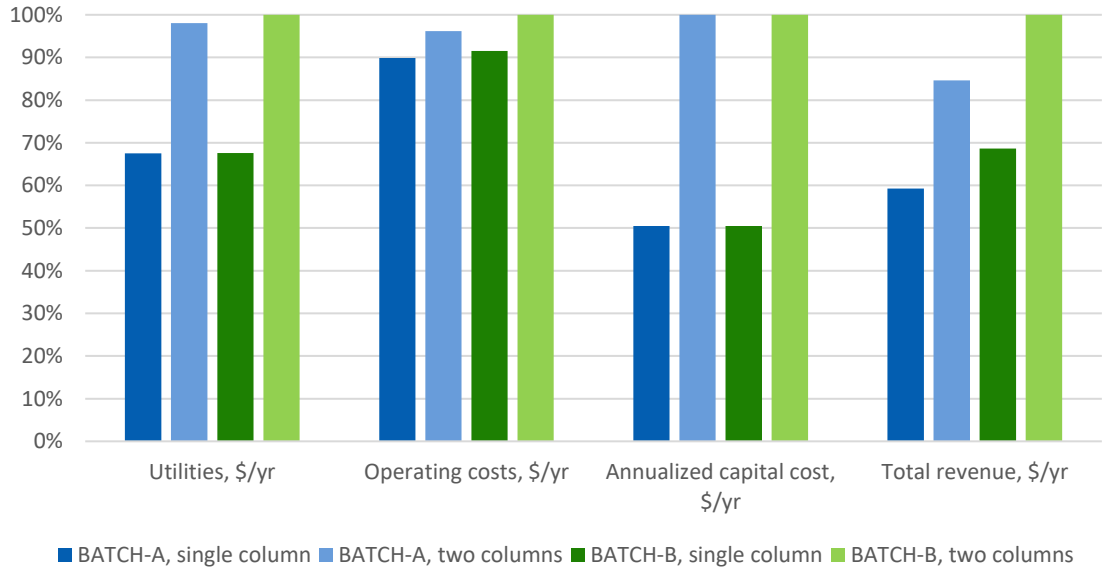

Figure 24. Comparing the normalized cost and revenue of different cases

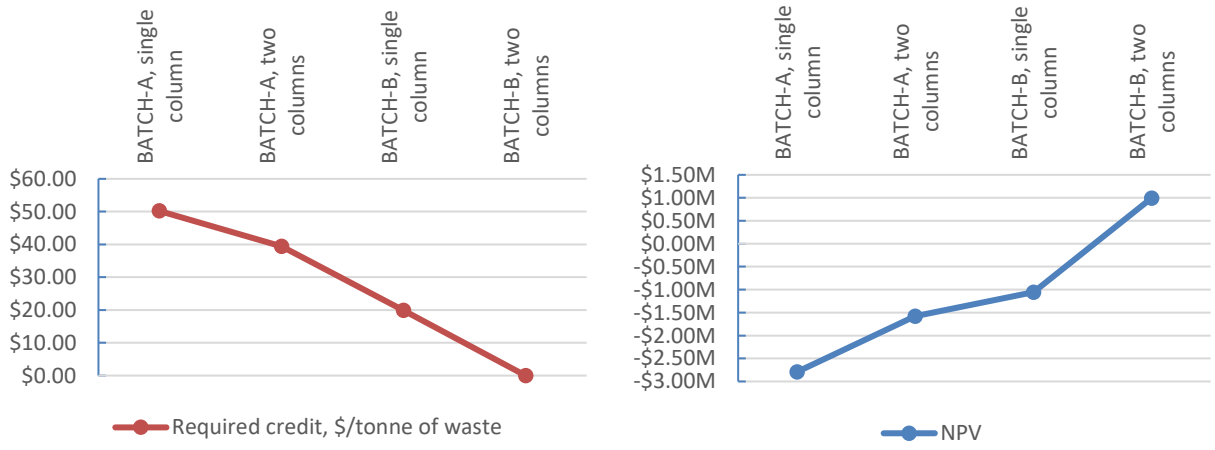

Figure 25. Comparing the NPV and the credit required of different cases

4.4.4. Key findings

The continuous process showed an ideal operation with very high product recovery rates. The batch distillation, however, provided operational flexibility, which is an important advantage when treating feed oils from waste streams that may vary in composition or quantity. This flexibility makes the semi-continuous process more viable when the feed characteristics are inconsistent.

In the batch configuration, the number of required columns was reduced to one or two (depending on the scale) to treat the available feed per year. In the optimal case for BATCH-A configuration, the recovery rate for the target products ranged from 47-70%. The BATCH-B configuration achieved larger recovery rates. Approximately 66-90% of the target products were recovered from each batch charge.

Comparison of the batch operation designs showed that BATCH-B, which used two controllers for the heating rate and the reflux ratio, performed more efficiently than BATCH-A. More of each target product was recovered in each batch cycle, and it resulted in a higher net present value. Although product separation was feasible with a single column, introducing a second, similar column further improved economic performance and enabled a profitable, self-sufficient design capable of processing all available yearly feedstock.

Batch time had a strong influence on economic performance. Shorter batch times enabled more batch runs per year, increasing total product recovery and yearly revenue. The scenarios with the shortest batch durations typically yielded the highest profit.

The maximum output of the controllers was also a critical factor. Lower reflux ratios reduced batch time and increased the number of cycles per year, although they produced slightly lower recovery rates. The shorter duration was more beneficial than the increase in recovery per batch resulting from higher reflux ratios. Similarly, a higher maximum heating rate improved profitability by accelerating column dynamics and reducing batch time.

A sensitivity analysis was performed to assess the impact of the maximum heating rate and the number of columns. Raising the maximum heating rate to 10 GJ/hr shortened the batch duration by 2.2 hours, but the increase was only 1%, which reduced the credit by just $4.28 per tonne of waste. Meanwhile, adding a second column proved to be more advantageous. With two columns, the batch plant became profitable, and the net present value increased to 0.99 million dollars.

5. Conclusion And Future Work

Conclusion

E-waste plastic pyrolysis offers a promising route for both energy and chemical recovery from e-waste plastic that would otherwise be landfilled or incinerated. In this work, the gas recovery and oil upgrading processes were designed and assessed for both continuous and semi-continuous operation. Using LCA, the environmental performance of the MW-assisted pyrolysis route was assessed and compared with that of the conventional incineration process. Additionally, the economic feasibility of the proposed upgrading process was evaluated through technoeconomic analysis.

The oil and gas streams in this study were obtained from an upstream microwave-assisted pyrolysis unit processing 25 tonnes of pre-treated e-waste per day, producing a halogen- and metal-free stream suitable for downstream separation. The continuous distillation configuration recovered toluene, ethylbenzene, and styrene with recovery rates above 80% using five columns, and adding two more columns could recover a high-purity phenol stream, and this configuration was considered the base case. The remaining by-products formed heavy and light residual oil streams suitable for energy recovery. However, the continuous process represented an ideal case, and small-scale waste treatment systems require greater operational flexibility. For this reason, a more practical semi-continuous process was developed to reduce the capital costs and improve flexibility.

The technoeconomic analysis considered an upgrading plant at the reference scale, and the feasibility of the process varied with key economic and design assumptions, including plant capacity and feed oil price. In the base case, which included seven distillation columns at the reference scale, the net present value (NPV) was -1.81 million dollars, and an external incentive of $29.34 per tonne of e-waste plastic treated was required to achieve profitability. When phenol recovery was omitted, the resulting reduction in capital and utility costs increased the NPV to $2.24 million, showing that the process was self-sufficient and required no external credit. The assumed feed oil was critical. When a price of $262 per tonne was used, the NPV decreased significantly, and the required external credit rose to about $157 and $91 for both the base and simplified design. Under these conditions, the plant capacities would require to increase to above roughly 40 and 52 tonnes of e-waste plastic per day to break even.

The environmental performance of the process was assessed using different electricity production mixes from various regions. The pyrolysis route gained substantial environmental credits due to the avoided production of valuable by-products, which would otherwise be produced from fossil fuel-based and emission-intensive routes. In many impact categories, the net impacts were negative, indicating an overall environmental benefit. When the global warming impact was considered, pyrolysis was preferred in Quebec regardless of the oil utilization route, whether the oil was distilled to recover chemicals or used directly as a fuel substitute. In Alberta and China,

however, incineration was favoured because it used less electricity and generated more steam, thereby replacing the carbon-intensive local power. Overall, the benefits of pyrolysis were more noticeable in regions with low-carbon electricity. A critical carbon-intensity threshold of approximately 0.582 kg CO_2-eq was identified, and above this value, incineration has a lower global warming impact than pyrolysis with chemical recovery.

While continuous processes offered very high product recovery rates, batch distillation provided greater flexibility and was therefore more viable for waste-derived feed oils. In the batch configuration, the number of columns was reduced to one while still achieving high recovery, for instance, BATCH-B recovered 66-90% of target products for each batch. Comparing batch designs showed that BATCH-B, which used two controllers for the heating rate and reflux ratio, recovered more product per batch and required a lower rate of $19.89 per tonne of waste as external credit. Adding a second column further improved economic performance and enabled a profitable, self-sufficient design with an NPV of $0.99 million, processing all available yearly feedstock.

Batch time and controller parameters significantly influenced the plant's economic performance. Shorter batch times increased the number of cycles per year, which raised the total product recovery and annual revenue. Lower reflux ratios and higher maximum heating rates generally reduced batch time and enhanced profitability, and in most scenarios, this effect outweighed the benefits of slightly higher recovery rates in longer batch cycles. However, this trend was consistently reliable. A sensitivity analysis confirmed that increasing the maximum heating rate to 10 GJ/hr, while keeping other parameters constant, shortened the batch by 2.2 hours but only marginally affected economic performance, reducing the credit required by $4.28 per tonne of waste and causing a negligible change in net present value.

Future work

Future work could expand the scope of this study beyond gas and oil recovery to include char recovery in both LCA and TEA analyses. The environmental and economic assessment of the batch process could also be extended, including the oil that remains in the pot after styrene recovery. The batch distillation process could also be expanded to enable the recovery of a light oil fraction with a high heating value. For a more comprehensive analysis, the hydrotreatment of the olefin-rich oil product could be investigated to transform it into a suitable fuel. Additionally, the economic assessment in this work relies on several assumptions about the upstream pyrolysis process, particularly the price of the feed oil. Including the upstream process in future simulations will enhance the robustness of the results and decrease uncertainty.

6. References

[1] P. R. Jadhao, E. Ahmad, K. K. Pant, and K. D. P. Nigam, "Environmentally friendly approach for the recovery of metallic fraction from waste printed circuit boards using pyrolysis and ultrasonication," *Waste Manag.*, vol. 118, pp. 150–160, Dec. 2020, doi: 10.1016/j.wasman.2020.08.028.

[2] "Global e-Waste Monitor 2024: Electronic Waste Rising Five Times Faster than Documented E-waste Recycling | UNITAR." Accessed: Jul. 17, 2025. [Online]. Available: https://unitar.org/about/news-stories/press/global-e-waste-monitor-2024-electronic-waste-rising-five-times-faster-documented-e-waste-recycling

[3] ewastemonitor, "GEM 2020," E-Waste Monitor. Accessed: Jul. 17, 2025. [Online]. Available: https://ewastemonitor.info/gem-2020/

[4] Á. Risco, D. Sucunza, and S. González-Egido, "Chemical recovery of waste electrical and electronic equipment by microwave-assisted pyrolysis: A review," *J. Anal. Appl. Pyrolysis*, vol. 159, p. 105323, Oct. 2021, doi: 10.1016/j.jaap.2021.105323.

[5] J. Dong, Y. Tang, A. Nzihou, Y. Chi, E. Weiss-Hortala, and M. Ni, "Life cycle assessment of pyrolysis, gasification and incineration waste-to-energy technologies: Theoretical analysis and case study of commercial plants," *Sci. Total Environ.*, vol. 626, pp. 744–753, Jun. 2018, doi: 10.1016/j.scitotenv.2018.01.151.

[6] P. Evangelopoulos, S. Arato, H. Persson, E. Kantarelis, and W. Yang, "Reduction of brominated flame retardants (BFRs) in plastics from waste electrical and electronic equipment (WEEE) by solvent extraction and the influence on their thermal decomposition," *Waste Manag.*, vol. 94, pp. 165–171, Jul. 2019, doi: 10.1016/j.wasman.2018.06.018.

[7] H. Wang, S. Zhang, B. Li, D. Pan, Y. Wu, and T. Zuo, "Recovery of waste printed circuit boards through pyrometallurgical processing: A review," *Resour. Conserv. Recycl.*, vol. 126, pp. 209–218, Nov. 2017, doi: 10.1016/j.resconrec.2017.08.001.

[8] J. Moltó, R. Font, A. Gálvez, and J. A. Conesa, "Pyrolysis and combustion of electronic wastes," *J. Anal. Appl. Pyrolysis*, vol. 84, no. 1, pp. 68–78, Jan. 2009, doi: 10.1016/j.jaap.2008.10.023.

[9] P. Das, J.-C. P. Gabriel, C. Y. Tay, and J.-M. Lee, "Value-added products from thermochemical treatments of contaminated e-waste plastics," *Chemosphere*, vol. 269, p. 129409, Apr. 2021, doi: 10.1016/j.chemosphere.2020.129409.

[10] R. Wang and Z. Xu, "Recycling of non-metallic fractions from waste electrical and electronic equipment (WEEE): A review," *Waste Manag.*, vol. 34, no. 8, pp. 1455–1469, Aug. 2014, doi: 10.1016/j.wasman.2014.03.004.

[11] D. V. Suriapparao, S. Batchu, S. Jayasurya, and R. Vinu, "Selective production of phenolics from waste printed circuit boards via microwave assisted pyrolysis," *J. Clean. Prod.*, vol. 197, pp. 525–533, Oct. 2018, doi: 10.1016/j.jclepro.2018.06.203.

[12] L. Esposito, L. Cafiero, D. De Angelis, R. Tuffi, and S. Vecchio Ciprioti, "Valorization of the plastic residue from a WEEE treatment plant by pyrolysis," *Waste Manag.*, vol. 112, pp. 1–10, 2020, doi: 10.1016/j.wasman.2020.05.022.

[13] G. F. Cardamone, F. Ardolino, and U. Arena, "About the environmental sustainability of the European management of WEEE plastics," *Waste Manag.*, vol. 126, pp. 119–132, May 2021, doi: 10.1016/j.wasman.2021.02.040.

[14] A. Bifulco, J. Chen, A. Sekar, W. W. Klingler, A. Gooneie, and S. Gaan, “Recycling of flame retardant polymers: Current technologies and future perspectives,” *J. Mater. Sci. Technol.*, vol. 199, pp. 156–183, Nov. 2024, doi: 10.1016/j.jmst.2024.02.039.
[15] Y. Liu, J. Zhang, X. Yang, W. Yang, Y. Chen, and C. Wang, “Efficient recovery of valuable metals from waste printed circuit boards by microwave pyrolysis,” *Chin. J. Chem. Eng.*, vol. 40, pp. 262–268, Dec. 2021, doi: 10.1016/j.cjche.2020.11.008.
[16] A. Andooz, M. Eqbalpour, E. Kowsari, S. Ramakrishna, and Z. A. Cheshmeh, “A comprehensive review on pyrolysis of E-waste and its sustainability,” *J. Clean. Prod.*, vol. 333, p. 130191, Jan. 2022, doi: 10.1016/j.jclepro.2021.130191.
[17] D. Lee *et al.*, “Characteristics of fractionated drop-in liquid fuel of plastic wastes from a commercial pyrolysis plant,” *Waste Manag.*, vol. 126, pp. 411–422, May 2021, doi: 10.1016/j.wasman.2021.03.020.
[18] R. Krzywda and B. Wrzesińska, “Simulation of the Condensation and Fractionation Unit in Waste Plastics Pyrolysis Plant,” *Waste Biomass Valorization*, vol. 12, no. 1, pp. 91–104, Jan. 2021, doi: 10.1007/s12649-020-00994-7.
[19] S. Belbessai, A. Azara, and N. Abatzoglou, “Recent Advances in the Decontamination and Upgrading of Waste Plastic Pyrolysis Products: An Overview,” *Processes*, vol. 10, no. 4, Art. no. 4, Apr. 2022, doi: 10.3390/pr10040733.
[20] J. Joo, E. E. Kwon, and J. Lee, “Achievements in pyrolysis process in E-waste management sector,” *Environ. Pollut.*, vol. 287, p. 117621, Oct. 2021, doi: 10.1016/j.envpol.2021.117621.
[21] T. Zhang *et al.*, “Microwave-assisted catalytic pyrolysis of waste printed circuit boards, and migration and distribution of bromine,” *J. Hazard. Mater.*, vol. 402, p. 123749, Jan. 2021, doi: 10.1016/j.jhazmat.2020.123749.
[22] A. Undri, M. Frediani, L. Rosi, and P. Frediani, “Reverse polymerization of waste polystyrene through microwave assisted pyrolysis,” *J. Anal. Appl. Pyrolysis*, vol. 105, pp. 35–42, Jan. 2014, doi: 10.1016/j.jaap.2013.10.001.
[23] Y.-F. Huang and S.-L. Lo, “Energy recovery from waste printed circuit boards using microwave pyrolysis: product characteristics, reaction kinetics, and benefits,” *Environ. Sci. Pollut. Res.*, vol. 27, no. 34, pp. 43274–43282, Dec. 2020, doi: 10.1007/s11356-020-10304-2.
[24] C. Khaobang, P. Sarabhorn, C. Siripaiboon, F. Scala, and C. Areeprasert, “Pilot-scale combined pyrolysis and decoupling biomass gasification for energy and metal recovery from discarded printed circuit board and waste cable,” *Energy*, vol. 245, p. 123268, Apr. 2022, doi: 10.1016/j.energy.2022.123268.
[25] J. Baena-González, A. Santamaria-Echart, J. L. Aguirre, and S. González, “Chemical recycling of plastic waste: Bitumen, solvents, and polystyrene from pyrolysis oil,” *Waste Manag.*, vol. 118, pp. 139–149, Dec. 2020, doi: 10.1016/j.wasman.2020.08.035.
[26] N. Hassibi, Y. A. Vega-Bustos, M. H. Aissaoui, G. Mauviel, and V. Burklé-Vitzthum, “Thermochemical Recycling of Polystyrene by Pyrolysis: Importance of the Reflux to Maximize the Production of Styrene and BTEX,” *Ind. Eng. Chem. Res.*, vol. 62, no. 34, pp. 13432–13439, Aug. 2023, doi: 10.1021/acs.iecr.3c01692.
[27] C. Areeprasert and C. Khaobang, “Pyrolysis and catalytic reforming of ABS/PC and PCB using biochar and e-waste char as alternative green catalysts for oil and metal recovery,” *Fuel Process. Technol.*, vol. 182, pp. 26–36, Dec. 2018, doi: 10.1016/j.fuproc.2018.10.006.

[28] I. de Marco *et al.*, “Pyrolysis of electrical and electronic wastes,” *J. Anal. Appl. Pyrolysis*, vol. 82, no. 2, pp. 179–183, Jul. 2008, doi: 10.1016/j.jaap.2008.03.011.
[29] R. Mishra, A. Kumar, E. Singh, and S. Kumar, “Recent Research Advancements in Catalytic Pyrolysis of Plastic Waste,” *ACS Sustain. Chem. Eng.*, vol. 11, no. 6, pp. 2033–2049, Feb. 2023, doi: 10.1021/acssuschemeng.2c05759.
[30] A. Fivga and I. Dimitriou, “Pyrolysis of plastic waste for production of heavy fuel substitute: A techno-economic assessment,” *Energy*, vol. 149, pp. 865–874, Apr. 2018, doi: 10.1016/j.energy.2018.02.094.
[31] S. Ügdüler, K. M. Van Geem, M. Roosen, E. I. P. Delbeke, and S. De Meester, “Challenges and opportunities of solvent-based additive extraction methods for plastic recycling,” *Waste Manag.*, vol. 104, pp. 148–182, Mar. 2020, doi: 10.1016/j.wasman.2020.01.003.
[32] J. Xiong *et al.*, “Pyrolysis treatment of nonmetal fraction of waste printed circuit boards: Focusing on the fate of bromine,” *Waste Manag. Res.*, vol. 38, no. 11, pp. 1251–1258, 2020, doi: 10.1177/0734242X19894621.
[33] R. Gao and Z. Xu, “Pyrolysis and utilization of nonmetal materials in waste printed circuit boards: Debromination pyrolysis, temperature-controlled condensation, and synthesis of oil-based resin,” *J. Hazard. Mater.*, vol. 364, pp. 1–10, Feb. 2019, doi: 10.1016/j.jhazmat.2018.09.096.
[34] A. López, I. de Marco, B. M. Caballero, M. F. Laresgoiti, and A. Adrados, “Dechlorination of fuels in pyrolysis of PVC containing plastic wastes,” *Fuel Process. Technol.*, vol. 92, no. 2, pp. 253–260, Feb. 2011, doi: 10.1016/j.fuproc.2010.05.008.
[35] J. Sun, W. Wang, Z. Liu, and C. Ma, “Recycling of Waste Printed Circuit Boards by Microwave-Induced Pyrolysis and Featured Mechanical Processing,” *Ind. Eng. Chem. Res.*, vol. 50, no. 20, pp. 11763–11769, Oct. 2011, doi: 10.1021/ie2013407.
[36] Y. Shen, X. Chen, X. Ge, and M. Chen, “Thermochemical treatment of non-metallic residues from waste printed circuit board: Pyrolysis vs. combustion,” *J. Clean. Prod.*, vol. 176, pp. 1045–1053, Mar. 2018, doi: 10.1016/j.jclepro.2017.11.232.
[37] H. Wang, S. Zhang, B. Li, D. Pan, Y. Wu, and T. Zuo, “Recovery of waste printed circuit boards through pyrometallurgical processing: A review,” *Resour. Conserv. Recycl.*, vol. 126, pp. 209–218, Nov. 2017, doi: 10.1016/j.resconrec.2017.08.001.
[38] W. J. Hall and P. T. Williams, “Removal of organobromine compounds from the pyrolysis oils of flame retarded plastics using zeolite catalysts,” *J. Anal. Appl. Pyrolysis*, vol. 81, no. 2, pp. 139–147, Mar. 2008, doi: 10.1016/j.jaap.2007.09.008.
[39] F. Vilaplana, A. Ribes-Greus, and S. Karlsson, “Microwave-assisted extraction for qualitative and quantitative determination of brominated flame retardants in styrenic plastic fractions from waste electrical and electronic equipment (WEEE),” *Talanta*, vol. 78, no. 1, pp. 33–39, Apr. 2009, doi: 10.1016/j.talanta.2008.10.038.
[40] D. S. Achilias, M.-A. Charitopoulou, and S. V. Ciprioti, “Thermal and Catalytic Recycling of Plastics from Waste Electrical and Electronic Equipment—Challenges and Perspectives,” *Polymers*, vol. 16, no. 17, Art. no. 17, Jan. 2024, doi: 10.3390/polym16172538.
[41] M. Attai and S. Farag, “Process for recycling contaminated solid materials and purification of gases,” WO 2021/237342 A1, Dec. 02, 2021
[42] K.-B. Park, Y.-S. Jeong, B. Guzelciftci, and J.-S. Kim, “Two-stage pyrolysis of polystyrene: Pyrolysis oil as a source of fuels or benzene, toluene, ethylbenzene, and xylenes,” *Appl. Energy*, vol. 259, p. 114240, Feb. 2020, doi: 10.1016/j.apenergy.2019.114240.

[43] T. Xayachak *et al.*, “Pyrolysis for plastic waste management: An engineering perspective,” *J. Environ. Chem. Eng.*, vol. 10, no. 6, p. 108865, Dec. 2022, doi: 10.1016/j.jece.2022.108865.
[44] M. Artetxe *et al.*, “Styrene recovery from polystyrene by flash pyrolysis in a conical spouted bed reactor,” *Waste Manag.*, vol. 45, pp. 126–133, Nov. 2015, doi: 10.1016/j.wasman.2015.05.034.
[45] A. Zayoud *et al.*, “Pyrolysis of end-of-life polystyrene in a pilot-scale reactor: Maximizing styrene production,” *Waste Manag.*, vol. 139, pp. 85–95, Feb. 2022, doi: 10.1016/j.wasman.2021.12.018.
[46] C. Muhammad, J. A. Onwudili, and P. T. Williams, “Catalytic pyrolysis of waste plastic from electrical and electronic equipment,” *J. Anal. Appl. Pyrolysis*, vol. 113, pp. 332–339, May 2015, doi: 10.1016/j.jaap.2015.02.016.
[47] A. Terapalli *et al.*, “Microwave-assisted *in-situ* catalytic pyrolysis of polystyrene: Analysis of product formation and energy consumption using machine learning approach,” *Process Saf. Environ. Prot.*, vol. 166, pp. 57–67, Oct. 2022, doi: 10.1016/j.psep.2022.08.016.
[48] R. Miandad, M. A. Barakat, A. S. Aburiazaiza, M. Rehan, and A. S. Nizami, “Catalytic pyrolysis of plastic waste: A review,” *Process Saf. Environ. Prot.*, vol. 102, pp. 822–838, Jul. 2016, doi: 10.1016/j.psep.2016.06.022.
[49] W. Zeb *et al.*, “Fractional distillation of waste plastic pyrolysis oil for isolating narrow hydrocarbons cuts,” *Fuel*, vol. 379, p. 133055, Jan. 2025, doi: 10.1016/j.fuel.2024.133055.
[50] M. Kusenberg *et al.*, “Assessing the feasibility of chemical recycling via steam cracking of untreated plastic waste pyrolysis oils: Feedstock impurities, product yields and coke formation,” *Waste Manag.*, vol. 141, pp. 104–114, Mar. 2022, doi: 10.1016/j.wasman.2022.01.033.
[51] J. n. Sahu *et al.*, “Feasibility study for catalytic cracking of waste plastic to produce fuel oil with reference to Malaysia and simulation using ASPEN Plus,” *Environ. Prog. Sustain. Energy*, vol. 33, no. 1, pp. 298–307, 2014, doi: 10.1002/ep.11748.
[52] H. K. V. Gurram, S. H. Pamu, and S. A. Singh, “Parametric studies on fractionation column design for the separation of plastic waste pyrolysis oil into valuable fuels,” *J. Environ. Chem. Eng.*, vol. 12, no. 2, p. 112390, Apr. 2024, doi: 10.1016/j.jece.2024.112390.
[53] W. Zeb *et al.*, “Purification and characterisation of post-consumer plastic pyrolysis oil fractionated by vacuum distillation,” *J. Clean. Prod.*, vol. 416, p. 137881, Sep. 2023, doi: 10.1016/j.jclepro.2023.137881.
[54] M. I. Jahirul, M. G. Rasul, F. Faisal, M. A. Sattar, and R. B. Dexter, “Standard diesel production from mixed waste plastics through thermal pyrolysis and vacuum distillation,” *Energy Rep.*, vol. 9, pp. 540–545, Oct. 2023, doi: 10.1016/j.egyr.2023.09.179.
[55] T. Rieger, J. C. Oey, V. Palchyk, A. Hofmann, M. Franke, and A. Hornung, “Chemical Recycling of WEEE Plastics—Production of High Purity Monocyclic Aromatic Chemicals,” *Processes*, vol. 9, no. 3, Art. no. 3, Mar. 2021, doi: 10.3390/pr9030530.
[56] U. R. Gracida-Alvarez, O. Winjobi, J. C. Sacramento-Rivero, and D. R. Shonnard, “System Analyses of High-Value Chemicals and Fuels from a Waste High-Density Polyethylene Refinery. Part 2: Carbon Footprint Analysis and Regional Electricity Effects,” *ACS Sustain. Chem. Eng.*, vol. 7, no. 22, pp. 18267–18278, 2019, doi: 10.1021/acssuschemeng.9b04764.
[57] U. R. Gracida-Alvarez, O. Winjobi, J. C. Sacramento-Rivero, and D. R. Shonnard, “System Analyses of High-Value Chemicals and Fuels from a Waste High-Density Polyethylene Refinery. Part 1: Conceptual Design and Techno-Economic Assessment,” *ACS Sustain.*

Chem. Eng., vol. 7, no. 22, pp. 18254–18266, Nov. 2019, doi: 10.1021/acssuschemeng.9b04763.
[58] D. Kim, Y. Shin, M. Lee, J. Lee, Y.-J. Lee, and J. W. Lee, "Energy-Efficient Design Sequences for the Purification of Styrene Monomer from the Pyrolysis Oil of Waste Polystyrene," *Ind. Eng. Chem. Res.*, vol. 63, no. 33, pp. 14761–14776, 2024, doi: 10.1021/acs.iecr.4c01004.
[59] Y. Liu, J. Qian, and J. Wang, "Pyrolysis of polystyrene waste in a fluidized-bed reactor to obtain styrene monomer and gasoline fraction," *Fuel Process. Technol.*, vol. 63, no. 1, pp. 45–55, 2000, doi: 10.1016/S0378-3820(99)00066-1.
[60] M. Holtkamp, M. Renner, K. Matthiesen, M. Wald, G. A. Luinstra, and P. Biessey, "Robust downstream technologies in polystyrene waste pyrolysis: Design and prospective life-cycle assessment of pyrolysis oil reintegration pathways," *Resour. Conserv. Recycl.*, vol. 205, p. 107558, Jun. 2024, doi: 10.1016/j.resconrec.2024.107558.
[61] R. Dahal, P. Uusi-Kyyny, J.-P. Pokki, T. Ohra-aho, and V. Alopaeus, "Conceptual design of a distillation process for the separation of styrene monomer from polystyrene pyrolysis oil: experiment and simulation," *Chem. Eng. Res. Des.*, vol. 195, pp. 65–75, Jul. 2023, doi: 10.1016/j.cherd.2023.05.039.
[62] A. Merkel, L. Plessing, G. A. Luinstra, M. Grünewald, and P. Biessey, "Development of a Separation Sequence for the Integration of a Styrene Recyclate into Polystyrene Production," *Chem. Ing. Tech.*, vol. 95, no. 8, pp. 1323–1331, 2023, doi: 10.1002/cite.202100210.
[63] U. Diwekar, *Batch Distillation: Simulation, Optimal Design, and Control, Second Edition*, 2nd ed. Boca Raton: CRC Press, 2011. doi: 10.1201/b11705.
[64] *Perry's Chemical Engineers' Handbook, Eighth Edition*, 8th ed. /. McGraw-Hill Education, 2008. Accessed: Feb. 18, 2025. [Online]. Available: https://www.accessengineeringlibrary.com/content/book/9780071422949
[65] H. Ismail and M. M. Hanafiah, "Evaluation of e-waste management systems in Malaysia using life cycle assessment and material flow analysis," *J. Clean. Prod.*, vol. 308, p. 127358, Jul. 2021, doi: 10.1016/j.jclepro.2021.127358.
[66] S. M. Alston and J. C. Arnold, "Environmental Impact of Pyrolysis of Mixed WEEE Plastics Part 2: Life Cycle Assessment," *Environ. Sci. Technol.*, vol. 45, no. 21, pp. 9386–9392, Nov. 2011, doi: 10.1021/es2016654.
[67] A. Schulte, M. Lamb-Scheffler, P. Biessey, and T. Rieger, "Prospective LCA of Waste Electrical and Electronic Equipment Thermo-Chemical Recycling by Pyrolysis," *Chem. Ing. Tech.*, vol. 95, no. 8, pp. 1268–1281, 2023, doi: 10.1002/cite.202300036.
[68] J. V. J. Krishna, S. S. Damir, and R. Vinu, "Pyrolysis of electronic waste and their mixtures: Kinetic and pyrolysate composition studies," *J. Environ. Chem. Eng.*, vol. 9, no. 4, 2021, doi: 10.1016/j.jece.2021.105382.
[69] D. Han, X. Yang, R. Li, and Y. Wu, "Environmental impact comparison of typical and resource-efficient biomass fast pyrolysis systems based on LCA and Aspen Plus simulation," *J. Clean. Prod.*, vol. 231, pp. 254–267, Sep. 2019, doi: 10.1016/j.jclepro.2019.05.094.
[70] "Production Occupations," Bureau of Labor Statistics. Accessed: Nov. 20, 2025. [Online]. Available: https://www.bls.gov/oes/2023/may/oes510000.htm
[71] M. S. Peters, K. D. Timmerhaus, and R. E. West, *Plant Design and Economics for Chemical Engineers*, 5th Edition. McGraw-Hill Education, 2003.

[72] Hydro-Québec, “Electricity Rates.” Accessed: Oct. 15, 2024. [Online]. Available: https://www.hydroquebec.com/data/documents-donnees/pdf/electricity-rates.pdf
[73] “Toluene - Sigma-Aldrich.” Accessed: Aug. 28, 2024. [Online]. Available: https://www.sigmaaldrich.com/CA/en/substance/toluene9214108883
[74] “Styrene price index,” businessanalytiq. Accessed: Oct. 20, 2024. [Online]. Available: https://businessanalytiq.com/procurementanalytics/index/styrene-price-index/
[75] “Ethylbenzene Price - Historical & Current | Intratec.us.” Accessed: Oct. 20, 2024. [Online]. Available: https://www.intratec.us/solutions/primary-commodity-prices/commodity/ethylbenzene-prices
[76] “Phenol Price - Current & Forecasts | Intratec.us.” Accessed: Oct. 20, 2024. [Online]. Available: https://www.intratec.us/solutions/primary-commodity-prices/commodity/phenol-prices
[77] N. R. C. Government of Canada, “Daily Average Wholesale (Rack) Prices for Furnace Oil (Daily only shows the last 60 days) | Energy Sources.” Accessed: Oct. 20, 2024. [Online]. Available: https://www2.nrcan.gc.ca/eneene/sources/pripri/wholesale_bycity_e.cfm?priceYear=2023&productID=15&locationID=66,8,39,29,17&frequency=D#priceGraph
[78] A. F. Schneider and X. Zeng, “Investigations into the transition toward an established e-waste management system in China: Empirical evidence from Guangdong and Shaanxi,” *Curr. Res. Environ. Sustain.*, vol. 4, p. 100195, Jan. 2022, doi: 10.1016/j.crsust.2022.100195.
[79] U. Arena and F. Ardolino, “Technical and environmental performances of alternative treatments for challenging plastics waste,” *Resour. Conserv. Recycl.*, vol. 183, 2022, doi: 10.1016/j.resconrec.2022.106379.
[80] Brooke E. Rogachuk and Jude A. Okolie, “Waste tires based biorefinery for biofuels and value-added materials production,” *Chem. Eng. J. Adv.*, vol. 14, p. 100476, 2023.
[81] “ReCiPe,” PRé Sustainability. Accessed: Nov. 21, 2025. [Online]. Available: https://pre-sustainability.com/articles/recipe/
[82] “electricity, high voltage, production mix - China, Guangdong (广东) - electricity, high voltage | ecoQuery.” Accessed: Nov. 21, 2025. [Online]. Available: https://ecoquery.ecoinvent.org/3.8/cutoff/dataset/25041/documentation
[83] “‘electricity, high voltage, production mix – Canada, Alberta – electricity, high voltage | ecoQuery,’” ecoQuery (ecoinvent). [Online]. Available: https://ecoquery.ecoinvent.org/3.8/cutoff/dataset/25136/documentation
[84] “electricity, high voltage, production mix - Canada, Ontario - electricity, high voltage | ecoQuery.” Accessed: Nov. 21, 2025. [Online]. Available: https://ecoquery.ecoinvent.org/3.8/cutoff/dataset/24998/documentation
[85] “electricity, high voltage, production mix - Brazil - electricity, high voltage | ecoQuery.” Accessed: Nov. 21, 2025. [Online]. Available: https://ecoquery.ecoinvent.org/3.8/cutoff/dataset/24688/documentation

7. Appendix

Table A1. Feed composition as defined in the simulation of the continuous process

Component ID	Component name	Mass fraction in feed (%)
TRANS-01	(E)-Stilbene	0.153%
ALPHA-01	,alpha,-Methylstyrene	1.633%
BIPHE-01	1,1'-Biphenyl, 4-methyl-	0.118%
1:2-D-01	1,2-Diphenylcyclopropane	0.412%
1:3-B-01	1,3-Dicyanobenzene	0.228%
DI-2--01	1,4-Benzenedicarboxylic acid, bis(2-ethylhexyl) ester	0.153%
2:4-D-01	2,4-Diphenyl-4-methyl-1-pentene	1.544%
ACENA-01	Acenaphthene	0.121%
N-ETH-01	Benzenamine, N-ethyl-	0.684%
ISOPR-01	Benzene, (1-methylethyl)-	3.250%
PHENY-01	Benzene, (phenoxymethyl)-	0.204%
2:3-D-01	Benzene, 1,1'-(1,1,2,2-tetramethyl-1,2-ethanediyl)bis-	0.353%
1:3-D-01	Benzene, 1,1'-(1,3-propanediyl)bis-	6.563%
BUTAN-01	Benzene, 1,1'-(1,4-butanediyl)bis-	0.225%
BUTAN-02	Benzene, 1,1'-(1-methyl-1,3-propanediyl)bis-	0.651%
BENZE-01	Benzene, 1-ethynyl-4-methyl-	0.176%
PHENY-02	Benzene, cyclopropyl-	0.266%
N-BUT-01	Benzene, n-butyl-	0.121%
N-ETH-02	Benzene, propyl-	0.198%
DIMET-01	Benzenemethanol, ,alpha,,,alpha,-dimethyl-	0.294%
BENZO-01	Benzonitrile	0.124%
PHENY-03	Benzyl nitrile	0.238%
1:2-D-02	Bibenzyl	0.166%
ETYLBENZ	Ethylbenzene	14.016%
FLUOR-01	Fluorene	0.136%
N-HEX-01	Hexadecane	0.132%
NAPHT-01	Naphthalene	0.361%
PCRESOL	p-Cresol	0.131%
PHENOLC9	p-Cumenol	5.848%
GLUTA-01	Pentanedinitrile	0.118%
METHY-01	Pentanedinitrile, 2-methyl-	0.121%
PHENOLC6	Phenol	6.705%
2:5-X-01	Phenol, 2,5-dimethyl-	0.138%
O-CRE-01	Phenol, 2-methyl-	0.268%
3:5-X-01	Phenol, 3,5-dimethyl-	0.131%
P-CUM-01	Phenol, 4-(1-methyl-1-phenylethyl)-	0.846%
BISPHENO	Phenol, 4,4'-(1-methylethylidene)bis-	1.014%

P-ETH-01	Phenol, 4-ethyl-	0.349%
STYRENE	Styrene	21.903%
TOLUENE	Toluene	6.984%
TRIPH-01	Triphenyl phosphate	0.138%
U-BBN	Benzenebutanenitrile	11.861%
U-COMP1	(+)-di-O-4-Toluoyl-D-tartaric acid	0.139%
U-COMP5	,alpha,-Methylstyrene	1.633%
U-COMP12	1-Chloro-6-phenylhexane	0.120%
U-COMP13	1H-Cyclopenta[l]phenanthrene, 2,3-dihydro-	0.273%
U-COMP14	1H-Indene, 1-(phenylmethylene)-	0.452%
U-COMP15	1H-Indene, 1-ethylidene-	0.178%
U-COMP17	1-Naphthalenamine, N-ethyl-	0.239%
U-COMP19	1-Propene, 3-(2-cyclopentenyl)-2-methyl-1,1-diphenyl-	0.538%
U-COMP21	2,2-Dimethyl-4-phenyl-2H-pyrrole	0.344%
U-COMP23	2,4-Diphenyl-4-methyl-2(E)-pentene	0.303%
U-COMP26	2-Cyano-4-phenylpentane	0.315%
U-COMP30	3-Aminophthalonitrile	0.155%
U-COMP32	3-Phenyl-2-pentenenitrile	0.937%
U-COMP33	4,6-Octadiyn-3-one, 2-methyl-	0.116%
U-COMP35	5H-Indeno[1,2-b]pyridine	0.659%
U-COMP37	Acridine, 9-phenyl-	0.171%
U-COMP39	Benzene, (1,3-dimethyl-3-butenyl)-	0.879%
U-COMP47	Benzene, 1,1'-(3-methyl-1-propene-1,3-diyl)bis-	0.786%
U-COMP62	Bicyclo[3,2,0]hept-2-ene, 4-isopropylidene-6-(cyanomethylene)-	0.320%
U-COMP64	Diazene, bis(2-phenylethyl)-	0.136%
U-COMP65	Diglycolic acid, di(phenethyl) ester	0.407%
U-COMP72	m-Ethylbenzonitrile	0.270%
U-COMP77	Naphthalene, 2,7-bis(1,1-dimethylethyl)-	0.581%
U-COMP87	Phenol, 2-(1-phenylethyl)-	0.248%
U-COMP93	Phenol, 4-(1-phenylethyl)-	0.403%
U-COMP96	Phenylglyoxylic Acid, 3-methylbutyl ester	0.142%
U-COMP97	Propanedinitrile, (1-methylethenyl)(phenylmethyl)-	0.184%

Table A 2. Midpoint impact assessment results for electricity production, referring to the production of 1 kWh of electricity

Impact Category	Unit	Electricity production					
		QC	AB	ON	BC	BR	CN
Fine particulate matter formation	*kg PM2.5 eq*	1.76E-05	7.07E-04	6.59E-05	4.37E-05	3.31E-04	1.44E-03
Fossil resource scarcity	*kg oil eq*	1.61E-03	2.21E-01	1.95E-02	2.22E-02	4.74E-02	1.72E-01
Freshwater ecotoxicity	*kg 1,4-DCB*	3.82E-03	3.03E-02	2.63E-03	6.36E-04	1.48E-03	7.95E-03
Freshwater eutrophication	*kg P eq*	2.46E-06	1.17E-03	6.68E-06	2.68E-06	2.28E-05	1.59E-04
Global warming	*kg CO_2-eq*	1.51E-02	7.98E-01	6.61E-02	6.24E-02	2.09E-01	8.88E-01
Human carcinogenic toxicity	*kg 1,4-DCB*	2.17E-03	5.96E-02	5.81E-03	2.48E-03	4.13E-03	2.67E-02
Human non-carcinogenic toxicity	*kg 1,4-DCB*	1.90E-02	1.18E+00	8.85E-02	1.06E-02	6.68E-02	3.98E-01
Ionizing radiation	*kBq Co-60 eq*	1.48E-04	1.42E-03	5.60E-01	3.02E-04	1.88E-02	9.16E-02
Land use	*m2a crop eq*	4.84E-03	5.49E-03	2.24E-03	2.78E-03	1.35E-02	1.33E-03
Marine ecotoxicity	*kg 1,4-DCB*	4.69E-03	4.16E-02	3.45E-03	8.43E-04	2.30E-03	1.11E-02
Marine eutrophication	*kg N eq*	2.36E-07	7.16E-05	1.04E-05	3.18E-07	2.53E-05	1.20E-05
Mineral resource scarcity	*kg Cu eq*	1.32E-04	2.16E-04	7.62E-04	1.21E-04	1.43E-04	3.13E-04
Ozone formation, Human health	*kg NOx eq*	2.98E-05	1.17E-03	1.13E-04	1.03E-04	3.74E-04	2.47E-03
Ozone formation, Terrestrial ecosystems	*kg NOx eq*	3.04E-05	1.19E-03	1.16E-04	1.05E-04	3.84E-04	2.47E-03
Stratospheric ozone depletion	*kg CFC11 eq*	4.91E-09	1.84E-07	2.63E-08	2.69E-08	4.68E-07	1.38E-07
Terrestrial acidification	*kg SO2 eq*	4.80E-05	2.29E-03	1.52E-04	1.23E-04	8.55E-04	3.29E-03
Terrestrial ecotoxicity	*kg 1,4-DCB*	1.18E-01	3.04E-01	2.88E-01	6.07E-02	2.97E-01	4.92E-01
Water consumption	*m3*	1.73E-02	2.24E-03	2.93E-02	2.48E-02	1.89E-02	2.54E-03

Table A 3. LCIA midpoint results of baseline scenario, referring to the treatment of 25 tonnes/day of E-waste through incineration

Name	Unit	Incineration (Baseline)					
		QC	AB	BC	ON	CN	BR
Fine particulate matter formation	*kg PM2.5 eq*	9.67	-3.07E+01	8.15	6.85	-7.36E+01	-8.69
Fossil resource scarcity	*kg oil eq*	-9.43E+01	-1.29E+04	-1.30E+03	-1.14E+03	-1.01E+04	-2.78E+03
Freshwater ecotoxicity	*kg 1,4-DCB*	-2.24E+02	-1.77E+03	-3.72E+01	-1.54E+02	-4.65E+02	-8.64E+01
Freshwater eutrophication	*kg P eq*	-1.44E-01	-6.85E+01	-1.57E-01	-3.91E-01	-9.31	-1.33
Global warming	*kg CO2-eq*	4.05E+04	-5.27E+03	3.78E+04	3.76E+04	-1.05E+04	2.92E+04
Human carcinogenic toxicity	*kg 1,4-DCB*	-1.27E+02	-3.49E+03	-1.45E+02	-3.40E+02	-1.56E+03	-2.42E+02
Human non-carcinogenic toxicity	*kg 1,4-DCB*	-1.11E+03	-6.88E+04	-6.21E+02	-5.18E+03	-2.33E+04	-3.91E+03
Ionizing radiation	*kBq Co-60 eq*	-8.69	-8.32E+01	-1.77E+01	-3.28E+04	-5.36E+03	-1.10E+03
Land use	*m2a crop eq*	-2.83E+02	-3.21E+02	-1.63E+02	-1.31E+02	-7.78E+01	-7.89E+02
Marine ecotoxicity	*kg 1,4-DCB*	-2.74E+02	-2.43E+03	-4.93E+01	-2.02E+02	-6.52E+02	-1.35E+02
Marine eutrophication	*kg N eq*	-1.38E-02	-4.19	-1.86E-02	-6.09E-01	-6.99E-01	-1.48E+00
Mineral resource scarcity	*kg Cu eq*	-7.72	-1.26E+01	-7.08	-4.46E+01	-1.83E+01	-8.39
Ozone formation, Human health	*kg NOx eq*	9.46E+01	2.76E+01	9.03E+01	8.97E+01	-4.81E+01	7.44E+01
Ozone formation, Terrestrial ecosystems	*kg NOx eq*	9.45E+01	2.70E+01	9.02E+01	8.95E+01	-4.84E+01	7.39E+01
Stratospheric ozone depletion	*kg CFC11 eq*	-2.87E-04	-1.08E-02	-1.57E-03	-1.54E-03	-8.10E-03	-2.74E-02
Terrestrial acidification	*kg SO2 eq*	3.19E+01	-9.93E+01	2.76E+01	2.59E+01	-1.58E+02	-1.53E+01
Terrestrial ecotoxicity	*kg 1,4-DCB*	-6.88E+03	-1.78E+04	-3.55E+03	-1.68E+04	-2.88E+04	-1.74E+04
Water consumption	*m3*	-1.01E+03	-1.31E+02	-1.45E+03	-1.71E+03	-1.49E+02	-1.11E+03

Table A 4. LCIA midpoint results of scenario A, referring to the treatment of 25 tonnes/day of E-waste through MW-assisted pyrolysis

Name	**Unit**	**Microwave-assisted pyrolysis (Scenario A)**					
		QC	**AB**	**BC**	**ON**	**BR**	**CN**
Fine particulate matter formation	*kg PM2.5 eq*	-27.62	4.58E+00	-2.64E+01	-2.54E+01	-9.83E+00	3.88E+01
Fossil resource scarcity	*kg oil eq*	-16492	-6.25E+03	-1.55E+04	-1.57E+04	-1.43E+04	-8.53E+03
Freshwater ecotoxicity	*kg 1,4-DCB*	-192.26	1.04E+03	-3.41E+02	-2.48E+02	-2.94E+02	4.48E-01
Freshwater eutrophication	*kg P eq*	-3.49	5.11E+01	-3.48E+00	-3.30E+00	-2.47E+00	3.82E+00
Global warming	*kg CO2-eq*	-18156	1.84E+04	-1.59E+04	-1.58E+04	-8.78E+03	2.26E+04
Human carcinogenic toxicity	*kg 1,4-DCB*	-532	2.15E+03	-5.18E+02	-3.62E+02	-4.04E+02	6.15E+02
Human non-carcinogenic toxicity	*kg 1,4-DCB*	-8308	4.57E+04	-8.70E+03	-5.06E+03	-5.84E+03	9.41E+03
Ionizing radiation	*kBq Co-60 eq*	-301	-2.42E+02	-2.94E+02	2.59E+04	5.60E+02	3.97E+03
Land use	*m2a crop eq*	133	1.63E+02	3.67E+01	1.16E+01	5.63E+02	-3.11E+01
Marine ecotoxicity	*kg 1,4-DCB*	-284.50	1.44E+03	-4.64E+02	-3.42E+02	-4.02E+02	1.67E+01
Marine eutrophication	*kg N eq*	-0.25	3.08E+00	-2.46E-01	2.26E-01	9.39E-01	2.98E-01
Mineral resource scarcity	*kg Cu eq*	-18.12	-1.42E+01	-1.86E+01	1.13E+01	-1.64E+01	-9.65E+00
Ozone formation, Human health	*kg NOx eq*	-38.54	1.49E+01	-3.51E+01	-3.46E+01	-2.00E+01	7.53E+01
Ozone formation, Terrestrial ecosystems	*kg NOx eq*	-42.85	1.11E+01	-3.94E+01	-3.88E+01	-2.41E+01	7.12E+01
Stratospheric ozone depletion	*kg CFC11 eq*	-0.0048	3.51E-03	-3.82E-03	-3.85E-03	1.92E-02	1.39E-03
Terrestrial acidification	*kg SO2 eq*	-66.76	3.80E+01	-6.33E+01	-6.19E+01	-1.96E+01	8.47E+01
Terrestrial ecotoxicity	*kg 1,4-DCB*	-34468	-2.57E+04	-3.71E+04	-2.65E+04	-2.45E+04	-1.70E+04
Water consumption	*m3*	540	-1.64E+02	8.89E+02	1.10E+03	5.94E+02	-1.50E+02

Table A 5. LCIA midpoint results of scenario B, referring to the treatment of 25 tonnes/day of E-waste through MW-assisted pyrolysis

Name	Unit	Microwave-assisted pyrolysis (Scenario B)					
		QC	AB	BC	ON	BR	CN
Fine particulate matter formation	*kg PM2.5 eq*	-25.84	5.20E+00	-2.47E+01	-2.37E+01	-8.22E+00	3.82E+01
Fossil resource scarcity	*kg oil eq*	-16011	-6.13E+03	-1.51E+04	-1.52E+04	-1.38E+04	-8.34E+03
Freshwater ecotoxicity	*kg 1,4-DCB*	-155	1.04E+03	-2.99E+02	-2.09E+02	-2.52E+02	3.08E+01
Freshwater eutrophication	*kg P eq*	-3.12	4.95E+01	-3.11E+00	-2.93E+00	-2.12E+00	3.94E+00
Global warming	*kg CO2-eq*	-16642	1.86E+04	-1.45E+04	-1.43E+04	-7.55E+03	2.26E+04
Human carcinogenic toxicity	*kg 1,4-DCB*	-477	2.11E+03	-4.63E+02	-3.13E+02	-3.48E+02	6.28E+02
Human non-carcinogenic toxicity	*kg 1,4-DCB*	-7408	4.47E+04	-7.78E+03	-4.28E+03	-4.99E+03	9.67E+03
Ionizing radiation	*kBq Co-60 eq*	-262	-2.05E+02	-2.55E+02	2.50E+04	5.67E+02	3.85E+03
Land use	*m2a crop eq*	133	1.62E+02	4.00E+01	1.58E+01	5.50E+02	-2.54E+01
Marine ecotoxicity	*kg 1,4-DCB*	-237	1.42E+03	-4.10E+02	-2.93E+02	-3.52E+02	5.33E+01
Marine eutrophication	*kg N eq*	-0.22	2.99E+00	-2.20E-01	2.34E-01	9.24E-01	3.03E-01
Mineral resource scarcity	*kg Cu eq*	-15.89	-1.21E+01	-1.64E+01	1.25E+01	-1.40E+01	-7.72E+00
Ozone formation, Human health	*kg NOx eq*	-35.68	1.58E+01	-3.24E+01	-3.19E+01	-1.75E+01	7.41E+01
Ozone formation, Terrestrial ecosystems	*kg NOx eq*	-39.61	1.24E+01	-3.63E+01	-3.58E+01	-2.12E+01	7.04E+01
Stratospheric ozone depletion	*kg CFC11 eq*	-0.0049	3.12E-03	-3.94E-03	-3.97E-03	1.86E-02	1.08E-03
Terrestrial acidification	*kg SO2 eq*	-63.59	3.74E+01	-6.02E+01	-5.89E+01	-1.67E+01	8.25E+01
Terrestrial ecotoxicity	*kg 1,4-DCB*	-31596	-2.32E+04	-3.42E+04	-2.39E+04	-2.17E+04	-1.47E+04
Water consumption	*m3*	536	-1.44E+02	8.72E+02	1.07E+03	5.85E+02	-1.30E+02

Table A 6. LCIA midpoint results of scenario C, referring to the treatment of 25 tonnes/day of E-waste through MW-assisted pyrolysis

Name	Unit	Microwave-assisted pyrolysis (Scenario C)					
		QC	AB	BC	ON	BR	CN
Fine particulate matter formation	*kg PM2.5 eq*	-2.32E+01	8.99E+00	-2.20E+01	-2.09E+01	-8.55E+00	4.33E+01
Fossil resource scarcity	*kg oil eq*	-1.27E+04	-2.41E+03	-1.17E+04	-1.18E+04	-1.05E+04	-4.70E+03
Freshwater ecotoxicity	*kg 1,4-DCB*	-1.79E+02	1.06E+03	-3.28E+02	-2.35E+02	-2.89E+02	1.33E+01
Freshwater eutrophication	*kg P eq*	-3.41E+00	5.12E+01	-3.40E+00	-3.21E+00	-2.46E+00	3.91E+00
Global warming	*kg CO2-eq*	-1.67E+04	1.98E+04	-1.45E+04	-1.43E+04	-7.68E+03	2.40E+04
Human carcinogenic toxicity	*kg 1,4-DCB*	-4.87E+02	2.19E+03	-4.73E+02	-3.17E+02	-3.96E+02	6.59E+02
Human non-carcinogenic toxicity	*kg 1,4-DCB*	-7.88E+03	4.62E+04	-8.27E+03	-4.63E+03	-5.65E+03	9.84E+03
Ionizing radiation	*kBq Co-60 eq*	-2.02E+02	-1.42E+02	-1.95E+02	2.60E+04	6.68E+02	4.07E+03
Land use	*m2a crop eq*	1.39E+02	1.70E+02	4.32E+01	1.81E+01	5.43E+02	-2.46E+01
Marine ecotoxicity	*kg 1,4-DCB*	-2.61E+02	1.46E+03	-4.41E+02	-3.19E+02	-3.73E+02	4.02E+01
Marine eutrophication	*kg N eq*	-2.35E-01	3.10E+00	-2.32E-01	2.40E-01	9.35E-01	3.12E-01
Mineral resource scarcity	*kg Cu eq*	-1.56E+01	-1.17E+01	-1.61E+01	1.38E+01	-1.50E+01	-7.10E+00
Ozone formation, Human health	*kg NOx eq*	-3.26E+01	2.08E+01	-2.92E+01	-2.87E+01	-1.65E+01	8.13E+01
Ozone formation, Terrestrial ecosystems	*kg NOx eq*	-3.65E+01	1.74E+01	-3.30E+01	-3.25E+01	-2.00E+01	7.76E+01
Stratospheric ozone depletion	*kg CFC11 eq*	-1.85E-03	6.50E-03	-8.19E-04	-8.48E-04	1.98E-02	4.39E-03
Terrestrial acidification	*kg SO2 eq*	-5.35E+01	5.13E+01	-5.00E+01	-4.87E+01	-1.58E+01	9.80E+01
Terrestrial ecotoxicity	*kg 1,4-DCB*	-3.15E+04	-2.28E+04	-3.42E+04	-2.36E+04	-2.31E+04	-1.40E+04
Water consumption	*m3*	5.41E+02	-1.63E+02	8.90E+02	1.10E+03	6.15E+02	-1.49E+02

Table A 7. LCIA midpoint results of scenario D, referring to the treatment of 25 tonnes/day of E-waste through MW-assisted pyrolysis

Name	Unit	Microwave-assisted pyrolysis (Scenario D)					
		QC	AB	BC	ON	BR	CN
Fine particulate matter formation	*kg PM2.5 eq*	-1.31E+01	8.05E+00	-1.23E+01	-1.16E+01	6.54E+00	3.06E+01
Fossil resource scarcity	*kg oil eq*	-1.22E+04	-5.46E+03	-1.16E+04	-1.16E+04	-1.05E+04	-6.96E+03
Freshwater ecotoxicity	*kg 1,4-DCB*	7.33E+01	8.86E+02	-2.46E+01	3.67E+01	2.67E+01	2.00E+02
Freshwater eutrophication	*kg P eq*	-2.15E-01	3.56E+01	-2.08E-01	-8.55E-02	6.42E-01	4.59E+00
Global warming	*kg CO2-eq*	-1.43E+03	2.26E+04	2.40E+01	1.38E+02	5.61E+03	2.54E+04
Human carcinogenic toxicity	*kg 1,4-DCB*	-8.19E+01	1.68E+03	-7.24E+01	2.98E+01	9.51E+01	6.72E+02
Human non-carcinogenic toxicity	*kg 1,4-DCB*	-8.90E+02	3.46E+04	-1.15E+03	1.24E+03	1.34E+03	1.08E+04
Ionizing radiation	*kBq Co-60 eq*	-3.14E+02	-2.75E+02	-3.09E+02	1.69E+04	2.30E+02	2.49E+03
Land use	*m2a crop eq*	1.20E+02	1.40E+02	5.64E+01	3.99E+01	4.45E+02	1.19E+01
Marine ecotoxicity	*kg 1,4-DCB*	6.35E+01	1.19E+03	-5.46E+01	2.55E+01	-2.92E+01	2.61E+02
Marine eutrophication	*kg N eq*	-3.81E-02	2.15E+00	-3.56E-02	2.74E-01	7.72E-01	3.21E-01
Mineral resource scarcity	*kg Cu eq*	-4.37E+00	-1.80E+00	-4.70E+00	1.50E+01	-1.36E-01	1.20E+00
Ozone formation, Human health	*kg NOx eq*	-1.34E+01	2.17E+01	-1.12E+01	-1.09E+01	5.12E+00	6.14E+01
Ozone formation, Terrestrial ecosystems	*kg NOx eq*	-1.47E+01	2.07E+01	-1.24E+01	-1.21E+01	3.54E+00	6.03E+01
Stratospheric ozone depletion	*kg CFC11 eq*	-9.45E-03	-3.96E-03	-8.78E-03	-8.80E-03	1.24E-02	-5.35E-03
Terrestrial acidification	*kg SO2 eq*	-3.92E+01	2.97E+01	-3.69E+01	-3.60E+01	1.58E+01	6.04E+01
Terrestrial ecotoxicity	*kg 1,4-DCB*	-8.83E+03	-3.09E+03	-1.06E+04	-3.60E+03	2.17E+03	2.67E+03
Water consumption	*m3*	5.28E+02	6.50E+01	7.57E+02	8.94E+02	5.15E+02	7.42E+01

Table A 8. Endpoint impact assessment results for all scenarios

Scenario	Area of protection	QC	AB	BC	ON	CN	BR
Baseline	Damage to human health	0.0409	-0.0517	0.0364	0.0329	-0.0669	0.0175
	Damage to ecosystems	1.16E-04	-8.46E-05	1.02E-04	9.73E-05	-7.89E-05	6.49E-05
	Damage to resource availability	-32.8404	-2313.2644	-461.8626	-403.2049	-983.2258	-918.4992
Scenario A	Damage to human health	-0.0367	0.0372	-0.0331	-0.0303	0.0493	-0.0157
	Damage to ecosystems	-6.50E-05	9.50E-05	-5.39E-05	-5.01E-05	9.05E-05	-2.10E-05
	Damage to resource availability	-6447.94	-4628.25	-6105.60	-6152.40	-5689.57	-5706.64
Scenario B	Damage to human health	-0.0338	0.0374	-0.0304	-0.0276	0.0491	-0.0132
	Damage to ecosystems	-5.94E-05	9.49E-05	-4.87E-05	-4.51E-05	9.05E-05	-1.65E-05
	Damage to resource availability	-6316.67	-4562.24	-5986.60	-6031.73	-5585.50	-5596.53
Scenario C	Damage to human health	-0.0323	0.0415	-0.0288	-0.0260	0.0537	-0.0137
	Damage to ecosystems	-5.72E-05	1.03E-04	-4.61E-05	-4.23E-05	9.83E-05	-1.65E-05
	Damage to resource availability	-4718.78	-2899.08	-4376.43	-4423.24	-3960.40	-4012.05
Scenario D	Damage to human health	-0.0089	0.0397	-0.0065	-0.0047	0.0477	0.0111
	Damage to ecosystems	-6.20E-06	9.89E-05	1.09E-06	3.55E-06	9.60E-05	3.09E-05
	Damage to resource availability	-5498.85	-4303.12	-5273.89	-5304.65	-5000.52	-4919.22

7.1. Regression models

BATCH-A

Variable	Description	Variable	Description
Y	Net revenue= Annual revenue - annual electricity cost	X_2	reflux controller gain
X_1	reflux controller maximum output	X_3 to X_7	specified pot heating rate for each operating step

Atmospheric :

$Y_1 = -168800 - 95269.27\ X_1 + 43387.9\ X_2 - 91717.17\ X_3 - 1030000\ X_4 + 159200\ X_5 + 805200\ X_6 - 333600\ X_7 + 60732.2\ X_1X_2 - 125100\ X_1X_3 + 250200\ X_1X_4 + 195800\ X_1X_5 - 1301000\ X_1X_6 + 940200\ X_1X_7 - 68753\ X_2X_3 - 254900\ X_2X_4 + 6520.32\ X_2X_5 + 483000\ X_2X_6 - 280000\ X_2X_7 + 185300\ X_3X_4 + 333300\ X_3X_5 + 2194000\ X_3X_6 - 2661000\ X_3X_7 - 31645.74\ X_4X_5 + 1014000\ X_4X_6 + 255700X_4X_7 - 81265.19\ X_1^2 - 130500\ X_2^2 - 367100\ X_3^2 - 279900\ X_4^2 - 45783.79\ X_5^2 + 144100\ X_1X_2X_3 - 211800\ X_1X_2X_4 + 125900\ X_1X_2X_5 + 35788.67\ X_1X_2X_6 - 19660.63\ X_1X_3X_4 + 231300\ X_1X_3X_5 - 138000\ X_1X_3X_6 - 68071.53\ X_1X_4X_5 + 259800\ X_2X_3X_4 - 153200\ X_2X_3X_5 - 152400\ X_1^2X_2 - 16106.07\ X_1^2X_3 + 6823.17\ X_1^2X_4 + 134300\ X_1^2X_5 + 33691.47\ X_1X_2^2 - 163800\ X_1X_3^2 + 75148.93\ X_1X_4^2 - 73416.99\ X_1X_5^2 + 147400\ X_2^2X_3 + 175600\ X_2^2X_4 - 92680.72\ X_2X_3^2 + 107600\ X_2X_4^2 + 335600\ X_3^2X_4 - 579100\ X_3X_4^2 - 28227.45\ X_4^2X_5 + 97910.15\ X_1^3 + 531.43\ X_2^3 + 582800\ X_3^3 + 22774.53\ X_4^3$

Vacuum :

$$
\begin{aligned}
Y_2 = {} & 180030 + 785.22422\ X_1 - 61026.40456\ X_2 + 50145.35125\ X_3 + 22682.17928\ X_4 \\
& + 207133\ X_5 - 200813\ X_6 + 190361\ X_7 + 1036.36821\ X_1X_2 \\
& + 209.64453\ X_1X_3 - 1329.36224\ X_1X_4 + 478.45066\ X_1X_5 + 1423.34443\ X_1X_6 \\
& - 1406.86133\ X_1X_7 + 2107.57143\ X_2X_3 - 16284.88172\ X_2X_4 + 4128.80068\ X_2X_5 \\
& + 41433.23279\ X_2X_6 - 20628.75723\ X_2X_7 - 24189.12898\ X_3X_4 + 43036.02334\ X_3X_5 \\
& + 6627.0734\ X_3X_6 - 25062.76693\ X_3X_7 + 1868.28337\ X_4X_5 + 39440.15807\ X_4X_6 \\
& - 22370.82784\ X_4X_7 - 50605.24382\ X_5X_6 + 51316.19575\ X_5X_7 - 19433.98869\ X_6X_7 \\
& - 30.3919\ X_1^2 + 382.68379\ X_2^2 - 10040.72133\ X_3^2 + 16889.80078\ X_4^2 \\
& - 41457.15734\ X_5^2 + 17039.10738\ X_6^2 - 4120.70884\ X_7^2
\end{aligned}
$$

BATCH-B

Variable	Description	Variable	Description
Y	Net revenue= Annual revenue - annual electricity cost	X_3	heating rate controller gain
X_1	heating rate controller output maximum	X_4	reflux controller gain
X_2	reflux controller maximum output		

Atmospheric :

$$Y_3 = -682698 + 726917\ X_1 + 25234.09768\ X_2 - 457178\ X_3 - 73110.00348\ X_4 - 11157.97081\ X_1X_2 + 49462.33465\ X_1X_3 + 45005.70872\ X_1X_4 + 8372.34063\ X_2X_3 + 1447.97356\ X_2X_4 - 2629.53323\ X_3X_4 - 98975.94837\ X_1^2 - 274.05135\ X_2^2 + 10987.29642\ X_3^2 - 10668.19125\ X_4^2 - 600.0901\ X_1X_2X_3 - 353.64257\ X_1X_2X_4 - 5456.92809\ X_1X_3X_4 + 311.75613\ X_2X_3X_4 + 1881.19325\ X_1^2X_2 + 10491.692\ X_1^2X_3 + 1813.88997\ X_1^2X_4 - 9.48117\ X_1X_2^2 - 11400.29382\ X_1X_3^2 - 2581.70038\ X_1X_4^2 - 6.86183\ X_2^2X_3 - 16.07982\ X_2^2X_4 - 785.51925\ X_2X_3^2 + 278.78886\ X_2X_4^2 + 982.70228\ X_3^2X_4 - 195.46443\ X_3X_4^2 - 5420.03667\ X_1^3 + 1.48843\ X_2^3 + 8303.09063\ X_3^3 - 447.84859\ X_4^3$$

BATCH-B Vacuum :

$$Y_4 = -411521 + 395054\ X_1 + 16175.33461\ X_2 - 58667.13125\ X_3 + 2678.13313\ X_4 - 1754.24089\ X_1X_2 - 875.44742\ X_1X_3 + 22632.58248\ X_1X_4 + 2342.28727\ X_2X_3 - 1567.0698\ X_2X_4 + 24580.7912\ X_3X_4 - 34515.62511\ X_1^2 - 103.03069\ X_2^2 - 23505.32683\ X_3^2 - 1935.89915\ X_4^2$$